# THE SEPTIC ABSCESS WALL: A CYTOKINE GENERATING ORGAN, INDUCING HEPATIC OUTFLOW FIBROSIS, SINUSOIDAL CONGESTION AND INFLAMMATION

**Adil Ceydeli**

**MD, 1998, Hacettepe Medical School**

**A Thesis submitted to the Graduate School of Biomedical Sciences, University of Medicine and Dentistry of New Jersey in partial fulfillment of the requirements for the MS Degree**

**Newark, New Jersey 07103**

**October, 2001**

# TABLE OF CONTENTS

# ACKNOWLEDGEMENT

I am indebted to the many special people, who have helped and who continue to support me.

First among them, I am very grateful to my mentor Dr. John H. Siegel. Dr. Siegel's encouragement and optimism has been a great contribution to my life and my surgical career. He is not only a good mentor but also a good friend. Although this project is completed, I hope that in the future we will work together again.

Many thanks to Dr. Iskender A. Sayek, who has been my mentor throughout my medical career and who encouraged me to follow this dream. My medical training began with Dr. Sayek and his advice has been invaluable.

I would like to thank Dr. Michael R. Condon who dedicated many hours in the laboratory and at home to my research. Dr. Condon's teaching of research techniques, provision of editorial suggestions and financial support are greatly appreciated.

I would like to thank Dr. Zoltan Spolarics for reviewing my thesis, and Dr. Richard Howland for proofreading my statistical analyses. I would also like to thank Jim Jetko and Cesar Fernandez for their technical help, as well as Romaine Wasserman, Amy Stolar and Norma Nicholson-Brown for their administrative support and friendship.

Finally, words cannot fully express the gratitude I have for my family. Mom, Dad, and Lucia; thank you for your love and support, without it this would not be happening. I love you all.

This project was funded with the Wesley J. Howe Professorship Account awarded to Dr. John H. Siegel.

# ABSTRACT

Sepsis is the systemic inflammatory response of the organism specifically against infectious causes. Sepsis is not a disease but a clinical syndrome, and if a culture negative patient develops the same clinical syndrome with an underlying reason other than infection, the syndrome is called Systemic Inflammatory Response Syndrome (SIRS). Sepsis and SIRS are closely related phenomena and both can cause multiple organ failure (MOF), which is responsible for 50% to 80% of all deaths in surgical intensive care units.

In this study, the cellular and molecular mechanisms of the systemic response to an intra-abdominal septic process have been investigated using a chronic septic rat fecal-agar pellet model. A sterile intra-abdominal (IA) abscess was produced by implantation of an autoclaved fecal-agar pellet in 7 animals, and the production of a septic abscess in 9 animals by implantation of a fecal pellet contaminated with $10^2$ CFU of E. coli and $10^9$ CFU of B. fragilis. There were 3 anesthesia controls.

**Hypothesis:** The abscess wall macrophages play a systemic inducer role in the host response by synthesizing IL-6 into the portal circulation, which in turn induces IL-6 and fibrinogen gene expression in the liver. Fibrinogen, secreted by liver and also produced by local abscess wall fibroblasts, plays a key role when converted to fibrin and then replaced by collagen, by assisting in walling off of the abscess and isolating the infection.

**Results:** At day 3, polymerase chain reaction (PCR) of sterile and septic abscess walls showed increased levels of TNF-alpha, IL-1 beta and IL-6 when compared to control small bowel wall. *In situ* hybridization of these cytokines confirmed the presence and the location of the mRNAs in the abscess walls. Portal vein IL-6 concentrations (ELISA) of sterile and septic abscess groups were also statistically higher than in the control group. The IL-6 and fibrinogen gene expression was markedly higher in the sterile and the septic livers, when compared to control liver, as a secondary response to the intra-abdominal inflammatory process, and the IL-6 and fibrinogen positive cells were uniquely located in pericentral vein area. Statistical comparisons were done by using Tukey-Kramer HSD, Student's t-test, and Dunnett's Method, and p value of less than 0.05 was considered statistically significant.

Circulating portal vein IL-6 concentrations in experimental groups:

| Groups | Mean (pg/ml) | 95% Confidence Intervals |
|---|---|---|
| Control | 4.20 | 4.14, 4.25 |
| Sterile | 8.83* | 7.47, 10.79 |
| Septic | 9.41* | 7.99, 11.43 |

*Significantly different from Control ($p<0.01$), power 90%.

**Conclusions:** Both the sterile and the septic abscess groups had walled-off abscesses and signs of peritonitis at post-implantation day 3. Both abscess walls had an increased amount of inflammatory cell infiltration with mRNA positive cells for IL-6 and fibrinogen, appearing to be responsible for the secondary inflammatory

changes seen in the liver. These cells play an endocrine role through the production and secretion of IL-6 into the portal circulation. The IL-6, which was originated from abscess wall reached the liver through the portal circulation and stimulated liver cells to produce local IL-6 and fibrinogen in a paracrine manner around the central vein parenchyma. The peri-central vein IL-6 and fibrinogen induction appears responsible for the hepatic collagen deposition and the resultant sinusoidal congestion, and appears to enhance the inflammatory cell sequestration in the liver in the chronic phase of sepsis/SIRS.

# INTRODUCTION

The inflammatory response is an adaptive mechanism of the organism to injury. It is a rapid process, peaking in 1-2 hours after trauma (1). During tissue injury a sequence of rapid and complex immune reactions occur. Hemostasis, the first response of the organism to injury, is achieved by the aggregation and activation of platelets, activation of coagulation pathways and by vascular contraction. Following hemostasis, injured cells and activated platelets produce large amounts of platelet activating factor (PAF), various growth factors and cytokines. These various factors cause a massive influx of neutrophils and macrophages to the site of injury. Neutrophils and macrophages have not only phagocytic functions, but also secrete many growth factors, such as PAF, leukotriens, prostaglandins, and cytokines, including Tumor Necrosis Factor-alpha (TNF-$\alpha$), Interleukin-1 beta (IL-1$\beta$), Interleukin-6 (IL-6), Interleukin-8 (IL-8), Interleukin-10 (IL-10), and Interleukin-12 (IL-12). Consequences of the massive influx of pro-inflammatory cells to the injured site include a stimulation of growth, activation of lymphocytes, attraction and activation of neutrophils, complement activation, and cell death.

These initial inflammatory responses provide protection to the host from injury, however, an excessive inflammatory response can damage the host itself through the release of lysosomal enzymes, elastase, and reactive oxygen radicals. There are variety of processes to control inflammation, preventing an excessive immune response, like heat shock proteins, antioxidant vitamins, acute-phase

proteins, receptor antagonists, prostaglandins and cytokines (2, 3). When these control mechanisms are not enough to control the inflammatory response, an excessive and autotoxic systemic inflammatory burst reaction will occur.

## A) DEFINITIONS OF SEPSIS/SIRS AND RELATED PHENOMENA:

Sepsis is the systemic inflammatory response of the organism specifically to infection. Sepsis is not a disease but a clinical syndrome. A correct and common definition of sepsis is important not only in establishing the pathophysiological mechanisms of sepsis but also in developing new therapeutical approaches in critically ill patients. The definitions of sepsis depend on clinical, laboratory and radiological abnormalities and do not include pathophysiologic, immunologic or biochemical mechanisms. A patient is considered septic if two or more of the following clinical conditions develop (4):

1) Temperature: > 38°C (100.4°F) or <36°C (96.8°F)
2) Heart Rate: > 90 beats/minute
3) Respiratory Rate: > 20 breaths/minute or PaCO2 < 32 torr
4) WBC > 12000/mmP$^3$ or < 4000/mm$^3$ or > 10% immature (band) forms

If a culture negative (unable to grow bacteria in the blood culture) patient develops two or more of the above criteria without infection, the clinical syndrome is called Systemic Inflammatory Response Syndrome (SIRS) (4). Some of the causes of SIRS include trauma, burns, acute pancreatitis, aspiration pneumonia, hemorrhagic shock, necrotic tissue, adrenal insufficiency, pulmonary embolism, dissecting or

ruptured aortic aneurysm, myocardial infarction, occult hemorrhage, cardiac tamponade, anaphylaxis, drug overdose, and tissue inflammation. (4, 5).

Bloodstream infection does not necessarily initiate the host defense response to sepsis. When a pathogen is isolated from the blood of a patient who presents signs of systemic infection, the infection is referred to as bacteraemia, viraemia or fungaemia depending upon the microorganism isolated.

Sepsis is called septic shock if hypotension is included in the clinical picture, and vasopressors/inotropes are frequently required to maintain blood pressure despite adequate fluid resuscitation (4). Septic shock is the progressive form of sepsis/SIRS and indicates severe perfusion and metabolic abnormalities that may include lactic acidosis, oliguria, or acute alteration in mental status.

Multiple organ failure (MOF) is the end stage of sepsis/SIRS, which affects one or more specific organ systems, and is usually a manifestation of a generalized inflammatory response, which is a closely related phenomenon to sepsis/SIRS (6). MOF was first described and published more than 20 years ago (7, 8) and is the cause of 50% to 80% of all deaths in surgical intensive care units (9). But the underlying mechanisms of MOF are still poorly understood and the treatment is usually supportive.

The local inflammatory response to an initially localized intra-abdominal infectious process in the normal sterile peritoneum is called intra-abdominal sepsis. Peritoneal levels of cytokines are elevated compared to the levels measured systemically, which suggests that peripheral blood cytokine levels represent only a very limited amount of the host response in a localized inflammatory process, such as

intra-abdominal abscess (5). If a non-infectious abdominal condition, such as operative trauma, triggers a cytokine-mediated inflammatory response, is referred to as a local inflammatory response syndrome (5). The terms intra-abdominal sepsis and local inflammatory response syndrome can be used instead of sepsis and systemic inflammatory response syndrome, respectively, if the origin of the inflammatory process is peritoneal and the inflammatory reaction is more intense in the local peritoneum than in the systemic circulation (5).

Early peritoneal soiling with microorganisms without invasion and with the lack of a local inflammatory response indicates abdominal contamination, and should not be confused with intra-abdominal sepsis or local inflammatory response syndrome. Traumatic perforation of the colon with peritoneal soiling is a common example of abdominal contamination and early irrigation of the soiling with antibiotic solutions may prevent or reduce the intra-peritoneal cytokine response and the development of intra-abdominal sepsis (5).

Tertiary peritonitis refers to when the bacterial peritonitis is cured with successful operations, effective antibiotic treatment and maximal supportive therapy but local and systemic inflammation persists. It has been shown that patients suffering from tertiary peritonitis may develop multiple organ failure and eventually die (10).

## B) PATHOPHYSIOLOGY OF SEPSIS/SIRS:

Therapy and prevention of sepsis/SIRS depends upon an understanding of the underlying pathophysiological mechanisms of the syndrome. Establishing the underlying cellular and molecular mechanisms is very important. In sepsis, even if the reason is due to bacterial infection, every patient can not be treated in the same way. Different organisms respond differently to antimicrobial agents and in most of the cases, administration of antimicrobial agents may be ineffective, since the underlying infection may have initiated the inflammatory response. Different etiologies other than microbial organisms may cause the same clinical syndrome by using similar cellular and molecular pathways, therefore it is crucial to establish these pathways in order to develop efficient therapies.

Pulmonary and intra-abdominal (IA) infections are typical causes of sepsis (6). Gram-negative (-) bacilli (E. coli) and anaerobes (B. fragilis) are more commonly the causes of IA septic abscess but other microorganisms like enterocci species, certain viruses and fungal organisms like candida species can also cause the septic syndrome (11). The host in an attempt to control the infection will produce a variety of factors such as, complement and coagulation factors, arachidonic acid metabolites, cytokines, and acute phase proteins. However, if this inflammatory response overwhelms the organism, it can cause damage to the host and possibly lead to multiple organ failure. Irrespective of the causing mechanism, MOF usually follows a course beginning with the lungs and progressing to the liver, gut and kidney. Bone marrow and heart are late sites of MOF and neurological symptoms may be seen early or late (6).

There are many proposed etiologies, which cause sepsis and which have been implicated in inducing further progression of sepsis to MOF, such as endotoxin, activated macrophages, cytokines, arachidonic acid metabolites, erythropoietin, endothelin and platelet activating factor (PAF).

Endotoxin, a lipopolysaccharide (LPS), is a molecule found in the cell walls of gram-negative microorganisms and is one of the most important and well-studied molecules underlying the pathophysiology of sepsis. It is composed of an O-linked polysaccharide chain, a core sugar, and a lipophilic fatty acid. The lipid portion of LPS (referred to as Lipid A) induces expression of cytokine genes through stimulation of receptors on the surface of target cells and activation of the nuclear factor kappa B (NF-κB). The products of these genes contribute to the inflammatory response and its destructive effects, i.e., hypotension and organ dysfunction (12).

Activated macrophages are the organizers of the systemic inflammatory response and are responsible for the cellular and molecular pathophysiology of sepsis/SIRS by producing cytokines and other pro-inflammatory molecules (13). Circulating monocytes, the source of macrophages, are attracted to the area of infection or tissue injury, enter the site by diapedesis and differentiate into activated macrophages.

Activated macrophages eliminate microorganisms, microorganism infected cells, and other cellular debris, but excessive activation of macrophages also causes the production and secretion of high levels of pro-inflammatory mediators, such as cytokines, which activate other pro-inflammatory cells like neutrophils and

endothelial cells. These high levels of systemic inflammatory mediators secreted by activated macrophages and other pro-inflammatory cells contribute to the development of sepsis/SIRS and distant organ failure.

There is always a sensitive balance between the above immunopathophysiological pathways and the anti-inflammatory response of the host against injury. The pro-inflammatory response fights against the agents that cause injury while anti-inflammatory responses try to balance this response in order to prevent further tissue damage to host itself. Roger Bone termed compensatory anti-inflammatory response syndrome (CARS), which he explained as the local and systemic anti-inflammatory responses of the organism against the local and systemic inflammatory response syndrome, which is mediated by anti-inflammatory cytokines (46). He also hypothesized that if SIRS and CARS are balanced, homeostasis occurs; when SIRS is predominant, apoptosis (programmed cell death) and organ failure is the result; when CARS is predominant, immunoparesis occurs (14).

## C) THERAPEUTIC APPROACHES AGAINST SEPSIS/SIRS:

The lack of an understanding of the underlying molecular mechanisms of sepsis has led to a heterogeneity of clinical trials, which has limited the validity of the investigations of sepsis and the production of new therapeutical approaches (4).

Many treatment modalities have been tried to decrease the morbidity and mortality from sepsis/SIRS, including external oxygenation, using extra corporeal membrane oxygenators, intra-aortic oxygenation, corticosteroids, vasoactive drugs, monoclonal antibodies to endotoxin, administration of nitric oxide, antioxidants, ketoconazole, ibuprofen, indomethacin, sodium nitroprusside, pentoxyfyline, antiendotoxin, anticytokine, aerosolized surfactant and more (15). Even if none of the above regimens have been shown to alter high mortality rate, it has been proposed that cyclooxygenase (COX) inhibitors, granulocyte-colony stimulating factor (G-CSF), interferon (IFN) and pentoxyfylin might be used as immunomodulatory agents in the near future (1).

Bactericidal permeability increasing protein (BPI) is one of the oxygen independent antibacterial mechanisms of host defense and it has been shown recently that administration of BPI in menengecocsic endotoxemia patients improved their prognosis (16). It is found in azurophilic granules of neutrophils and has two domains. BPI has 45% amino acid (aa) identity with lipoprotein binding protein (LBP), and both genes exist on chromosome 20 (16). BPI is a potent binder of endotoxin and is bactericidal to gram-negative rods. The N terminal domain has its bactericidal activity. BPI has neutralizing effects on endotoxin both *in vivo* and *in*

*vitro*. It has been shown that BPI has effects on IL-6 by decreasing its circulating levels (16).

Drugs used in sepsis, are usually for improving the clinical picture without affecting the underlying cause, and some pathology specific therapies don't have significant results probably because of the heterogeneity of the experimental studies due to lack of a definition, which describes underlying pathologies of sepsis. For this reason, future clinical studies of new therapies must serve two purposes:

a) To establish the disease mechanisms by showing that the specific biological mediator is the cause of organ dysfunction or death.

b) To test the efficacy of the drug's ability to modify the actions of the targeted mediator.

**D) CYTOKINES:**

Cytokines are intercellular signaling molecules, which have polypeptide or glycopeptide structures. They have a direct effect in the modulation of infectious or inflammatory processes. Most cytokines have multiple sources, multiple targets and multiple functions. Activated macrophages and monocytes are two major sources of cytokine production, with differing patterns of cytokine production in different inflammatory conditions. Cytokines are not stored in cells, and their relatively rapid appearance in injury depends on their active gene transcription and translation by the activated cell (17). Cytokines produce their effects by binding to specific cellular receptors and activating intra cellular signaling and gene transcription (18). Cytokines modulate immune cell activity, differentiation, proliferation and survival. They also

have synergistic and antagonistic affects on other cytokines by regulating their production and their receptor activity.

Lyoumi et al (19), have shown that IL-6 and other cytokines, such as TNF-alpha and IL-1 beta, predominantly function in a paracrine (effecting surrounding cells) and/or autocrine (effecting itself) fashion and are not endocrine mediators. There are two groups of cytokines, pro-inflammatory and anti-inflammatory:

The cytokines, which are produced during and participate in the inflammatory processes, are called pro-inflammatory cytokines and act by activating the production and secretion of inflammatory modulators and also directing inflammatory cells to the site of the injury.

Anti-inflammatory cytokines are also produced during the inflammatory processes but they act to attenuate the inflammatory process and prevent cellular damage.

Pro and anti-inflammatory cytokines work in a balance when modulating the inflammatory processes. This balance is a double edge sword, that changing this sensitive balance to either side can cause a poor and even fatal prognosis. An exaggerated pro-inflammatory cytokine response will cause sepsis/SIRS and may lead to MOF and death whereas unbalanced anti-inflammatory cytokine response will render the organism immunocomprimised and susceptible to overwhelming infectious morbidity (14).

Pro and anti-inflammatory cytokines also have regulatory effects on the systemic inflammatory response by affecting the apoptosis (programmed cell death) of the immuno-active cells (15). In the normal host, apoptosis is the principal

mechanism of sequestration of dysfunctional immune cells including macrophages. The apoptosis of these immune-active cells prevents a further systemic pro-inflammatory response (20). Some pro-inflammatory cytokines, such as TNF-α, IL-1, IL-2, IL-3, IL-6, GM-CSF, IFN-γ, and bacterial products (endotoxin) have been shown to delay macrophage and neutrophil apoptosis in vitro, while anti-inflammatory cytokines, such as IL-4 and IL-10, induce apoptosis in activated monocytes (15, 21).

**a) Pro-inflammatory Cytokines:**

Tumor necrosis factor-alpha (TNF-α), interleukin-1 (IL-1), interleukin-2 (IL-2), interleukin-6 (IL-6), interleukin-8 (IL-8), interleukin-12 (IL-12), interleukin-15 (IL-15), interleukin-18 (IL-18), interferon-gamma (IFN-γ), and granulocyte macrophage-colony stimulating factor (GM-CSF) are among the major pro-inflammatory cytokines (15), and participate in the inflammatory processes by activating the production and secretion of inflammatory modulators and directing inflammatory cells to the site of injury..

***Tumor necrosis factor-alpha (TNF-α):*** TNF-α is one of the earliest and most potent mediators in response to acute injury, infections or endotoxin administration. Monocytes/macrophages and T cells are the main sources of TNF-α production. TNF-α is an important inducer of muscle catabolism and cachexia by shunting the necessary amino acids to the hepatic circulation from the systemic circulation as energy substrates (17). TNF-α has been shown to effect the activation of coagulation,

increase the expression or release of adhesion molecules, prostaglandin $E_2$ ($PGE_2$), platelet-activating factor (PAF), glucocorticoids, and eicosonoids (22).

***Interleukin-1 (IL- 1):*** Activated macrophages and endothelial cells are the main sources of IL-1 production. There are 2 types of IL-1; IL-1α and IL-1β. IL-1α exerts its functions by cellular contacts. IL-1α has similar effects with TNF-α and it can be detected in the circulation (23). IL-1 has a half-life of approximately 6 minutes, which makes its detectibility in acute injury more difficult (17).

IL-1 induces the classic inflammatory febrile response to injury by activating the local prostaglandins in the anterior hypothalamus. It is also the cause of decreased pain threshold after surgery by inducing the secretion of beta endorphins from the pituitary gland and upregulating the central opioid-like receptors (24).

IL-1 may also interact with TNF-alpha to induce muscle proteolysis (25).

***Interleukin-2 (IL-2):*** IL-2 has immuno-modulatory effects by inducing T-cell proliferation, immunoglobulin production and maintaining gut barrier integrity. Decreased IL-2 expression is associated with the transient immunocompromise stage of the surgical patient (26).

***Interleukin-6 (IL-6):*** TNF-α and IL-1 are the major inducers of IL-6 production from almost all cells and tissues. Following acute injury, circulating IL-6 levels are detectable in 1 hour and peak in 4 to 6 hours, but the circulating levels of IL-6 can persist for as long as 10 days, which makes it valuable not only in the acute phase of inflammatory response but also during the chronic phase (17). Circulating IL-6 levels are indicators of the extent of the tissue injury during operations and are

more sensitive than the duration of the surgical procedure itself. IL-6 has regulatory effects on the acute-phase response, and is a major inducer of hepatic acute phase protein production in injury and convalescence. It produces fever, stimulates the production of arginine vasopressin, causes thrombocytosis and increases the production of metal-binding protein, metallothionein, in acute inflammation (27). It shows its pro-inflammatory effects by both inducing neutrophil activation and delaying the sequestration of these cells (28). It activates lymphocytes and stimulates growth (3). It is an important growth factor, especially following hepatectomy, and an essential initiator of hepatic regeneration (2). It has also been shown that, IL-6 has a protective effect during the first day of vaccinia virus infection, and if it is induced early pre-infection, it supports regenaration by enhancing the protein production in the liver (29).

Although IL-6 is one of the major pro-inflammatory cytokines, there is recent data, that it also has anti-inflammatory effects (30). IL-6 shows its anti-inflammatory effects by attenuating the activities of pro-inflammatory cytokines, TNF-$\alpha$ and IL-1, by inducing the secretion of TNF receptors and IL-1 receptor antagonists (31).

***Interleukin-8 (IL-8):*** IL-8 is a major chemoattractant and a potent activator of neutrophils (32). It is produced by monocytes, endothelial cells, fibroblasts, and neutrophils (5).

***Interleukin-12 (IL-12):*** IL-12 has a primary role in cellular immunity by inducing the differentiation of T Helper-1 (TH-1) cells. IL-12 promotes both neutrophil and coagulation activity, and modulates the pro and anti-inflammatory

mediator production. In fecal peritonitis, it has been shown that IL-12 administration has decreased mortality (33).

***Interleukin-15 (IL-15):*** IL-15 has similar effects as IL-2 by promoting lymphocyte activation and proliferation (34, 35). It potentiates the activity of neutrophils against fungal infections by inducing IL-8 production and NF-κB activation (36, 37).

***Interleukin-18 (IL-18):*** IL-18 is a relatively newly described pro-inflammatory cytokine, which has similar functions as IL-12. It used to be known as IFN-γ inducing factor. IL-18 levels are increased during sepsis and remain high as long as 21 days and show parallelism with the severity of sepsis (15). IL-18 is increased during gram-positive (+) sepsis compared to gram-negative (-) sepsis, and IL-18 is the only cytokine, which has this property (15, 38).

***Interferon-gamma (IFN-γ):*** Activated human T helper cells produce IFN-γ. Pro-inflammatory cytokines, IL-12 and IL-18, also show their biological effects via IFN-γ. IFN-γ also induces the production of pro-inflammatory cytokines, IL-2, IL-12, and IL-18 (39, 40). IFN-γ can be detected in the circulation by 6 hours and may remain high for as long as 8 days. IFN-γ may activate macrophages, and alveolar macrophage activation by IFN-γ after major trauma or surgery is responsible for acute lung inflammation.

***Granulocyte macrophage-colony stimulating factor (GM-CSF):*** GM-CSF is effective in inducing the production, maturation and recruitment of leukocytes to the

sites of injury for a normal inflammatory cytokine response. It is potentially important in wound healing, since macrophages are the main cells in wound healing.

**b) Anti-inflammatory Cytokines:**

Interleukin-4 (IL-4), interleukin-5 (IL-5), interleukin-6 (IL-6), interleukin-9 (IL-9), interleukin-10 (IL-10), and interleukin-13 (IL-13) are among the major anti-inflammatory cytokines and their levels increase as counter-inflammatory mediators in trauma. T Helper-2 (TH-2) cells regulate the secretion of these anti-inflammatory cytokines (1, 15). IL-4, IL-10 and IL-13 especially increase immediately after trauma.

***Interleukin-4 (IL-4):*** IL-4 has its major effects on the humoral immune system (41). Cluster Designation-8 (CD-8) positive lymphocytes are the source of IL-4 after trauma and has been related with poor outcome (1). IL-4 has potent anti-inflammatory effects by downregulating the pro-inflammatory cytokines, IL-1, TNFα, IL-6, and IL-8, which are produced by activated macrophages. IL-4 also shows its anti-inflammatory effects by decreasing the toxic oxygen radical production. It also amplifies the anti-inflammatory effects of glucocorticoids by increasing the macrophages' susceptibility.

***Interleukin-10 (IL-10):*** IL-10 is the most important anti-inflammatory cytokine and it has irreversible effects (15). IL-10 has modulatory roles on TNF-α and IL-18 simply by attenuating their pro-inflammatory effects. IL-10 is also immunosuppressive and inhibits T cell proliferation and may augment susceptibility

to repeated invasion of microorganisms. In animal experiments, IL-10 has been shown to decrease the mortality in septic peritonitis (42). Anti-IL-10 treatment increased peritoneal TNF-α and IL-6 levels in the cecal ligation and perforation (CLP) model. But in clinical trials, excessive IL-10 levels were also consistent with bacterial overload and mortality, and anti-IL-10 has been shown to improve outcome (43). TNF-α and IL-12 may induce IL-10 levels (1) during sepsis, but there is disagreement on the importance of its magnitude (43). IL-10 has a targeted delivery, being the greatest where the inflammatory event is intense, not to cause immunoparesis (43).

***Interleukin-13 (IL-13):*** IL-13 has similar effects with IL-4. It is one of the major anti-inflammatory cytokines and it shows its effects by inhibiting nitric oxide production and pro-inflammatory cytokine expression. It also inhibits IL-1 activity by secreting inhibitory IL-1 receptor antagonist, IL-1ra (44).

## E) T HELPER CELLS: THE ORGANIZERS OF IMMUNOMODULATION:

There are two functional subgroups of T Helper lymphocytes, TH-1 and TH-2.

TH-1 cells are related with cell-mediated immunity and activated TH-1 lymphocytes induce the activation of monocytes, B lymphocytes, and cytotoxic T lymphocytes. The TH-1 response is more potent in lesser injuries and more effective against microbial infections than the TH-2 response. In more severe injuries, TH-2 response is favored and naive T helper cells are shifted toward TH-2 lymphocytes. TH-2 lymphocytes are related with antibody-mediated immunity and they are not as effective as the TH-1 response against microbial infections. Activated TH-2 cells induce the activation of eosinophils, mast cells, and B lymphocyte, which produce immunoglobulin subtypes IgG4 and IgE. IgG4 and IgE are poor complement activators and the least efficient opsonizing antibodies.

Both of these T helper lymphocytes can induce the production of certain cytokines and certain cytokines can also activate these two subgroups of T helper cells. While both TH-1 and TH-2 cells produce IL-3, TNF-$\alpha$, and GM-CSF, the TH-1 response is further characterized by the production of IFN-$\gamma$, IL-2, IL-12 and TNF-$\beta$ (lymphotoxin), and the TH-2 cell response is further characterized by the production of IL-4, IL-5, IL-6, IL-9, IL-10, and IL-13.

IFN-$\gamma$, TNF, IL-1 and IL-12 can stimulate the TH-1 response and IL-12 is the most potent cytokine among all. IL-4, IL-5, IL-6, IL-10 and glucocorticoids can stimulate TH-2 response and IL-4 is the most effective stimulant among all. IL-4 and

IL-10 are main inhibitors of the TH-1 response, while IFN-γ is the main inhibitor of the TH-2 response.

The TH-2 response is predominantly immunosupressive and anti-inflammatory due to the activation of anti-inflammatory cytokines. Immunosupression and susceptibility to infections after major trauma and burns is due to shifting of naive T cells toward TH-2 lymphocytes and subsequent immunosuppressive effects (5, 17)

**F) SEPSIS AND LIVER:**

The liver is the largest internal organ in the human body, weighing approximately 1.7 kg in an adult (4% of the total body weight). It is reddish in color and positioned immediately beneath the diaphragm and in the right upper quadrant of the abdominal cavity.

The liver cells or hepatocytes form plates that are one or two cells thick and separated from each other by large capillary spaces called sinusoids. The hepatic plates are arranged into functional units called liver lobules. In the center of each lobule is the central vein, and at the periphery three portal triads (composed of hepatic artery, bile duct and portal vein branches). Central veins are the exits of various metabolites along with the venous blood from the liver, and all central veins merge to produce the right and left hepatic veins, and then connect to the inferior vena cava, which finally empties into the systemic circulation.

The liver is the central organ in whole body metabolism, and also an essential organ of natural immunity response by production of acute-phase proteins, complement and cytokines, and has a rich blood supply consistent with its important metabolic and immunomodulatory functions. Liver blood flow is approximately 1.5 L/min, which comprises 30% of the total blood volume. There is also a high amount of oxygen consumption in the liver, i.e. 20-25% of the total blood oxygen is used by the liver.

The liver is the only organ in the human body, which has a dual circulation. Seventy percent of the blood supply is maintained by the portal vein, and the rest is supplied by the hepatic artery. There is a reciprocal regulation between these two vessels that is, if the portal blood flow to the liver decreases, hepatic artery blood flow will increase to compensate for the diminished portal supply. If the hepatic artery blood flow decreases, compensatory portal blood supply will increase. Both portal vein and hepatic artery pour their blood into the sinusoids in the portal triad where the portal vein, hepatic artery and main bile duct come together. The portal vein carries various molecules from the gut to the liver and then to the systemic circulation, whereas the hepatic artery supplies the liver with oxygen. The bile ducts transport bile, produced by the hepatocytes, to the gastrointestinal system for lipid absorption.

Portal and hepatic blood flow will mix with each other in the portal triad and will travel together along the sinusoids throughout the liver, and after metabolic and immunologic changes, they will finally come to the central vein, which is located in the middle of each liver lobule.

The liver is composed of parencymal and non-parencymal cells. Hepatocytes are the parencymal cells of the liver and they compose 70% of all liver cells and 90% of all liver mass. Kupffer cells (hepatic macrophages), ITO cells (fat storing cells), sinusoidal endothelial cells, and PIT cells (liver natural killer cells) are among the non-parencymal cells of the liver, and compose only 30% of all liver cells and 10% of the liver mass.

***Hepatocytes:*** Hepatocytes have various functions. Their main function is to maintain the basal metabolic homeostasis and are responsible for the adaptation to metabolic needs of the peripheral organs. They achieve their metabolic functions by modulating all carbohydrate, protein and lipid metabolism. Hepatocytes also have an exocrine function, that they produce and secrete bile to the gut, which aids absorbtion of lipids from the gastrointestinal system.

Hepatocytes have also immunomodulatory functions other than their main metabolic functions. They produce and secrete inflammatory molecules like cytokines and acute phase proteins in response to injury to modulate the inflammatory response.

***Kupffer Cells:*** Kupffer cells are fixed hepatic macrophages, and they represent the largest and most concentrated population of macrophages in the human body (17), which is 80% of all resident macrophages. Their origin is monocytes but they can also proliferate locally. They are long lived cells. Their main function is to filter various molecules coming from the gut via the portal circulation, and to prevent the access of these molecules into the systemic circulation. They have various surface receptors, such as galactose, Fc, fibronectin, complement, mannose scavenger and

LPS receptors. They also phagocytosize red blood cells, opsonized bacteria and other particular matter, such as fibrin, DNA, debris, complement coated matter, yeast, parasites, modified proteins and LPS with their receptors, thereby eliminating them from the circulation.

Kupffer cells also have immunomodulatory functions. They produce inflammatory mediators, such as cytokines and lipid mediators, and are sources of reactive oxygen intermediates and nitric oxide. TNF-$\alpha$ is the major cytokine produced by Kupffer cells in response to systemic and localized inflammation. They also produce the cytokines, IL-1, IL-6, TGF-$\beta$, hepatic growth factor (HGF), and the lipid mediators, PAF, prostaglandin-$D_2$ ($PGD_2$), $PGF_{2a}$ and thromboxane-$A_2$ ($TxA_2$).

***Sinusoidal endothelial cells:*** The liver has a special type of endothelial cell, which is called the sinusoidal endothelial cell. These cells lie parallel to the hepatocytes starting from the portal triad and ending at the central vein. Sinusoidal endothelial cells have fenestrations, which allows the communication of the portal circulation and its ingredients with the hepatic cells. The placement of sinusoidal cells between the hepatic cells and blood circulation not only produces a protective cellular barrier but also allows transcytosis of important molecules and hormones to the hepatic interstisium by their fenestrations.

Sinusoidal endothelial cells bind modified proteins by their surface scavenger receptors, and are responsible for the uptake and degradation of hyaluronic acid by binding it to their hyaluronan receptors. They show some metabolic functions through

binding glycosidases, proteinases and proteinase-inhibitor complexes to their mannose receptors.

Sinusoidal cells also produce and secrete cytokines, such as IL-6, TNF-α, IL-1, TGF-β, and other inflammatory mediators, such as $PGE_2$, $PGD_2$, prostocyclin ($PGI_2$) and NO, in response to injury.

They are also responsible for the recruitment of inflammatory cells, such as polymorphonuclear leukocytes (PMN), monocytes, and PIT cells, by producing adhesion molecules on their surfaces. The production of these adhesion molecules on sinusoidal cells is increased in inflammation, and these surface receptors interact with the corresponding molecules located on the membranes of inflammatory cells, and recruit them to the site of the injury.

***PIT cells:*** Natural Killer (NK) cells of the liver are called PIT cells, and they exist in the liver as resident cells for weeks. There are as many PIT cells as Kupffer cells in the liver, and they participate in cell killing. Their accumulation in the liver is IL-2 dependent, and is increased in response to infections and tumors. Other than their killing fuctions, they also produce inflammatory mediators.

***ITO cells:*** ITO cells are fat storing cells of the liver and, are also called stellate cells. They are located behind the endothelial cells and are not in direct contact with the bloodstream. They compose 5-6% of all liver cells but in chronic inflammation their number increases. Since they are fat storing cells of the liver, they are also the storing sites of fat soluble vitamins like A and E. Especially 90% of all

the body's vitamin E is stored in liver ITO cells. ITO cells have a long life span, and are important in liver microcirculation, especially in response to sepsis.

They are very sensitive to cytokine stimulation, and the inflammatory stimuli change their structure. In normal situations they have moderate matrix synthesis, and are composed of passive (non-contractile) strings, such as desmin and vimentin. In response to injury, ITO cells become myofibroblastic, highly contractive, and actin filaments (contractile) take place of desmin and vimentin strings. Their matrix synthesis is also stimulated and they start to produce collagen. They loose their lipid doplets along with the fat soluble vitamins. The structural change of stellate cells in response to injury makes them responsible for the contraction of sinusoids, and contractive function of ITO cells modulate the microcirculation of the liver in sepsis.

**G) ACUTE-PHASE RESPONSE:**

The acute-phase response is one of the defense mechanisms of the organism against inflammation, and characterized by systemic changes in the body. It controls the inflammatory process by eliminating or isolating the inflammatory insult to avoid systemic dissemination, and also is responsible for the maintenance of the cardiovascular and metabolic physiology of the body in order to fight against various insults. There are two kinds of acute-phase changes in the inflammatory processes:

1) Changes in the concentrations of many plasma proteins, which are known as the acute phase proteins (APP's).

2) A large number of behavioral, physiologic, biochemical, and nutritional changes.

Fever, neurological alterations, loss of appetite, muscular pain, leukocytosis, hypothermia, hyperglycemia, increased protein catabolism in the skeletal muscle with transfer of amino acids to the liver to support acute-phase protein synthesis, and hormonal changes by the activation of the pituitary-adrenal axis are the systemic signs and symptoms of the acute-phase response, which are mostly caused by cytokines, produced during the inflammatory process (45). The systemic signs and symptoms, along with the type of positive acute-phase proteins seen in the acute-phase response depend on the type of the injury, damaging agent, the organ, and the extent of the injury.

The changes in the concentrations of acute-phase proteins (APP's) mostly depend on their production by hepatocytes. Infection, trauma, surgery, burns, tissue infarction, various immunologically mediated and crystal-induced inflammatory conditions cause abundant changes in the plasma concentrations of APP' s, while heavy exercise, heatstroke, labor, psychological stress cause moderate changes (27). There are two types of acute phase proteins:

**a) Positive Acute Phase Proteins:** The plasma concentrations of the positive acute-phase proteins increase by at least 25% of the normal levels during inflammatory disorders (27). Complement system proteins (C3, C4, C9, Factor B, C1 inhibitor, C4b-binding protein, Mannose-binding lectin), coagulation and fibrinolytic system proteins (Fibrinogen, Plasminogen, Tissue plasminogen activator, Urokinase, Protein S, Vitronectin, Plasminogen-activator inhibitor 1), antiproteases ($\alpha$1-Protease

inhibitor, α1-Antichymotrypsin, Pancreatic secretory trypsin inhibitor, Inter-α-trypsin inhibitors), transport proteins (Ceruloplasmin, Haptoglobin, and Hemopexin), and proteins that participate in inflammatory responses (Secreted phospholipase A2, Lipopolysaccharide-binding protein, Interleukin-1 receptor antagonist, Granulocyte-colony stimulating factor), C-reactive protein (CRP), serum amyloid A (SAA), α-Acid glycoprotein, fibronectin, ferritin, and angiotensinogen are examples of the positive acute-phase proteins.

**b) Negative Acute Phase Proteins:** The plasma concentrations of the negative acute-phase proteins decrease by at least 25% of the normal levels during inflammatory disorders (27). Albumin, transferrin, transthyretin, α2-HS glycoprotein, α-fetoprotein, thyroxine-binding globulin, insulin-like growth factor I, and factor XII are among the negative acute-phase proteins.

Cytokines are the most important activators of acute phase proteins. IL-6, IL-1β, TNF-α, IFN-γ, TGF-β, IL-8 are all pro-inflammatory cytokines, which activate the acute-phase response, but among them, IL-6 is the chief stimulator (27).

There are two main animal models, which have been used to study the acute-phase response and the regulation of acute-phase proteins by cytokines:

a) Induction of a local-sterile inflammation (muscle abscess) in rats by injection of subcutaneous turpentine.

b) Induction of systemic inflammation in mice by administration of bacterial lipopolysaccharide (LPS) intraperitoneally or intravenously.

The acute-phase response and hepatic acute-phase protein synthesis are both regulated by different cytokines in local-sterile inflammation caused by turpentine injection and in systemic inflammation caused by LPS administration.

In turpentine-induced local inflammation, local increases in IL-1β and TNF-α are followed by a systemic circulatory increase in IL-6 levels, and only the increased concentrations of IL-6 are responsible for the induction of hepatic acute-phase protein synthesis, whereas IL-1β, TNF-α and IL-6 are all responsible for the increase in acute-phase protein production in systemic inflammation, and TNF-α is the principal one (19, 46, 47). The stimulation of the pituitary-adrenal axis and the increase in systemic glucocorticoid concentrations are caused by cytokines in the acute-phase response, and further support the hepatic acute-phase protein synthesis by cytokines.

Combinations of cytokines have additive, inhibitory or synergistic effects in the regulation of acute-phase protein gene expression. IL-1 and TNF-α have synergistic effects with IL-6 in the induction of C-reactive protein (CRP) and serum amyloid A (SAA) genes, but have inhibitory effects on the induction of the fibrinogen gene stimulated by IL-6 (27). IL-1 does not have a major effect on the induction of the CRP gene, but is definitely required for the full induction of the mouse serum amyloid P (SAP) gene (an acute phase protein structurally similar to CRP) together with IL-6 (48). Both IL-1 and IL-6 synergistically induce serum amyloid A (SAA) in synovial fibroblast cells, and are present at significantly high levels in the synovial fluid of arthritis patients (49).

There is also species-dependent variability in the types of the acute-phase proteins produced during inflammation and their regulation by cytokines. The major positive acute-phase proteins are α2-macroglobulin in rats, serum amyloid P (SAP) in mice, and C-reactive protein (CRP) together with serum amyloid A (SAA) in humans (46). IL-1β is the major cytokine, which modulates the acute-phase response in mice (50), and IL-6 is the principal acute-phase mediator in rats and in humans (51, 52). IL-6 is necessary but not sufficient for the induction of hCRP gene, but it is not required for murine SAA gene induction (47).

Cytokines also have modulatory effects on negative acute-phase protein regulation. IL-1β and TNF-α decrease the expression of growth hormone receptors on hepatocytes, which subsequently decreases the responsiveness to growth hormone and insulin-like growth factor-I (27), whereas IL-6 reduces transferrin synthesis, thus decreasing serum iron, an important catalyst of free radical formation (3).

Several other mechanisms other than cytokines also regulate acute-phase protein synthesis. Hormonal regulation is one mechanism, of which the sex steroids are among the most important and well-studied ones. They not only regulate acute-phase protein synthesis, but also modulate other inflammatory mediators. It has been shown that males have more immunosupression and worse prognosis than females in shock and trauma, and this is partly because of the high concentrations of IL-6 release by Kupffer cells in males, and the positive effects of estrogen on the improvement of cardiac and immune functions (53). Testosterone, the male sex steroid, has been shown to directly regulate gene expression of some of the acute-phase proteins. In

mice, basal expression of the C-reactive protein (CRP) gene requires testosterone, but no such requirement for the gene encoding serum amyloid P has been demonstrated. IL-6 is necessary for the induction of the CRP gene in male mice, but either LPS or testosterone is required in addition to IL-6 in females (48). Sex steroids also affect the concentrations of several other inflammatory mediators, such as cytokines, chemokines, and T Helper cells. IL-8 levels and, so the neutrophil chemotaxis, are less in females, and they are more susceptible to viral-induced diseases (54).

Hormones other than sex steroids, such as cortisol, glucocorticoids, and catecholamines, also regulate the acute-phase response indirectly by modulating the cytokine response. These hormones all have anti-inflammatory functions. Cortisol and glucocorticoids show their anti-inflammatory effects by decreasing TNF-α and IL-1β gene expression, inducing cyclooxygenase-2 (COX-2) and adhesion molecule production (55), whereas catecholamines show their anti-inflammatory effects by inhibiting endotoxin-induced TNF-α and IL-1β production, and by stimulating IL-10 production. It has been shown that catecholamines have effects in the management of septic shock patients by increasing cardiac index (56).

Malnutrition is another important factor in the regulation of acute-phase proteins by cytokines. In severe malnutrition, the cytokine levels in whole blood are decreased, and the acute-phase response impaired. It has been shown that, concentrations of pro-inflammatory cytokines, such as TNF-α and IL-6, in whole blood, as well as CRP and Serum Amyloid A (SAA) responses to diphteria-pertussis-tetanus vaccine were impaired in severely malnourished children (57). It has also

been shown that, expression of the alpha-2 macroglobulin gene is dependent on IL-6 induction, and is increased in malnourished rats, whereas α-1 glycoprotein is regulated by a complex of cytokines, and there is no increase in the serum protein concentration in malnutrition (19).

The acute-phase proteins have various functions in the regulation of the inflammatory processes as well as in normal situations. They may have effects on one or more inflammatory stages. Especially changes in their concentrations, which are useful to clinicians, since they reflect the presence and intensity of an inflammation, even if they do not give any information about the etiology. Currently the most widely used indicators of the acute-phase response are erythrocyte sedimentation rate (ESR) and plasma CRP concentration. The functions of acute-phase proteins are:

***C reactive protein:*** CRP was first discovered in the 1930s in the plasma of patients, who had acute pneumococcal pneumonia and so named, because it reacted with the Pneumococcal C-polysaccharide (27, 58).

CRP has pro-inflammatory effects, and in the acute phase response, its secretion, but not its synthesis is greatly increased (27). It is a component of the innate immune system. It recognizes foreign pathogens and damaged cells by binding to phospholipid components, and then initiates the elimination of these targeted cells through activation of the complement system and by macrophage opsonization. CRP also induces inflammatory cytokines.

CRP has also been shown to exhibit anti-inflammatory effects, such as, preventing the adhesion of neutrophils to endothelial cells by decreasing the surface

expression of L-selectin, inhibiting the generation of superoxide by neutrophils, and stimulating the synthesis of interleukin-1 receptor antagonist (IL-1ra) by mononuclear cells.

***Serum amyloid A:*** SAA has the potential to influence cholesterol metabolism during inflammation by binding to high density lipoproteins (HDL). It also causes the adhesion and chemotaxis of phagocytic cells and lymphocytes.

***Complement System Proteins:*** Many of the complement components are acute-phase proteins, and have central pro-inflammatory roles in immunity by inducing leukocyte chemotaxis.

***Haptoglobin and hemopexin:*** Both molecules are antioxidants, and have been shown to have anti-inflammatory actions.

***Fibrinogen*:** Fibrinogen is one of the major acute-phase proteins produced in response to intra-abdominal sepsis and contributes to coagulation, wound healing, surface structure, and supports the lattice functions needed for entrapment of foreign material (80).

***Transthyretin****:* Transthyretin is a negative acute-phase protein, and inhibits IL-1 production by monocytes and endothelial cells.

***α-1 antitrypsin and antichymotrypsin:*** They modulate inflammatory events and protect the organism against tissue damage.

***IL-1 receptor antagonist:*** IL-1ra is a naturally occurring anti-inflammatory protein, that inhibits the effects of IL-1 both in vitro and in vivo. It also has been shown to reduce the severity of inflammation in several animal models (11). It

exhibits many properties similar to acute-phase proteins (APP), such as elevated serum levels after inflammation, in vitro production by human primary hepatocytes and Hepatic G2 cells, stimulation of production by IL-1β and IL-6, and regulation of transcription by NF-κB and C/ EBP family members. IL-1ra production is enhanced in both human primary hepatocytes and hepatoma cells by IL-1β alone or in combination with IL-6, and this is the first report describing a protein that acts as a class 1 acute-phase protein in both normal hepatocytes and hepatoma cells (11).

The expression of the positive acute-phase protein genes is mainly regulated at the transcriptional level, but it has been shown that the mRNA of the acute-phase proteins might also be increased by posttranscriptional stabilization (2, 27). The acute-phase proteins are divided into two subgroups, Class 1 and Class 2, based on the transcriptional activation by cytokine-stimulated transcriptional factors (2, 27). Haptoglobin, CRP, SAA, α-1 acid glycoprotein and hemopexin are examples of the Class 1 positive acute-phase proteins, whereas fibrinogen, α-1 antichymotrypsin, and α-1 antitrypsin are examples of the Class 2. IL-1 like cytokines (IL-1β, TNF-α) can only regulate the transcription of Class 1 acute-phase protein genes, whereas IL-6 like cytokines (IL-6, leukemia inhibitory factor, oncostatin M, ciliary neurotrophic factor, cardiotropin-1, IL-11) regulates the gene expression of both Classes of acute-phase proteins.

Both IL-1 like and IL-6 like cytokines first bind to their specific membrane-bound receptors, and activate various intra-cellular signal transduction pathways. The Sphingomyelinase/Ceramide signal transduction pathway is unique for Class 1 acute-

phase protein genes, and may only be activated by IL-1 like cytokines, whereas the JAK/STAT (**S**ignal **T**ransducer and **A**ctivator of **T**ranscription) pathway is specific for Class 2 genes, and may be only activated by IL-6 like cytokines. There is a third signal transduction pathway, the MAP-kinase pathway, which can be activated by both IL-1 like and IL-6 like cytokines. Following the induction of signal transduction, each signal transduction pathway activates a specific transcription factor, which ultimately activates the expression of acute-phase protein genes. The Sphingomyelinase/ceramide pathway activates the NF-κB transcription factor, JAK/STAT pathway activates STAT transcription factors, and MAP-kinase pathway activates a C/EBP family member of transcription factors (C/EBPβ). The activated transcription factors, then recognize target sequences in the promoter region of Class 1 and Class 2 acute-phase protein genes, and activate the expression of these genes. As mentioned above, NF-κB (activated by Sphingomyelinase/Ceramide pathway) can only recognize and activate the promoter regions of Class 1 acute-phase proteins, and STAT (activated by JAK/STAT pathway) transcription factors are specific for the promoter regions of Class 2 acute-phase proteins. C/EBPβ transcription factors (activated by MAP-kinase pathway) are able to recognize and activate the target sequences in the promoter regions of both Class 1 and Class 2 acute-phase proteins (45, 47). Neverthless, Class 1 acute-phase protein gene expression can be stimulated by NF-κB and C/EBPβ transcription factors, which are activated by a series of intra-cellular signal transduction pathways, induced by IL-1 like and IL-6 like cytokines,

respectively, whereas Class 2 acute-phase protein gene expression can only be activated by IL-6 like cytokines, via C/EBPβ and STAT transcription factors.

# RATIONALE

Sepsis is the systemic inflammatory response of the host to infection, and may occur after major trauma or surgery. It is not a disease but a clinical syndrome, and hepatic failure is a common manifestation of septic decompensation. Even though there are a large number of studies investigating sepsis in the literature, there is no specific treatment for the prevention or management of septic hepatic failure other than non-specific supportive care, and sepsis is still the leading cause of deaths in intensive care units.

The future treatment modalities of sepsis will depend on our understanding of the underlying pathophysiological mechanisms. In order to study and define the underlying mechanisms of sepsis and develop effective treatment modalities, we need animal models, which mimic the course of sepsis in patients. Most of the current animal models can only give information about the acute-phase of sepsis, and are incapable of studying the whole picture, which we usually see in patients.

For this reason, we used a well-established, reliable, and highly reproducible chronic septic rat fecal-agar pellet model. This model has been previously shown to follow a similar course of sepsis as seen in patients, and is able to give information about not only the acute hyperdynamic phase, but also the chronic hypercathabolic phase and metabolic fuel-energy shift as well. The chronic septic rat model has the advantage of allowing the study of SIRS at the same time with comparison to the septic process as well as controls.

The aim of this study was to characterize the immunopathophysiological mechanisms of the systemic inflammatory response against sterile and septic insults in order to guide the future studies, and help the development of therapeutic modalities.

# MATERIALS AND METHODS

## A) EXPERIMENTAL DESIGN AND THE CHRONIC SEPTIC RAT FECAL-AGAR PELLET MODEL:

The chronic septic rat fecal-agar pellet model was first reported in 1984 by Nakatani et al (59). It is a highly reproducible chronic intra-abdominal abscess model in rats. Rats were randomly assigned to three groups, namely control, sterile abscess, and septic abscess. The control group was anesthetized but did not go under laparotomy, while sterile and septic fecal-agar pellets were implanted into the abdominal cavity of the sterile and septic abscess groups, respectively. The septic fecal-agar pellets were inoculated with $10^2$ CFU/pellet of Escherichia coli and $10^9$ CFU/pellet of Bacteriodes fragilis prior to implantation as described previously by Nakatani et al (60). All animals were sacrificed 72 hours after pellet implantation.

### Chronic Septic Rat Fecal-Agar Pellet Model Protocol:

Male Sprague-Dawley rats, weighting 175-200 g, were ordered from Charles River Breeding Laboratories (Wilmington, MA) through Research Animal Facility, UMDNJ, and were maintained on regular rat chow and tap water until pellet implantation day.

B. fragilis colonies were grown on a Sheep Blood Agar (SBA) plate in an anaerobic chamber at 37°C five days prior to implantation day. The colonies were then transferred to a previously prepared and autoclaved cooked-meat medium at the

end of three days, and were left in the 37°C incubator for two more days for further growth. Meanwhile Escherichia coli were plated on Tripticase Soy Agar (TSA) two days prior to pellet implantation day and incubated at 37°C overnight, then transferred to 5 ml of sterilized Tripticase Soy Broth (TSB) and left one more night in the incubator for colony growth.

All rats were labeled and randomized into control (no laparotomy), sterile abscess (sterile pellet implantation), and septic abscess (pellet implantation containing $10^2$ CFU of E. coli and $10^9$ CFU of B. fragilis) groups prior to implantation day using JMP statistical software. All rats were weighted daily starting pre-operative day 2 until the sacrifice day (Post-implantation day 3).

Fecal-agar pellets were prepared by first pulverizing dry rat feces, and then mixing with certain amount of Tripticase Soy Agar and water (Table 1) on pellet implantation day.

**Table 1. The amounts of Tripticase Soy Agar, rat dried feces, and water to prepare certain number of pellets**

| | Number of pellets | | | | | | |
|---|---|---|---|---|---|---|---|
| | **5** | **10** | **15** | **18** | **20** | **24** | **30** |
| **TSA** | 0.207 g | 0.414 g | 0.62 g | 0.744 g | 0.826 g | 0.992 g | 1.24 g |
| **Feces** | 1.733 g | 3.466 g | 5.2 g | 6.24 g | 6.93 g | 8.34 g | 10.4 g |
| **Water** | 5.9 ml | 11.7 ml | 17.6 ml | 21.1 ml | 23.5 ml | 28.2 ml | 35.2 ml |

Following the preparation of the feces-agar mixture, syringe plungers were pulled to the 1.5 ml line and filled with the mixture. The plungers were then pulled further down in order to prevent over boiling during the autoclave process, capped

with chrome caps, placed in a glass beaker upright, and autoclaved using short-liquid cycle (sterile time 15 minutes, dry time 0). The autoclaved pellets were kept in incubator at 37ºC until ready to add bacteria.

The incubated cooked-meat medium was transferred into a sterilized 50 ml screw cap PC centrifuge tube and centrifuged at 13,000 rpm in a Beckman J2-21 (angle rotor) for 10 minutes at 4°C. After the spin, the excess supernatant was poured off until 3 ml of the supernatant was left in the tube. The B. fragilis pellet was then resuspended in the remaining 3 ml supernatant.

Serial dilutions of the resuspended B. fragilis pellet were performed using sterile water as the diluent. 100 µl of full strength B. fragilis suspension was inoculated to each pellet while 100 µl of $1:10^6$, $1:10^7$, and $1:10^8$ dilutions were plated onto SBA plates in duplicate and incubated at 37°C in an anaerobic chamber for 2 days in order to confirm the amount of B. fragilis inoculated to each pellet.

The E. coli was centrifuged at 11,000 rpm in Beckman J2-21 (angle rotor) for 10 minutes at 4°C. After which, the supernatant was decanted, and the E. coli pellet was resuspended in 5 ml of sterile water.

A Beckman's spectrophotometer was set at 660 nm and calibrated by using 1 ml of sterile water in a sterile cuvet. After the calibration, resuspended E. coli was added to the sterile cuvet containing 1 ml of sterile water, until the spectrophotometer absorbance reading was approximately 0.083-0.085 (Vary et al. previously showed in their laboratory work that, 100 µl of $1:10^5$ dilution of the E. coli suspension, which had 0.083-0.085 absorbance would give approximately $10^2$ CFU of E. coli/100µl).

Each pellet was inoculated with 100 μl of $1:10^5$ dilution of E. coli suspension, and 100 μl of $1:10^4$, $1:10^5$, and $1:10^6$ dilutions were plated onto TSA plates in duplicate and incubated at 37°C for approximately 18-24 hours to confirm the amount of E. coli inoculated to each pellet.

Pellets, which were prepared by inoculating 100 μl of full strength B. fragilis suspension and 100 μl of $1:10^5$ diluted E. coli per each, were stored on ice until the surgical procedure.

On the implantation day, rats were first anesthetized by using a mixture of ketamine/acepromazine (0.09 ml/100 g body weight), injected intramuscularly into their right thighs.

Each rat was placed on a board in the supine position (Figure 1). The abdomen was shaved, and the surgical area was prepped and draped in a routine sterile fashion (Figure 2).

A 2-cm midline incision was performed in the lower abdominal area of the sterile and septic groups, using a #15 blade. Depending on the experimental group, a sterile or septic pellet was implanted into the right lower quadrant of the rat (Figure 3). The control group received anesthetic only, and no laparotomy was performed.

**Figure 1. Preparation of the rats for the pellet-implantation surgery.** The surgical instruments required for the surgery are shown.

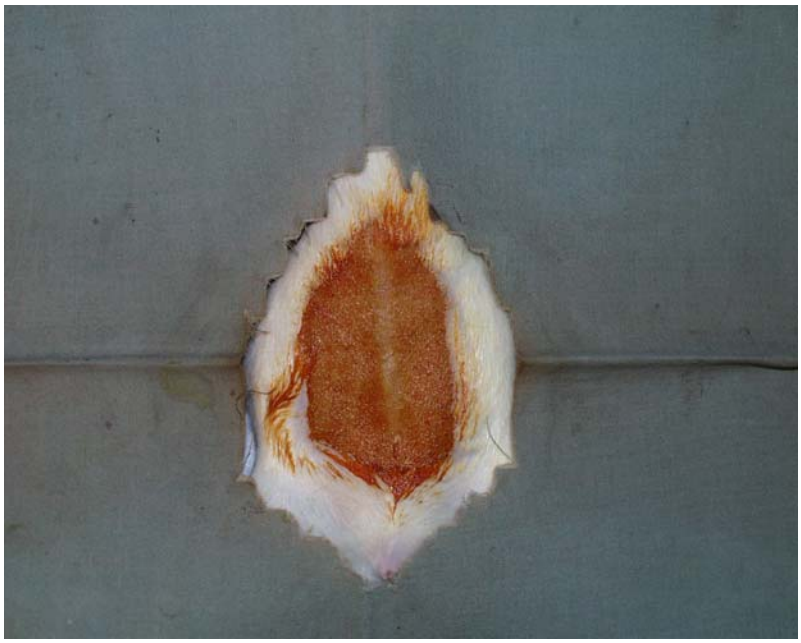

**Figure 2. Preparation of rats for pellet-implantation surgery.** Prepped and draped surgical area is shown.

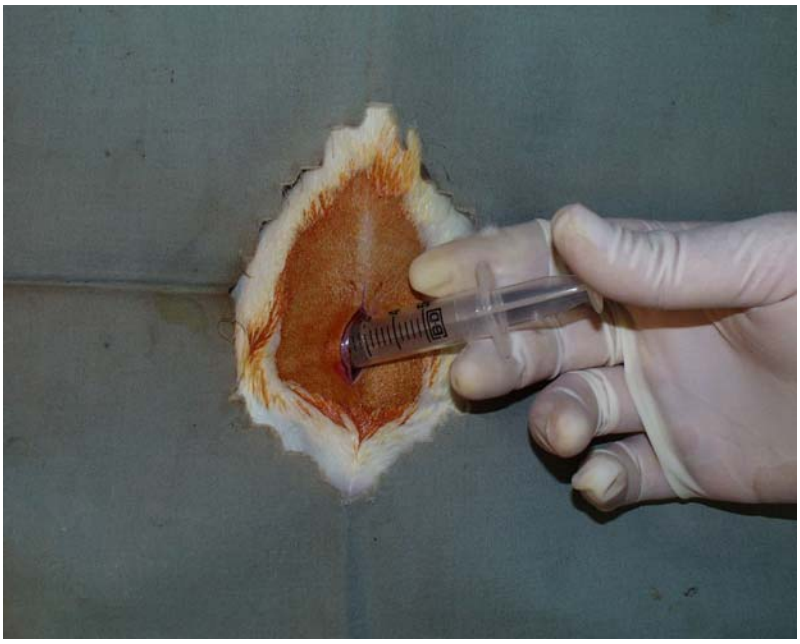

**Figure 3. Pellet implantation following laparotomy through midline incision.**

**Figure 4. Closure of the abdominal incision with 3-0 Vicryl (inner muscle layer) and Ethilon (skin) suture materials.**

Following the implantation, the inner muscular layer was approximated with absorbable 3-0 Vicryl suture material using a running suturing technique, and the skin was closed with non-absorbable 3-0 Nylon suture material using interrupted matris suturing technique (Figure 4).

The operated rat was placed in a cage on its right side (implanted pellet side), and the surgical area was prepared for the subsequent rat. These steps were repeated for each rat and all the rats were returned to the Research Animal Facility at the end.

All the mortality was recorded during the post-operative period, and only the animals that survived until post-operative day 3 were included in the statistical analyses. The original E. coli and B. fragilis inoculums to each pellet were calculated by counting the E. coli and B. fragilis dilution plates at the post-operative period.

On post-operative day 3, the surviving rats were brought to the laboratory, and anesthetized with a mixture of ketamine and acepromazine (0.09 ml/100 g body weight). The skin and the subcuticular layers were carefully dissected, intraperitoneal space was entered, and whole walled off abscess along with the other visceral organs were exposed.

After photography of the gross abscess and viscera, the pre-hepatic portal vein and post-hepatic inferior vena cava were catheterized using 22 gage angiocatheters. Blood samples were collected simultaneously from both the pre-hepatic portal vein and post-hepatic inferior vena cava into two separate 3 cc heparinized syringes. All blood samples were immediately transferred to 1.5 ml Eppendorf tubes, kept on ice until all the tissue samples were collected.

Immediately after collecting blood samples, the right lobe of the liver was clamped, and two separate pieces of liver were rapidly excised. One piece was flush frozen in liquid nitrogen for isolation of RNA and cryosectioning, and stored at -80°C until needed for analysis. The second piece was placed in 10% buffered formalin fixative solution for morphological and in situ hybridization studies.

After the liver sampling, the abscess was carefully dissected from the adjacent small intestine. A piece of abscess wall was flush frozen, while the rest was fixed as above.

The sacrifice protocol was applied for each animal, except for the control group. The rats in the control group were also anesthetized with the same type and dose of anesthetic, blood and liver samples were obtained from the same locations using the same techniques, but no abscess sampling was performed. After collecting all the samples, animals were exsanguinated under anesthesia.

At the completion of tissue collection, the blood samples were centrifuged at 12,000 rpm for 10 minutes to obtain plasma for Enzyme Linked-Immuno-Sorbent Assay (ELISA) analyses. The plasma samples were transferred to 0.5 ml Eppendorf microfuge tubes, and flush frozen in liquid nitrogen and stored at -80°C until ELISA analyses were performed.

**B) STATISTICAL ANALYSIS:**

Data was analyzed using the JMP statistical software, alpha value of 0.05 was used in all statistical analyses, and p values were considered as statistically significant below the alpha value of 0.05. According to the software protocol, two rules had to be maintained before testing the significance of the experimental results. The first was that, the data had to be normally distributed and the second that, the variances of data had to be equal. In all analyses, normality of the distribution was detected by histogram, outlier box plot, normal quantile plot and the Shapiro-Wilk W Test for Normality. If the data was not normally distributed, it was transformed to achieve the normal distribution, and the transformed data was tested for equal variances using the O'Brien and Brown-Forsythe tests. If these two tests did not support the equality of variances, the Welch Anova Test was used as an alternative, which tests the equality of means, allowing the standards not being equal.

Following the transformation of the data, multiple pairwise comparisons of the means, of the three experimental groups, were performed using the Tukey-Kramer test (Tukey's Honest Significant Difference test) instead of the Student's t-test (LSD test). The Tukey-Kramer test was used, since it is more sensitive and conservative, and the probability of making type 1 error (incorrectly rejecting null hypothesis) is high in multiple pairwise comparisons in the Student's t-test.

Both portal vein and inferior vena cava circulating cytokine (TNF-$\alpha$, IL-1$\beta$ and IL-6) levels were measured in each animal. Portal vein cytokine level was the first paired response and the inferior vena cava cytokine level was the second one per rat. The difference between the circulating cytokine levels of the portal vein and the

inferior vena cava was calculated for each rat, and the distribution tested for normality and equality of variances. If the distribution of the difference was normal, the paired t-test was used; if not, then the Wilcoxon Signed-Rank non-parametric test was applied to test the significance of the difference between the portal vein and the inferior vena cava circulating cytokine levels.

In the paired t-test, portal vein cytokine levels were represented on the X horizontal axis, while the inferior vena cava cytokine levels were represented on the Y vertical axis. Y was fitted by X, using JMP statistical software, and a scatterplot, showing the portal vein value on the X-axis and the inferior vena cava value on the Y-axis, was obtained. The paired t-test was run on this scatterplot, and a black 45-degree reference line passing through the origin, which represented where two columns were equal, a solid red line with a 45-degree slope, which indicated the line of fit, and the two red lines around the line of fit, which showed the 95% confidence interval, were obtained. If the two red lines, showing the confidence interval, included the black line through the origin, then it was interpreted as the two means were not significantly different; if the confidence interval did not include the black line, then it was concluded, that there was a statistically significant difference at the 0.05 alpha level. The scatterplot gave a good idea of each variable's distribution, as well as the distribution of the difference. It also provided information about the correlation structure. If the portal vein and inferior vena cava variables were positively correlated, they laid closer to the red line of fit, and the variance of the difference was small; if the two variables were negatively correlated, then most of the variations were perpendicular to the red line of fit, and the variance of the difference was large.

In the paired t-test, it was this variance of difference that scaled the difference in a t-test, and determined whether the difference was statistically significant or not.

In the Wilcoxon Signed-Rank non-parametric test, the difference of the cytokine levels between the portal vein and the inferior vena cava was compared with the hypothesized zero (0) value, since our null hypothesis was that there was no difference between the portal vein and the inferior vena cava circulating cytokine levels in each specific group, and the difference had to be 0. The actual estimate, indicating the difference, was tested with the hypothesized 0 value, and if the t ratio had a p value of 0.05 or higher, then it was decided that there was enough evidence to accept the null hypothesis (no statistically significant difference between the portal vein and the inferior vena cava circulating cytokine levels in the specified experimental group). If the t ratio had a p value of less than 0.05, then it was decided that there was enough evidence to reject the null hypothesis and accept the alternate one (statistically significant difference between portal vein and inferior vena cava circulating cytokine levels).

The linear regression analysis of the portal vein and inferior vena cava cytokine (TNF-alpha, IL-1 beta and IL-6) levels were performed at the end of the statistical analyses to indicate the correlation between the two sources.

## C) TISSUE FIXATION, PROCESSING, EMBEDDING AND SECTIONING:

**a) Tissue Fixation:** Fixation is the first step in preparing a tissue sample for examination under the light microscope. Since the tissues would also be used for in situ hybridization procedures, 4% paraformaldehyde was used as a fixative to avoid overfixation of the tissue samples with traditional 10% neutral buffered formalin. 4% paraformaldehyde is a less harsh fixative than 10% neutral buffered formalin, providing good signals during *in situ* hybridization while allowing the tissue to retain a normal morphologic structure.

4 % paraformaldehyde was prepared fresh and used for all tissue samples. Two grams of paraformaldehyde was dissolved in 30 ml of water in a beaker on a hotplate. 200 µl of 2M NaOH was added to help dissolve the paraformaldehyde, after which 200 µl of HCl was added to buffer the 2M NaOH. 5 ml of 10X PBS was added and the solution was adjusted to a final volume of 50 ml with water.

10-15 ml of fixative was added into 15 ml sterile conical tubes. Following the sacrifice of the rats, tissues were immediately placed into the labeled sterile conical tubes including the fixative. The tissues were fixed for 4 hours at room temperature on a rocking board to help the infiltration of fixative into the samples. After 4 hours, the fixative solutions of the samples were replaced with 50% alcohol and washed 3 times, 20 minutes each, on a rocking board. After the 3$^{rd}$ wash, the 50% alcohol was replaced with 70% alcohol and the samples washed 3 times, for 20 minutes each. Tissues were stable at room temperature in the final 70% ethanol wash.

**b) Processing:** Tissues were processed after fixation in order to infiltrate the tissue with an embedding medium. The embedding medium penetrates, surrounds, and stabilizes the tissue so that it can be sectioned using a rotary microtome.

Tissue processing started with dehydrating the samples by incubation in a series of gradually more concentrated solutions of alcohol. Following the dehydration step, tissues were incubated in two changes of xylene, an organic clearing agent, which removed any alcohol and prepared the tissues for infiltration with embedding medium (Table 2). Finally the samples were infiltrated with paraffin wax embedding medium in order to provide a stable and protective environment in and around the tissues.

**Table 2. The solutions used in tissue processing.**

| Container | Solution | Incubation duration |
|---|---|---|
| **1** | 50% alcohol | 30 minutes-1 hour |
| **2** | 70% alcohol | 30 minutes-1 hour |
| **3** | 90% alcohol | 30 minutes-1 hour |
| **4, 5** | 100% alcohol | 30 minutes-1 hour |
| **6, 7** | Xylene | 30 minutes-1 hour |
| **8, 9** | Paraffin at 60°C | 1 hour |

The incubation times were 30 minutes to 1 hour depending on the size of the sample and incubations were done with agitation to allow the infiltration of the tissues with processing solutions.

**c) Embedding:** The purpose of embedding tissues in paraffin wax is to provide a stable environment for proper sectioning. The same type of paraffin that was used for processing was also used for embedding purposes.

The embedding molds were filled with molten paraffin on a 60°C hot plate and three different tissues representing different experimental groups were removed from the processing cassettes and placed in each embedding mold. The embedded tissues were immediately cooled on an ice plate for proper crystallization.

Following rapid cooling of the embedded tissues, an embedding cassette was placed on top of each embedding mold and filled with paraffin to assure maximum stability of the paraffin block in the microtome. Paraffin blocks were immediately replaced on ice for further solidification. After the paraffin was completely set, the blocks were removed from the embedding molds, and the excess paraffin trimmed. The paraffin blocks were either sectioned or stored at room temperature for future sectioning.

**d) Sectioning:** Tissues were sectioned and mounted on slides for examination with a light microscope. Paraffin sectioning of the blocks was done with a rotator microtome (Olympus Cut 4060) that operates with a screw feed. It was able to move the paraffin block up and down while advancing a preset number of micrometers with each revolution of the fine advance wheel. The microtome was equipped with a knife holder, which allowed the use of disposable knife blades. The knife and microtome were set as described in Table 3.

**Table 3. The rotator microtome settings.**

| | |
|---|---|
| Micrometer setting | 4-6 microns |
| Knife wedge angle | 15° to 18° |
| Knife bevel angle | 27° to 32° |
| Clearance angle, or knife tilt in relation to the block | 3° to 8° |

Paraffin blocks were cooled on ice for 30 minutes before sectioning. After which, 4-6 microns thick sections were cut and floated on a bath. Using Sigma Diagnostics' Silane-Prep™ Microscope Slides, sections were mounted. Following the mounting, slides were incubated in a 65°C oven for 1 hour to adhere the sections on the slides.

**D) HEMATOXYLIN & EOSIN STAIN:**

Hematoxylin & Eosin (H&E) Stain is a quick and easy way of evaluating the tissue morphology and fixation. In properly fixed tissues, H&E reveals enough information about the overall tissue structure allowing the distinguishing of various cell types and tissue components. It also gives a general idea about tissue inflammation and helps to decide whether the tissue is in normal conditions or not.

Nuclei of the cells are stained blue with various chromatin patterns, which helps to differentiate various cell types, especially to distinguish the different types of white blood cells. There is a clear contrast between the cell nucleus and cytoplasm. Erythrocytes and eosinophilic granules are stained bright pink to red color, and the cytoplasm along with the other tissue elements are stained various tones of pink.

**Hematoxylin & Eosin Stain Procedure:**

Sections were deparaffinized in three changes of xylene for 5 minutes each. After deparaffinization, sections were rehydrated in a series of graded alcohols, starting with two changes of 100% alcohol, followed by one change of 95% alcohol and one change of 70% alcohol, and ending with tap water. Each rehydration step was done for 2 minutes. Slides were incubated in filtered Harris Hematoxylin for 4 minutes, and then rinsed in several changes of tap water to get rid of the excess Hematoxylin stain. The final wash in tap water was for 5 minutes to enhance blue color development. The sections were then counteracted with eosin for 3 minutes.

Tissue sections were dehydrated in two changes of 95% and 100% ethanol and cleared in two changes of undiluted xylene. Finally the tissue sections were applied a permanent mounting media and covered with glass coverslips.

**E) MYELOPEROXIDASE STAIN:**

Sigma Diagnostics® Peroxidase (Myeloperoxidase) kit was used (Procedure No. 391). Peroxidase (Myeloperoxidase) kit is a cytochemical staining system for polymorphonucleocytes in blood or bone marrow films. This assay was used to measure inflammatory cell infiltration of tissues and to differentiate the various inflammatory cells in cryosectioned tissue samples.

Diaminobenzidine (DAB) is a benzidine substitute for peroxidase cytochemistry but was not as attractive as benzidine itself to histochemists because it has less tinctorial power than benzidine. Hanker and associates improved DAB methodology and made it more suitable and popular for differentiating granulocytes,

their precursors and monocytes from cells of lymphoid origin (61-63). According to their protocol, the brown reaction product is first intensified with copper salts followed by application of Gill's modified Papanicolau stain, resulting in intense gray-black granules at sites of neutrophil and monocyte myeloperoxidase (64).

$$\text{DAB} + H_2O_2 \xrightarrow{\text{MP}} \text{Oxidized DAB (light Brown Pigment)}$$

$$\text{Oxidized DAB} + Cu(NO_3)_2 \longrightarrow \text{Grey-Black Pigment}$$

The reaction product is further intensified and characteristic color imparted to neutrophils, eosinophils, and basophils, when it is treated with Gill's modified Papanicolaou stain. Neutrophils and their precursors show gray-black intracellular granulation, while monocytes stain less intensely. Eosinophils stain red-orange while basophils stain blue. Lymphocytes do not show peroxidase activity and so do not stain in this protocol.

**Myeloperoxidase Stain Procedure:**

a) The contents of 1 Diaminobenzidine vial, Catalog No. 391-1, were first dissolved in 50 ml TRIZMA® Working Solution.

b) A series of staining jars containing Gluteraldehyde-Acetone Fixative Solution, Diaminobenzidine Solution (prepared in step a), Copper Nitrate Solution, Hematoxylin Solution (Gill No 3, Catalog No. GHS-3), Scott's Tap Water Substitute,

Gill's Modified EA (Catalog No. 391-5), two dishes of 95% ethanol, two dishes of absolute ethanol and three dishes of xylene were set up.

c) Immediately prior to fixing slides, 0.5 ml of 1% hydrogen peroxide was added to the Diaminobenzidine solution prepared in step a and mixed thoroughly.

d) The fresh frozen and cryosectioned slides were fixed in Gluteraldehyde-Acetone Fixative Solution for 1 minute at 4°C.

e) Following fixation, the slides were rinsed in deionized water for 30 seconds.

f) The slides were incubated in Diaminobenzidine/Peroxide solution for 45 seconds.

g) The slides were again rinsed in deionized water for 30 seconds.

h) After the second rinse, the slides were incubated in a staining jar containing Copper Nitrate Solution for 2 minutes with gentle agitation.

i) The samples were rinsed in deionized water for 30 seconds after the Copper Nitrate Solution incubation.

j) The sections were immersed in Hematoxylin Solution, Gill No. 3, Catalog No. GHS-3, for 8 seconds (4 dips).

k) Following Hematoxylin immersion, the slides were washed with 2 changes of deionized water for 5 seconds each with agitation.

l) The slides were immersed in Scott's Tap Water Substitute Working Solution for 12 seconds (6 dips).

m) The tissues were washed in 2 changes of deionized water for 5 seconds.

n) After the washing step, tissues were incubated in Gill Modified EA, Catalog No. 391-5, for 1 minute.

o) The slides were dehydrated by rinsing in 2 changes of 95% ethanol for 3 seconds each, followed by 2 changes of absolute ethanol for 3 seconds each.

p) Finally the slides were cleared by washing them in 3 changes of xylene for 3 seconds each.

q) After the clearing step, the slides were mounted in permanent mounting media and examined microscopically.

**F) GOMORI'S ONE-STEP TRICHROME STAIN (*Gomori, Sheehan and Hrapchak*):**

The purpose of the trichrome stain was to identify an increase in collagenous connective tissue fibers. In the one-step trichrome procedure, a plasma stain (chromotrope 2R) and a connective tissue fiber stain (fast green FCF, light green, or aniline blue) are combined in a solution of phosphotungstic acid, to which glacial acetic acid has been added. Phosphotungstic acid is responsible for the red staining of muscle and cytoplasm, whereas the tungstate ion is specifically taken up by collagen, and the connective tissue fiber stain is subsequently bound to this complex, causing green or blue color of collagen, depending on the counterstain used.

**Gomori's One-Step Trichrome Stain Procedure:**

a) Sections were deparaffinized and hydrated as previously stated, and then rinsed well in distilled water.

b) The slides were incubated in Bouin's solution for 1 hour at 56°C.

c) They were removed from the oven, and allowed to cool, then washed in running water until the yellow color disappeared.

d) Following the rinsing in distilled water, the sections were stained in Weigert's hematoxylin for 10 minutes.

e) They were washed in running water for 10 minutes, and stained in Gomori's trichrome stain for 15-20 minutes.

f) After Gomori's trichrome stain, they were differentiated in 0.5% acetic acid for 2 minutes.

g) Sections were dehydrated, cleared, and mounted with synthetic resin at the end of the procedure.

**G) OIL RED O METHOD FOR NEUTRAL FATS:**

The purpose of the Oil Red O Method was to show lipid deposition in the liver sections. The effects of sepsis/SIRS on lipid metabolism of the liver, as well as degrading material containing fat, such as cell membranes, may be demonstrated with fat stains. Since the staining with oil-soluble dyes requires greater solubility of the dye in lipoid substances than in the usual hydroalcoholic dye solvents, the dye used was more soluble in tissue lipid than in the solvent in which it was dissolved, and was not water-soluble.

**Oil Red O Stain Procedure:**

a) Frozen liver tissues were cryosectined, fixed in 40% formaldehyde for 1 minute, and washed in tap water.

b) Sections then were stained in oil red O for 10 minutes.

c) Following the rinsing of the slides, they were stained in Harris' hematoxylin containing acetic acid (4ml glacial acetic acid/96 ml hematoxylin) for 1 minute.

d) The sections were washed in tap water, and then dipped in ammonia water.

e) They were then washed in tap water for the last time, and mounted with an aqueous mounting medium, and the edges of the coverslips were sealed.

## H) *IN SITU* HYBRIDIZATION:

*In situ* hybridization is a powerful and sensitive tool for the analysis and localization of specific mRNA expression within cells or tissues. It is a relatively simple and fast procedure that does not require mRNA extraction or electrophoresis, unlike Northern blot hybridization or nuclease protection assays, neither of which provides information on the location or the specific cell type that expresses the genes of interest. A limitation of Northern and RNase protection assays is that, messages that are expressed in a limited number of cells will be diluted during the RNA extraction.

*In situ* hybridization was performed using Ambion's mRNA *locator* ™-Hybridization Kit (*In Situ* Hybridization Kit-Catalog # 1800) and mRNA *locator*™-Biotin Detection Kit for *In Situ* Hybridization (Catalog # 1805). Hybridization was performed as described by the manufacturer. Briefly, following tissue fixation in 4%

paraformaldehyde, the tissues were dehydrated and embedded in paraffin. Five-micron sections were cut and adhered to Sigma Diagnostics' Silane-Prep™ Microscope Slides. Sections were deparaffinized by several washes in xylenes. After deparaffinizing, tissue sections were rehydrated through a graded series of alcohols and finally air-dried. Hybridizations were performed over night at 37°C. Signals were detected using a streptavidine-alkaline phosphatase conjugate and NBT/BCIP solution for color development.

In each *in situ* hybridization experiment, a positive and negative control slide was included. The positive control was supplied in the kit, and was used to ensure the reagents were working. Negative controls were sections, either minus the probe or pretreated with RNase A. The minus probe slide was done to control for endogenous biotin or alkaline phosphatase activity, which might skew the results. The RNase treated slides controlled for non-specific hybridization of the oligomer.

**In Situ Hybridization Protocol:**

**a) Deparaffinization, Rehydration, and Equilibration:**

Tissue sections were processes as shown in Table 4. Briefly, sections were deparaffinized, rehydrated through a graded series of alcohols and finally in DEPC-treated nuclease-free water. The samples were then equilibrated in 1X Tris Buffer, which is the reaction buffer for the subsequent proteinase K digestion step. This step allows the *in situ* hybridization (ISH) reagents to infiltrate the tissue section, giving the probe access to the target RNA.

**Table 4. The solutions used in deparaffinization, rehydration and equilibration.**

| Dish # | Solution | Incubation time |
|---|---|---|
| 1, 2, 3 | xylene | 5 minutes each |
| 4, 5, 6 | 100% alcohol | 2 minutes each |
| 7 | 90% alcohol | 2 minutes |
| 8 | 70% alcohol | 2 minutes |
| 9 | 50% alcohol | 2 minutes |
| 10 | Nuclease-free water | 2 minutes |
| 11 | 1X Tris Buffer | 2 minutes |

**b) Proteinase K Digestion:**

Proteinase K enzyme digestion step is crucial for the success of ISH. The fixing solution, paraformaldehyde, cross-links amino groups on the side chains of amino acids and the cross-linking of the proteins preserves the histological structure of the tissue, but also makes the nucleic acids in the samples inaccessible for hybridization. Proteinase K digestion first breaks the cross-links that stabilize the proteins, and then it removes some of the proteins from the cellular backbone to allow the probe to hybridize with the nucleic acids. This is a critical step, because if the proteinase K digestion is not enough, the nucleic acids will not be accessible for the hybridization, if the samples are over digested with proteinase K, then the tissue morphology will be poor or completely destroyed, making the localization of hybridization signal impossible.

To obtain a good signal-to-noise ratio as well as good preservation of tissue morphology, the digestion step has to be optimized based on the fixative being used, the fixation temperature and period, and the type of the tissue itself. The proteinase K digestion step was optimized by using serial concentrations and digestion periods on the samples. The best results were obtained with a 40 μg/ml concentration of

proteinase K digestion for 30 minutes at 37°C for liver and abscess wall samples, which were fixed in 4% paraformaldehyde for 4 hours at room temperature.

50 μl of the above proteinase K concentration was used per slide and the samples were carefully covered with glass coverslips and incubated in a 37°C incubator for 30 minutes in a humid chamber. Following the incubation, the coverslips were carefully removed and the samples were washed 3 times in 1X Tris Buffer, for 4 minutes each.

**c) RNase Treatment for negative control slides:**

After the third wash with 1X Tris Buffer, negative control slides were treated with 5 Units/μl of RNase for 60 minutes in a 37°C incubator. 50 μl of above RNase concentration was used per negative control slide. Following the RNase treatment, tissues were washed in 1X Tris Buffer 3 times, for 5 minutes each.

**d) Hybridization:**

Synthetic anti-sense oligonucleotide probes for both IL-6 and fibrinogen were used. Each slide, except for the negative minus probe control slides, was hybridized with the same concentration of oligo-nucleotide probe for the same duration of time at the same temperature in a humid chamber.

The oligonucleotide probes were specific for rat IL-6 and fibrinogen, respectively, and were made in the Molecular Biology Department, UMDNJ, and biotinylated at their $5^1$-primer ends.

Optimization of probe concentration, duration of hybridization and the hybridization temperature are crucial steps for the success of ISH. Low probe concentration, less duration of hybridization and high hybridization temperature may cause weak or no signal, while higher probe concentrations, increased period of hybridization time and low hybridization temperatures may cause strong signal but may also cause high and non-specific background.

Hybridization was optimized by using serial probe dilutions, hybridizing the samples in different temperatures, and allowing the hybridization occur in different duration of times, changing from 4 hours to overnight. A good signal to noise ratio for liver and abscess wall was obtained at a concentration of 40 ng/μl of probe, for overnight hybridization at 37°C in a humid chamber.

The probes were diluted to final concentration in *In Situ* Hybridization Buffer provided by the kit. 50μl of 40 ng/μl probe concentration was used per slide (2 μg/slide). The samples were covered with coverslips after applying the probe and incubated at 65°C for 5 minutes in a humid chamber. This short duration of high temperature incubation was necessary to denature the RNA in the tissue specimens without denaturing genomic DNA. Since single stranded oligonucleotide probes were used, they did not need to be denatured prior to hybridization. After the incubation at 65°C for 5 minutes, the slides were placed in a 37°C incubator in a humid chamber for overnight hybridization.

Following hybridization, the samples were washed in pre-warmed (50°C) 2X and 1X In Situ Wash Solutions for 4 minutes each, and the tissues were ready for biotin detection and color development.

**e) Incubation of Slides with Strepavidin-Alkaline Phosphatase Conjugate:**

Non-isotopic detection of hybridized biotinylated probe is faster, safer and a more sensitive approach than traditionally used radioactive detection. Detection of the biotinylated probes that have been hybridized to RNA in tissue sections occurs by binding of streptavidine-alkaline phosphatase conjugate to the biotinylated probe.

Strepavidine-alkaline phosphatase (AP) conjugate, which was provided by Ambion's biotin detection kit (Catalog # 1805), was first diluted in 1X Tris Buffer (1:3000 dilution of the stock). Right before adding the Strep-AP to the samples, the slides were incubated at 70°C for 5 minutes in a humid chamber in order to inhibit the endogenous alkaline phosphatase activity. Following the 5-minute incubation, 50µl of diluted Strep-AP conjugate was applied to each slide and the samples incubated at 37°C incubator for 30 minutes in a humid chamber. After the incubation, the slides were washed in 1X Tris Buffer for 2 times, 4 minutes each.

**f) Detection of Hybridized Signals using NBT/BCIP:**

NBT/BCIP are used as substrates for Strep-AP, and the interaction of Strep-AP with NBT/BCIP will generate a blue/purple colored signal within cells or tissues.

After the Strep-AP incubation and washes, 50µl of NBT/BCIP solution was applied to each slide. In this step, 200 µg/ml concentration of levamisole, a known alkaline phosphatase inhibitor, was added to 50µl of NBT/BCIP solution in order to block the endogenous alkaline phosphatase activity.

After adding the NBT/BCIP solution to the slides, they were incubated at 37°C for about 1.5-2 hours in a humid chamber to allow the color development and once the desired color intensity was achieved, the color development was ended by rinsing the slides in DEPC-treated nuclease free water 2 times for 4 minutes each.

**g) Dehydration, Clearing, and Mounting:**

After termination of the color development, the samples were dehydrated in a series of increasing concentrations of alcohol and ending with xylene wash, as outlined in Table 5.

**Table 5. The solutions used in dehydration and clearing.**

| Dish # | Solution | Incubation time |
|---|---|---|
| 1 | 50% alcohol | 2 minutes |
| 2 | 70% alcohol | 2 minutes |
| 3 | 90% alcohol | 2 minutes |
| 4, 5, 6 | 100% alcohol | 2 minutes each |
| 7, 8 | Xylene | 2 minutes each |

Following the dehydration steps, one to two drops of xylene based permanent mounting media was applied to the slide and carefully covered with glass coverslips and observed under the light microscope.

## I) ENZYME LINKED-IMMUNO-SORBENT ASSAY (ELISA):

The BioSource Cytoscreen™ Rat Interleukin-6 (raIL-6), Rat Tumor Necrosis Factor-Alpha (raTNF-α), and Rat Interleukin-1 Beta (raIL-1β) Kits were used for in vitro quantitative determination of raIL-6, raTNF-α, and raIL-1β, in rat serum.

The BioSource Cytoscreen™ raIL-6, raTNF-α, and raIL-1β kits are solid phase sandwich Enzyme Linked-Immuno-Sorbent Assay (ELISA). An antibody specific for the cytokine of interest has been coated onto the wells of the microtiter strips provided by the kit. Samples, standards of known concentration, and control specimens are pipetted into these wells.

During the first incubation, the cytokine antigens, which are found in samples or in standards of known cytokine content, bind to the antibody, which is immobilized the wells of the microtiter strips. After washing of the unbound antigens, a biotinylated antibody specific for the interested cytokine is added. During this second incubation, the biotinylated second antibody binds to the antigen, which has been immobilized during the first incubation.

After removal of excess second antibody, Streptavidine-Peroxidase enzyme is added. This enzyme binds to the biotinylated second antibody and completes the four-member sandwich. After the incubation of this four-member sandwich, all unbound enzyme is removed by washing, and finally a substrate solution for Streptavidine-Peroxidase enzyme is added, and the reaction between this enzyme and the substrate produces color. The intensity of this colored product is directly proportional to the concentration of the interested cytokine present in the original specimen and by

reading the microtiter plate in a microplate reader will quantify the specific cytokine concentration found in the serum of the subject.

**Assay Method: Procedure and Calculations:**

All twelve 8-well strips were used for each kit because of the high number of samples to be analyzed. All samples, standards, and controls were run in duplicate.

Two wells were reserved for chromogen blank and left empty. 100 μl of the Standard Diluent Buffer was added to zero wells for raIL-6 and raIL-1β kits while only 50 μl of the Standard Diluent Buffer was used for raTNF-α kit.

100 μl of standards were added to the designated wells for the standard curves for raIL-6 and raIL-1β kits and 50 μl of standards were added for raTNF-α kit. 50 μl of Standard Diluent Buffer along with 50 μl of sample was added to each well and tapped gently on the side of the plates for mixing in raIL-6 and raIL-1β kits. In raTNF-α kit, only 50 μl of sample was used without adding any Standard Dilution Buffer.

In raIL-6 and raIL-1β kits, plates were covered for incubation after adding the samples, but in raTNF-α kit, 50 μl of biotinylated anti-TNF-α (Biotin Conjugate) solution was pipetted into each well except chromogen blanks before the incubation step and was covered afterwards for incubation. Incubation was achieved at 37°C for 2 hours for raIL-6 kit, while raTNF-α kit was incubated at room temperature for 1 hour and raIL-1β kit was also incubated at room temperature but for 1 hour and 30 minutes.

Following the first incubations, all the solutions were aspirated from the wells and all wells were washed 4 times with diluted wash solution of all three kits.

After the washing step, 100 μl of biotinylated anti IL-6 (Biotin Conjugate) solution and 100 μl of biotinylated anti-IL-1β solution was added to each well except the chromogen blanks, in raIL-6 kit, and raIL-1β kit, respectively, and the solutions were mixed by tapping the sides of the plates gently. The plates of these two kits were then covered again and incubated at room temperature for 1 hour.

In raTNF-α kit, following the first wash, 100 μl of Streptavidine-HRP Working Solutions were added to each well except the chromogen blanks before the second incubation. Then the raTNF-α plate was also covered and incubated for 45 minutes at room temperature. After the second incubations, all three plates were aspirated and washed for 4 times each.

Following the second washings in raIL-6 and raIL-1β kits, 100 μl of Streptavidine-HRP Working Solutions were added to each well except for the chromogen blanks in both kits. Then both plates were covered again and incubated at room temperature for 30 minutes.

In raTNF-α kit, 100 μl of Stabilized Chromogen was pipetted in each well before the 3$^{rd}$ incubation. After adding 100 μl of Stabilized Chromogen to the wells, raTNF-α kit was incubated for 30 minutes at room temperature and in the dark without being covered.

After the 3$^{rd}$ incubation of raIL-6 and raIL-1β kits, 100 μl of Stabilized Chromogen was also added to the wells and both kits were incubated for 30 minutes

at room temperature and in the dark without covering. Immediately after pipetting Stabilized Chromogen to the well, the liquid in the wells turned in blue.

Following the adding of the Stabilized Chromogen step, 100 µl of Stop Solution was pipetted into the wells of all three kits, and the plates were tapped gently for mixing. In this step, the solutions in the wells turned yellow from blue color.

After completing the blocking of enzyme reaction by adding Stop Solution, the absorbance of each well of all plates was read at 450 nm having blanked the plate reader against a chromogen blank composed of 100 µl of each Stabilized Chromogen and Stop Solution.

All plates were read right after completing the ELISA protocol in a pre-programmed microplate reader. The absorbance of standards was plotted against the standard concentrations using curve fitting software and the concentrations of the unknown samples were automatically calculated using the standard curve fit by software and the results were analyzed by JMP statistical software.

**J) RNA EXTRACTION AND DETECTION:**

RNA was isolated from frozen tissues by the modified acid/phenol. Briefly, tissues were placed in 1 ml of a denaturing solution containing, 4M guanidium, 25 mM sodium acetate (pH4), 0.1 M 2-mercaptoethanol, 0.5% sarkosyl, and homogenized using a Labortechnik Ultra-Turrax T8 IKA homogenizer.

After homogenization, 100µl of 2 M sodium acetate (pH 4) was added to each sample and mixed thoroughly. An equal volume of water-saturated phenol was added and mixed, and 200µl of 49:1 chloroform/isoamyl alcohol was added. The mixture

was incubated on ice for 15 minutes. The homogenates were then centrifuged in a Sorvall RC-5B Refrigerated Superspeed Centrifuge for 20 minutes at 9000 rpm and 4°C. After the centrifugation, the upper aqueous phase, which contained RNA from the tissues, was transferred into a fresh tube. An equal volume of 100% isopropanol (1 volume) was added to each tube, and the solution was placed at -20°C to precipitate the RNA. RNA's were pelleted by centrifugation for 10 minutes at 9000 rpm and 4°C, and the supernatant disregarded. The RNA pellet was rinsed with 70% EtOH, and dissolved in DEPC treated water.

RNA concentrations were determined spectrophotometrically as follows: 1 μl of the stock RNA suspension was added to 99 μl of DEPC treated water. This 1:100 dilution of RNA was measured on a Beckman DU Series 60 Spectrophotometer using a Nucleic acid Soft-Pas Module. Following the measurement of the concentrations, samples were uniformly loaded and the integrity verified by using ethidium bromide staining. Briefly, a mini agarose gel was casted by dissolving 0.25 g of agarose in 25 ml of 1X TAE. The dissolved agarose was poured into a 6X10 cm tray and allowed to cool for 15-20 minutes at room temperature. RNA's were diluted to a concentration of 1 μg/μl and, 1 μg loaded.

After loading the gel, 25 μl of ethidium bromide was added into the cathodic reservoir of the electrophoretic chamber, and the gel was run 30 minutes at 50 volts constant voltage. At the end of 30 minutes, the mini gel was observed under UV light to determine if the two ribosomal RNA bands (18S and 28S) were apparent as sharp bands.

## K) NORTHERN HYBRIDIZATION OF RNA FRACTIONED BY AGAROSE-FORMALDEHYDE GEL ELECTROPHORESIS:

**a) Sample Preparation:** Total cellular RNA (10 μg) was incubated with 25 μl of RNA loading buffer (0.75 ml deionized formamide, 0.15 ml 10X MOPS, 0.24 ml formaldehyde, 0.1 ml deionized RNase-free water, 0.1 ml glycerol, 0.08 ml 10% bromophenol blue) at 65°C for 15 minutes. Immediately after heating, the samples were put on ice and 1μl of ethidium bromide was added to each sample, and centrifuged.

**b) Gel Preparation and Electrophoresis:** Agarose (1g) was mixed with 10 ml 10X MOPS and 72 ml DEPC treated autoclaved water in an RNase-free flask. The agarose was then dissolved by boiling the suspension in a microwave. The dissolved agarose was allowed to cool to 50°C, to which was added 18 ml of 37% formaldehyde. The solution was gently mixed and then poured into an 11X14 cm gel casting rack. The gel was allowed to solidify for 30 minutes before using. The RNA's were fractionated by electrophoresis in 1X MOPS buffer for 2 hours at 100 volts constant voltage at room temperature.

**c) Visualization and Photography of RNA:** Following electrophoresis, the gel was directly visualized and photographed on a short wave transilluminator (302 nm or 254 nm) using a yellow filter and Polaroid type 665 PN film. The exposure time was 1 s at fstop8.2.

**d) RNA Transfer:** After electrophoresis, the gel was washed with distilled water 3 times for 5 minutes each wash at room temperature to eliminate excess formaldehyde. Transfer was done by capillary action, using a double layer of Whatmann 3 MM paper as a wick. The transfer solution was 10X SSC. The gel was placed on top the Whatmann paper, and then a prewet membrane (Magna Graph Nylon membrane) was placed on the gel. Two pieces of Whatmann paper were then layered over the membrane, followed by a stack of absorbent paper towels. Transfers were allowed to proceed over night at room temperature. After the transfer, the nylon membrane was observed under UV light, and the position of the ribosomal 18 and 28S bands marked. The RNA was fixed to the membrane by baking for 30 minutes at 80°C in a vacuum oven. The membrane was then washed for 1 hour at 65°C in 0.1X SSC/0.5% SDS. After the 1 hour wash, the solution was decanted, and the membrane stored at 4°C, until ready to hybridize.

**e) Oligonucleotide Primers and Kinase End Labeling:** The following oligonucleotide probes were used in this study; rat alpha fibrinogen hybridization oligonucleotide (5'CCCTAGCTCCCATGTACCTG3'); rat IL-6 anti-sense (5'GACTGATGTTGTTGACAGCCACTGC3'), rat IL-6 sense (5'GCAGTGGCTGTCAACAACATCAGTC3'), and rat ribosomal 18S (5'GCCGTGCGTACTTAGAC3'). Primers were selected using the Primer 3 software (Rosen and Skaletsky, 1998). All oligos were synthesized by the New Jersey Medical School Molecular Resource Facility.

Oligonucleotides were end labeled using T4 polynucleotide kinase and γ-[$^{32}$P] ATP. Briefly, 100 pmol of oligonucleotide was added to 5X forward reaction buffer, γ-[$^{32}$P] ATP, and 10 U of T4 polynucleotide kinase. The reaction was incubated at 37°C for 30 minutes. The labeling reaction was terminated by the addition of EDTA. The labeled oligonucleotide probe was purified using a spin column of sephadex G-50. One microliter of the probe was counted in a scintillation counter to determine the number of counts per microliter.

**f) Pre-hybridization, Hybridization:** Membranes were pre-hybridized in 20 ml of hybridization solution of 6X NET (20X NET is 3M NaCl, 20 mM EDTA, and 0.3M Tris-HCl, pH 8.0), 5X Denhardt's, 0.1% SDS, and 250 μg/ml heat-denaturated yeast t-RNA. The oligonucleotide probe was added to the membrane hybridized over night at 50°C.

Membranes were washed four times, each for 10 minutes at room temperature in 200 ml of 6X NET, 0.5% SDS. The final wash was conducted for 10 minutes at the hybridization temperature.

Membranes were wrapped in saran wrap and PhosphoImaged over night. Images were analyzed using PhosphorImager™ SI and ImageQuant™ Software (Molecular Dynamics, Sunnyvale, Ca). Membranes were hybridized to the rat 18S ribosomal oligomer, which was used to normalize signals.

# EXPERIMENTAL RESULTS

## A) THE EFFECTS OF INTRA-ABDOMINAL SEPTIC AND STERILE ABSCESSES ON THE MORTALITY AND THE MORBIDITY RATES:

Animals were divided into three groups, control (n=22), sterile (n=27), and septic (n=98). No mortality was observed in control and sterile groups during the first 3 day prior to sacrifice in all 7 experiments, whereas in the septic group, a mortality rate ranging from 0-100%, depending on the amount of bacteria inoculated in the fecal pellets, was observed. All the septic group mortalities were observed during the first 48 hours after the pellet implantation, and no further deaths were observed in the following 24-hour period. All surviving animals in all groups were sacrificed under anesthesia at 72-hour post-implantation.

Septic pellets were inoculated with$10^9$ CFU/pellet of B. fragilis, which had no effect on mortality rate as previously reported by Vary et al (60), whereas the amount of E. coli inoculated was responsible for the mortality rate seen in our experiments (Table 6 and Figure 5).

The mortality was directly associated with the number of E. coli inoculated, and only those experiments, which resulted in a 60-75% mortality were included in statistical analyses in order to achieve equality of variances.

**Table 6. Bacteria counts and mortality rates by experiments.** Number of septic animals, number of septic deaths, mortality rate, initial pellet E. coli and B. fragilis counts are shown for each batch of animals.

| Exp. # | # of septic animals | # of deaths | Mortality Rate | E. coli counts (CFU/pellet) | B. fragilis counts (CFU/pellet) |
|---|---|---|---|---|---|
| 1 | 12 | 8 | 66.6 | 145 | $10^{-9}$ |
| 2 | 23 | 10 | 43.5 | 85 | $10^{-9}$ |
| 3 | 19 | 14 | 73.6 | 140 | $10^{-9}$ |
| 4 | 12 | 12 | 100 | 221 | $10^{-9}$ |
| 5 | 11 | 0 | 0 | 0 | $10^{-9}$ |
| 6 | 11 | 2 | 18.2 | 8 | $10^{-9}$ |
| 7 | 10 | 7 | 70 | 100 | $10^{-9}$ |

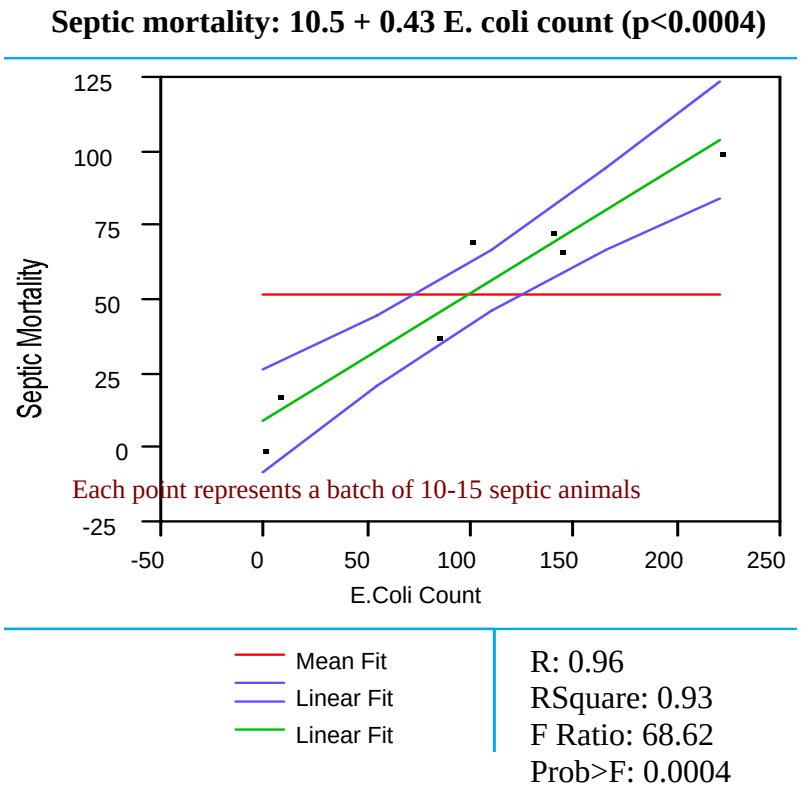


**Figure 5. Linear regression analysis of septic mortality rate by E. coli counts.** Red line: mean fit, green line: linear fit, blue lines: 95% confidence curves of the linear fit.

Figure 5 shows a linear regression analysis of the septic mortality rate as a function of the number of E. coli inoculated into the septic pellets. The F ratio of the linear regression analysis has a p value of 0.0004, showing a statistically significant direct correlation between mortality rate and E. coli pellet counts (Blue colored 95% confidence curves of the linear fit does not include the red colored mean fit, confirming the significant correlation).

The coefficient of determination (Rsquare) is 0.93, indicating that 93% of the data can be explained by the linear regression model, while the coefficient of correlation (R) of 0.96 suggests a close to perfect direct correlation between the two variables. The intercept term has an estimated value of 10.5, and a t ratio, whose p value is 0.16, indicates that the linear fit passes through the intercept.

The morbidity of the animals was evaluated by using parameters, such as weight changes, amount of chow and water intake, and general appearance. Following pellet implantation, both sterile and septic animals appeared sick during the first 48-hour period. They had diarrhea, crusted eyes, lack of mobility, and lower amounts of chow and water intake, when compared to the control group.

No statistically significant difference in the weights of sterile and septic groups was observed compared to controls in pre-operative days 2 and 1 (p values were 0.57 and 0.56, respectively). One day after the implantation, both sterile and septic animals had statistically significant amount of weight loss when compared to their pre-operative levels (p: 0.0002 and p: 0.0001, respectively). Septic animals continued to loose weight until 48 hours after pellet implantation, which was statistically significant, when compared to their 24-hour post-operative period (p:

0.006), whereas sterile animals were observed to gain weight by 48-hour post-operative period, however this gain was not statistically significant (p: 0.10). Starting from 48-hour post-operative period until 72-hour period, septic animals started to gain weight, while sterile animals continued to gain weight, and the weight gain of both groups was statistically significant during this time period (p: 0.0004 and p<0.0001, respectively), when compared to their weights on post-operative day 2. Control animals gained statistically significant amount of weight each day compared to previous day, starting from the pre-operative day 2 until the sacrifice day (72 hours after anesthesia treatment) (Figure 6).

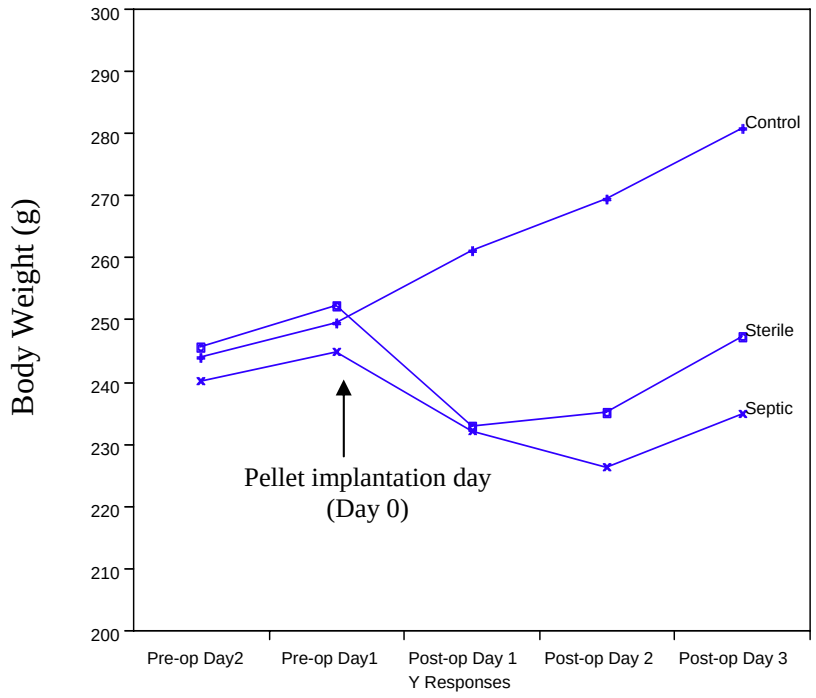


**Figure 6. Weight changes among the experimental groups from pre-operative day 2 to post-operative day 3.**

There was no significant difference among the weights of all three groups before the implantation surgery (in pre-operative days 2 and 1). After the pellet implantation surgery, the weights of the control group were statistically higher, compared to both sterile and septic groups in all time periods, while no significant difference between the weights of sterile and septic groups was observed (Table 7).

**Table 7. Weight change of control, sterile and septic animals during experiment time frame.** Standard Errors of the Means (SEM) are also shown.

| Groups | Pre-op day 2 | Pre-op day 1 | Post-op day 1 | Post-op day 2 | Post-op day 3 |
|---|---|---|---|---|---|
| Control | 244 ± 3 g | 250 ± 3 g | 261 ± 4 g | 269 ± 4 g | 281 ± 6 g |
| Sterile | 246 ± 5 g | 252 ± 7 g | 233 ± 5 * g | 235 ± 5 * g | 248 ± 6 * g |
| Septic | 240 ± 4 g | 245 ± 4 g | 232 ± 4 * g | 227 ± 4 * g | 235 ± 5 * g |

* Significantly different from control group ($p<0.0001$)

## B) THE INTRA-ABDOMINAL SEPTIC AND STERILE ABSCESSES: THE ANATOMY, HISTOLOGY AND THE PATHOPHYSIOLOGY OF ABSCESS DEVELOPMENT:

### 1) The Gross Anatomy of the Intra-abdominal Abscess Development:

Figure 7 shows the intra-abdominal anatomy of the rat and the abscess development three days after fecal-pellet implantation under sterile and septic conditions. The small intestine, colon, rectum and spleen are marked for anatomical orientation, and the abscess wall is indicated by arrows in both the sterile and septic groups.

Figure 7-A shows the intra-abdominal anatomy of a control rat, which has neither anatomical nor clinical pathology. A midline incision was performed to show the anatomy, and the visceral organs are marked. The liver occupies more than 1/3 of the intra-peritoneal cavity, and is located on the epigastrium extending to both upper quadrants. Most of the right lower quadrant as well as the right hypocondrium is occupied by small intestine, whereas colon, especially the sigmoid, is located on the left side.

Figure 7-B illustrates a gross intra-abdominal sterile abscess on post-implantation day 3. The abscess is located on the right side, since this is the side where the initial fecal-pellet was implanted. The sterile abscess wall is pointed out with arrows in the picture. The abscess is almost completely walled off with clear color fragile fibrinous tissue. The abscess is so fragile in the sterile group that the

wall, which is attached to the parietal peritoneum on the anterior side is split off when opening the abdomen, and stayed attached to the peritoneum.

Figure 7-C is the picture of the macroscopic intra-abdominal septic abscess on post-implantation day 3. The abscess is again located on the right side as per animal protocol. The septic abscess wall is marked with arrows. The abscess is completely walled off, and has a much thicker white color fibrinous tissue when compared to the sterile abscess wall. The thick fibrinous tissue almost covers all the fecal-pellet, except for a couple of small spots, which stayed attached to parietal peritoneum when opening the abdominal cavity. Intra-abdominal adhesions are also well seen around the septic abscess formation, attaching the small bowel together as well as to the localized inflammation.

**2) Hematoxylin & Eosin Stain of the Intra-abdominal Abscess Wall:**

Figure 8 shows the H&E stain of the sterile and septic abscess walls at 10X, 20X and 40X magnifications, indicating the basic morphology and inflammatory cell infiltration of the abscess wall. Figure 8 A-C are the histological sections of the sterile abscess wall, whereas Figure 8 D-F are of the septic one. Abscess cavity as well as serosal layer of the abscess wall, are marked in the sections.

Both sterile and septic abscess walls have different histological layers along the abscess wall. The first layer of the abscess wall (inner layer), which surrounds the necrotic center of the abscess cavity (AC), is composed of increased amounts of inflammatory cells. The second layer also has inflammatory cell infiltration, but the numbers are much less compared to inner layer. The second layer (intermediate layer)

is mainly composed of extracellular matrix, which gives strength as well as elasticity to the abscess wall. The third layer of the abscess wall (outer layer) is the serosal portion of the wall (S), which is basically the extension of the extracellular matrix that separates the abscess wall from the surrounding environment. There does not seem to be any significant difference between the sterile and septic abscess walls in terms of inflammatory cell infiltration, as shown by H&E stain.

**3) Detection of Interleukin-6 (IL-6) Gene Expression in the Intra-abdominal Abscess Wall:**

The presence of IL-6 gene expression in the sterile and septic abscess walls was confirmed by polymerase chain reaction (PCR) technique, and the specific locations of IL-6 producing cells in the sterile and septic abscess walls were detected by *in situ* hybridization technique. Figure 9 shows the gene expression of IL-6, detected by *in situ* hybridization, in the sterile (A-C) and the septic (D-F) abscess walls at 10X, 20X and 40X magnifications. Necrotic center of abscess cavity and the outside serosal layer are labeled, and IL-6 positive cells (purple) are indicated by arrows.

Both sterile and septic abscess walls have IL-6 positive cells, indicating the stimulated gene expression of IL-6 in response to both sterile and septic stimuli. There is no significant difference in terms of the quantity of the IL-6 expressing cells, between sterile and septic abscess walls, but there is an obvious difference in the location and the morphology of these cells between the two groups.

In the sterile abscess wall, the IL-6 expressing cells are uniquely located at the intermediate layer, where the extracellular matrix is prominent (Figure 9 A-C), whereas in the septic abscess wall, the IL-6 positive cells are mostly concentrated in the inner layer, where the inflammatory cell infiltration is dominant (Figure 9 D-F).

There is also a marked difference in the morphology of IL-6 expressing cells between the sterile abscess wall (Figure A-C), in which the cells are fusiform, and the septic abscess wall (Figure D-F), in which the cells are round.

**4) Detection of Fibrinogen Gene Expression in the Intra-abdominal Abscess Wall:**

Figure 10 shows the fibrinogen gene expression in the sterile (A-C) and the septic (D-F) abscess walls, detected by *in situ* hybridization. The images are compared at 10X, 20X and 40X magnifications. The abscess cavity and serosal layer are labeled for orientation, and the fibrinogen positive cells (purple) are marked with arrows.

There is no significant difference in terms of the quantity of fibrinogen positive cells between the two groups, even if the septic abscess wall seem to have a great amount of positive cells than the sterile abscess one, but the location and the morphology of the fibrinogen expressing cells show a major difference between the two groups. The fibrinogen expressing cells are located at the intermediate layer of the sterile abscess wall (Figure 10 A-C), where the extracellular matrix and fibrous tissue are prominent, whereas the fibrinogen positive cells are concentrated in the inner part of the septic abscess wall (Figure 10 D-F), where the inflammatory cell infiltration is markedly dominant. The location of fibrinogen producing cells showed a closed proximity to the IL-6 positive cells in both sterile and septic abscess walls.

The morphology of the fibrinogen expressing cells also show a difference, which is consistent with the location of the particular cell. The fibrinogen positive cells are fusiform shape in the sterile abscess wall, since they are located at the connective tissue layer of the wall. On the other hand, the fibrinogen expressing cells are mostly round in shape in the septic one, as they are located at the inner layer.

**5) Gomori's One-Step Trichrome Stain of the Intra-abdominal Abscess Wall:**

Figure 11 shows the trichrome stain of the abscess walls of the sterile (A-C), and the septic (D-F) groups at 10X, 20X and 40X magnifications, indicating the deposition of the collagenous connective tissue fibers in the abscess wall. Abscess cavity and serosal layer are marked, and collagen fibers are indicated by arrows.

The sterile and septic abscess walls show a significant difference in terms of collagen deposition, in which collagen is deposited in a scattered pattern in sterile abscess wall and does not take much space compared to septic abscess wall, in which collagen is deposited in a concentrated pattern, taking almost all of the space of the intermediate layer (extracellular matrix). The collagen in the septic abscess wall produces a thick layer starting from the intermediate layer and extending through the serosal layer, which is consistent with the gross picture of the septic abscess wall (Figure 7-C).

**C) THE EFFECTS OF INTRA-ABDOMINAL SEPTIC AND STERILE ABSCESSES ON THE PORTAL VEIN AND THE POST-HEPATIC INFERIOR VENA CAVA PLASMA PRO-INFLAMMATORY CYTOKINE (TNF-α, IL-1β, IL-6) LEVELS:**

**1) The Portal Vein and the Post-Hepatic Inferior Vena Cava Plasma Tumor Necrosis Factor-alpha (TNF-α) Levels:**

**a) Distributions of the Portal Vein Plasma TNF-α Raw and Transformed (TNF-$\alpha^{-3}$) Data:**

As illustrated in Figure 12, the portal vein TNF-α data was not normally distributed (The Shapiro-Wilk W test had a p value of less than 0.0001).

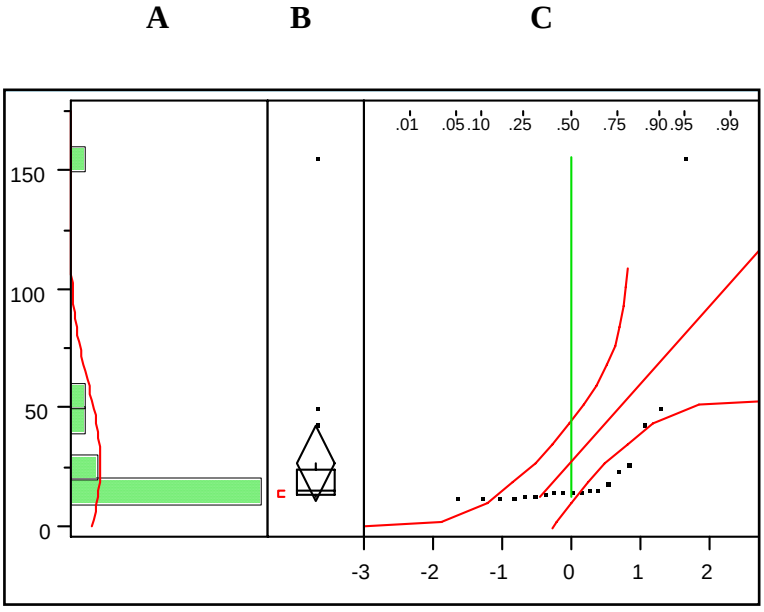


**Figure 12. Distribution of PV TNF-α Raw Data.** Histogram (A), Outlier Box Plot (B), and Normal Quantile Plot (C) of the distribution are shown.

All data was transformed for statistical analyses. Figure 13 shows the distribution of the transformed portal vein TNF-α data, in which (–3rd) power of portal vein TNF-α raw data (TNF-$\alpha^{-3}$) was used to support normal distribution. Shapiro-Wilk W Test of the transformed data had a p value of 0.15, which was greater than the 0.05 alpha value.

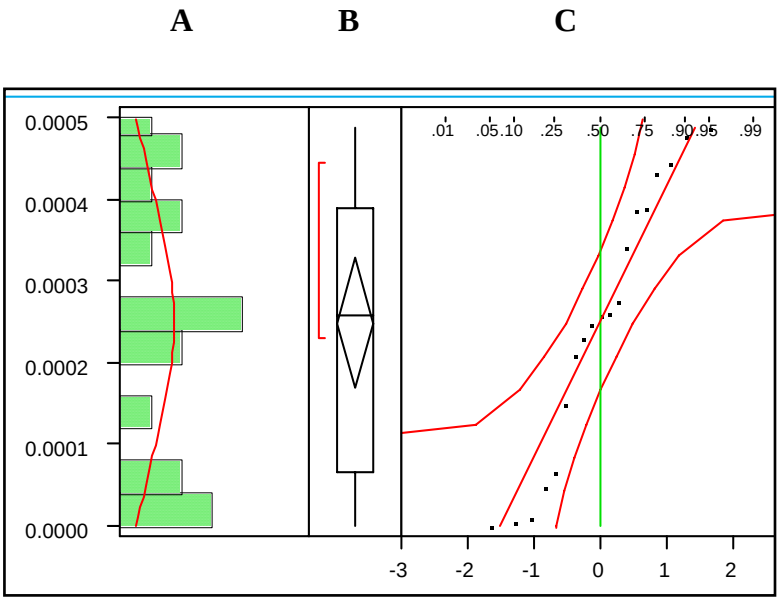


**Figure 13. Distribution of PV TNF-α Transformed (TNF-$\alpha^{-3}$) Data.** Histogram (A), Outlier Box Plot (B), and Normal Quantile Plot (C) of the distribution are shown.

Confirmation of the equality of variances of the transformed portal vein TNF-α data has been done by using O'Brien and Brown-Forsythe Tests of homogeneity, which had F ratios that had p values of 0.28 and 0.17 (>0.05), respectively, and was assumed that there were no statistically significant differences between the experimental subjects (rats), and the variances of the subjects were equal.

**b) Oneway Analysis of Variance (Oneway Anova) of the Transformed Portal Vein Plasma TNF-α Levels, and Comparisons of the Means of Control, Sterile, and Septic Groups by using Tukey's Honest Significant Difference Test (Tukey-Kramer HSD):**

There were a total of 19 portal vein TNF-α observations, and the coefficient of determination (RSquare) of the whole model was 34%, which indicated that only 34% of the data could be explained by the oneway anova model. The whole model, which was provided by fitting the response variables (portal vein TNF-α concentrations) by the predictor variables (experimental groups), had an F ratio, which had a p value of 0.04, indicated that, at least one of the experimental groups was statistically different from the others in terms of portal vein TNF-α concentrations, however the significance of this statistical difference was questionable, since the p value of the whole model (0.04) was close to the 0.05 alpha level, and that the power of the whole model was only 64%, which showed that the experiment did not have enough power to detect the differences in the portal vein plasma TNF-α levels among the control, sterile and the septic groups, since the acceptable levels of power begin at 70%.

When we compared the means of the portal vein TNF-α transformed levels of three experimental groups by using the Tukey's Honest Significant Difference test (Tukey-Kramer HSD), we found that only the mean of the sterile group was statistically different from the mean of the control group, and did not show a

statistically significant difference from the mean of septic group. No significant difference was found between the control and septic groups.

**c) Means and 95% Confidence Intervals of Portal Vein Plasma TNF-α Levels in Original Values:**

After analyzing the statistical differences among the experimental groups, the 95% confidence interval of the transformed data for each group was calculated by the addition and subtraction of each group's standard error of the mean to the mean of the same group. These 95% confidence interval values were converted back to the original values by retaking the –(1/3) power of the transformed values. Figure 14 and Table 8 show the means and 95% confidence intervals of the portal vein plasma TNF-α levels in original values.

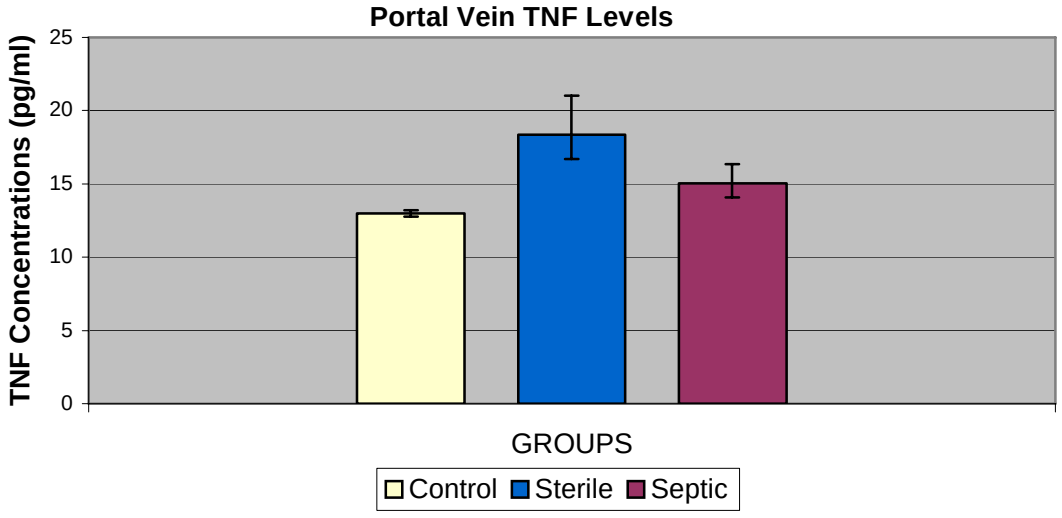


**Figure 14. The portal vein plasma TNF-α levels in control, sterile, and septic groups.** Means and standard error of the means are shown in original (non-transformed) values.

**Table 8. Means and 95% confidence intervals of the portal vein TNF-α concentrations are shown in original values.**

| Groups | Means (pg/ml) | 95% Confidence Intervals |
|---|---|---|
| Control | 12.98 | 12.78, 13.19 |
| Sterile | 18.36* | 16.68, 21.03 |
| Septic | 15.04 | 14.08, 16.33 |

*Significantly different from Control ($p<0.04$)

**d) Distributions of the Inferior Vena Cava Plasma TNF-α Raw and Transformed (TNF-$\alpha^{-3}$) Data:**

As can be seen in Figure 15, the inferior vena cava TNF-α data was not normally distributed (The Shapiro-Wilk W test had a p value of less than 0.0001).

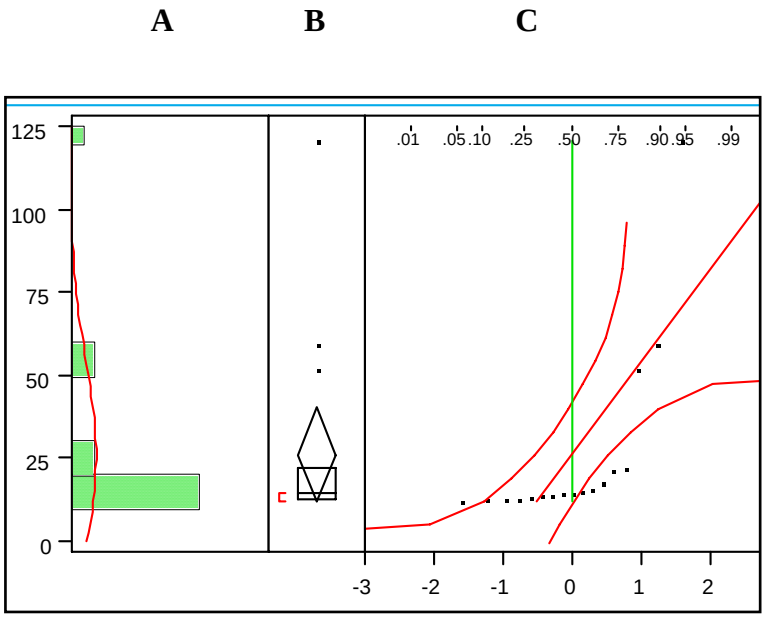


**Figure 15. Distribution of IVC TNF-α Raw Data.** Histogram (A), Outlier Box Plot (B), and Normal Quantile Plot (C) of the distribution are shown.

All data was transformed for statistical analyses. Figure 16 shows the distribution of transformed inferior vena cava TNF-α data, in which ($-3^{rd}$) power of portal vein TNF-α raw data (TNF-$\alpha^{-3}$) was used to support normal distribution. Shapiro-Wilk W Test of the transformed data had a p value of 0.23, which was greater than the 0.05 alpha value.

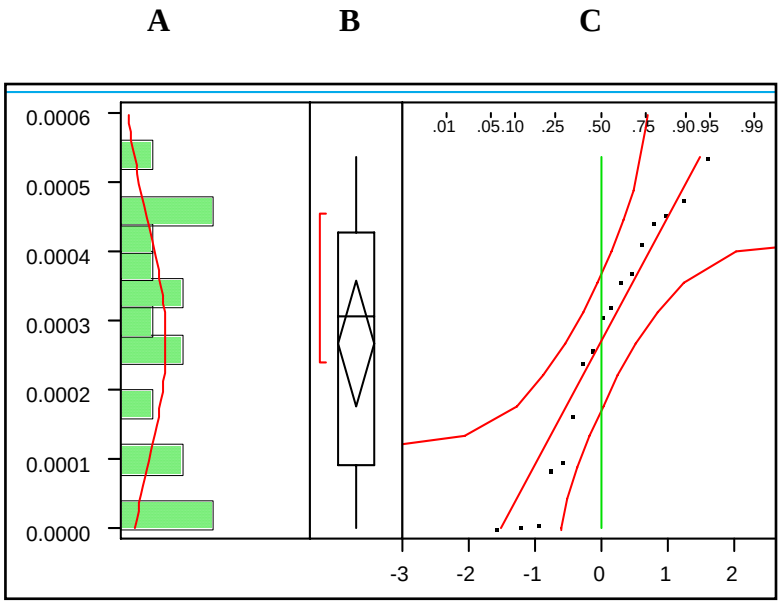


**Figure 16. Distribution of IVC TNF-α Transformed (TNF-$\alpha^{-3}$) Data.** Histogram (A), Outlier Box Plot (B), and Normal Quantile Plot (C) of the distribution are shown.

Confirmation of the equality of variances of the transformed IVC TNF-α data was done by using O'Brien and Brown-Forsythe Tests of homogeneity, which had F ratios that had p values of 0.74 and 0.38 (>0.05), respectively, and was assumed that there were no statistically significant differences between the experimental subjects (rats), and the variances of the subjects were equal.

**e) Oneway Analysis of Variance (Oneway Anova) of the Transformed Inferior Vena Cava Plasma TNF-α Levels, and Comparisons of the Means of Control, Sterile, and Septic Groups by using Tukey's Honest Significant Difference Test (Tukey-Kramer HSD):**

A total of 17 inferior vena cava TNF-α observations were used for this analysis. The coefficient of determination (RSquare) of the whole model was 32%, which indicated that only 32% of the data could be explained by the oneway anova model. The whole model had an F ratio, which had a p value of 0.07, indicated that, there was no statistically significant difference among the inferior vena cava TNF-α levels of the control, sterile and the septic groups at a chosen 0.05 alpha level, but the power of the whole model was only 52%, which suggested that the experiment did not have enough power to detect differences in the inferior vena cava plasma TNF-α levels among the control, sterile and the septic groups.

**f) Means and 95% Confidence Intervals of Inferior Vena Cava Plasma TNF-α Levels in Original Values:**

The 95% confidence interval of the transformed data for each group was calculated as outlined previously. Figure 17 and Table 9 show the means and 95% confidence intervals of the inferior vena cava plasma TNF-α levels in original values.

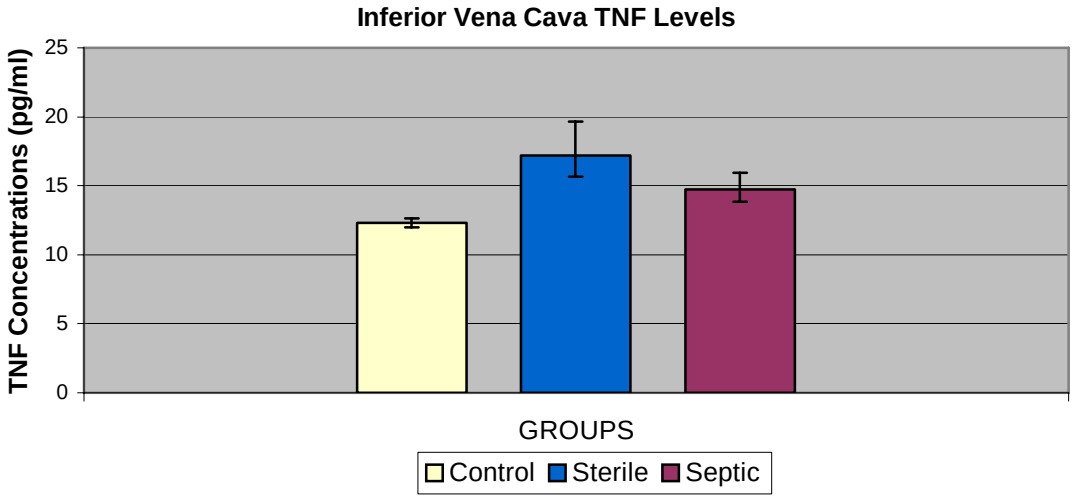


**Figure 17. The inferior vena cava plasma TNF-α levels in control, sterile, and septic groups.** Means and standard error of the means are shown in original (non-transformed) values.

**Table 9. Means and 95% confidence intervals of the inferior vena cava TNF-α concentrations are shown in original values.**

| Groups | Means (pg/ml) | 95% Confidence Intervals |
|---|---|---|
| Control | 12.32 | 12.01, 12.66 |
| Sterile | 17.21 | 15.65, 19.67 |
| Septic | 14.75 | 13.86, 15.94 |

**g) Analysis of the Differences Between the Portal Vein and the Inferior Vena Cava Circulating TNF-α Concentrations in Sterile Abscess Group:**

The distribution of the difference in the portal vein and the inferior vena cava TNF-α levels in the sterile group was not normally distributed, so the Wilcoxon Signed-Rank non-parametric test was used, which had a p value of 0.36, indicating

that there was no statistically significant difference between the plasma TNF-α levels of the portal vein and the inferior vena cava in the sterile abscess group.

**h) Analysis of the Differences Between the Portal Vein and the Inferior Vena Cava Circulating TNF-α Concentrations in Septic Abscess Group:**

The distribution of the difference in the portal vein and the inferior vena cava TNF-α levels in the septic group was not normally distributed, so the Wilcoxon Signed-Rank non-parametric test, which had a p value of 0.64, was used, and indicated that there was no statistically significant difference between the plasma TNF-α levels of the portal vein and the inferior vena cava in the septic abscess group.

**i) Linear Regression Analysis of the Transformed Portal Vein and Inferior Vena Cava TNF-α Values:**

Figure 18 shows a linear regression analysis of the portal vein and the inferior vena cava circulating TNF-α levels in all control, sterile, and septic groups. The legend of the figure represents the transformed TNF-α data. The F ratio of the model had a p value less than 0.0001, suggesting a statistically significant correlation between the TNF-α levels of the portal vein and the inferior vena cava. A coefficient correlation (R) value of 0.97, strongly suggested a direct correlation between the two sources of TNF-α.

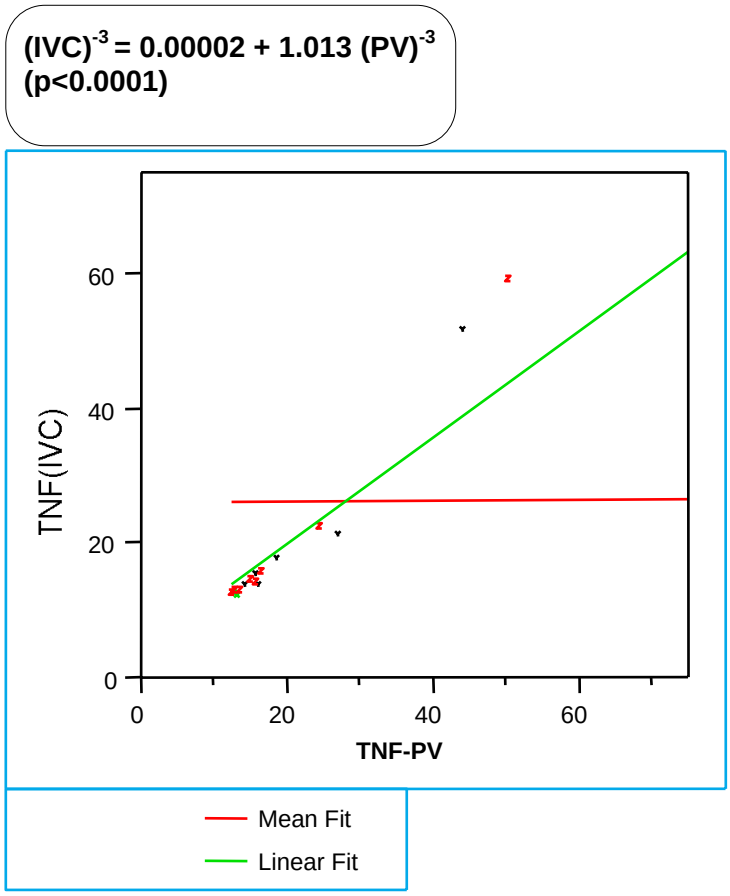


**Figure 18. The linear regression analysis of the portal vein and inferior vena cava TNF-α levels.** Linear fit and mean fit are shown.

**2) The Portal Vein and The Post-Hepatic Inferior Vena Cava Plasma Interleukin-1 Beta (IL-1β) Levels:**

**a) Distributions of the Portal Vein Plasma IL-1β Raw and Transformed (1/IL-1β) Data:**

Examination of Figure 19 shows that the portal vein IL-1β data was not normally distributed (The Shapiro-Wilk W test had a p value less than 0.0007).

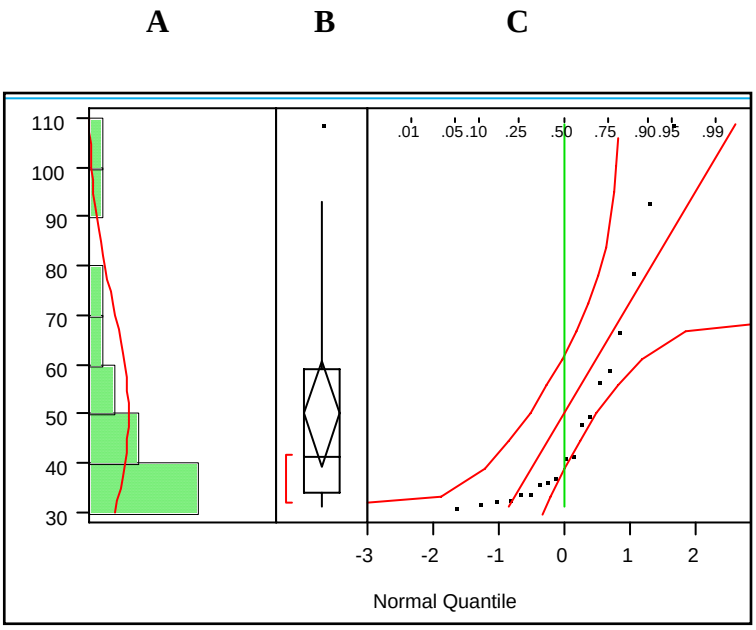


**Figure 19. Distribution of PV IL-1β Raw Data.** Histogram (A), Outlier Box Plot (B), and Normal Quantile Plot (C) of the distribution are shown.

All data was transformed for statistical analyses. Figure 20 shows the distribution of transformed portal vein IL-1β data, in which the reciprocal of the portal vein IL-1β raw data (1/IL-1β) was used to support normal distribution (The

Shapiro-Wilk W test had a p value of 0.09, which was greater than the 0.05 alpha value).

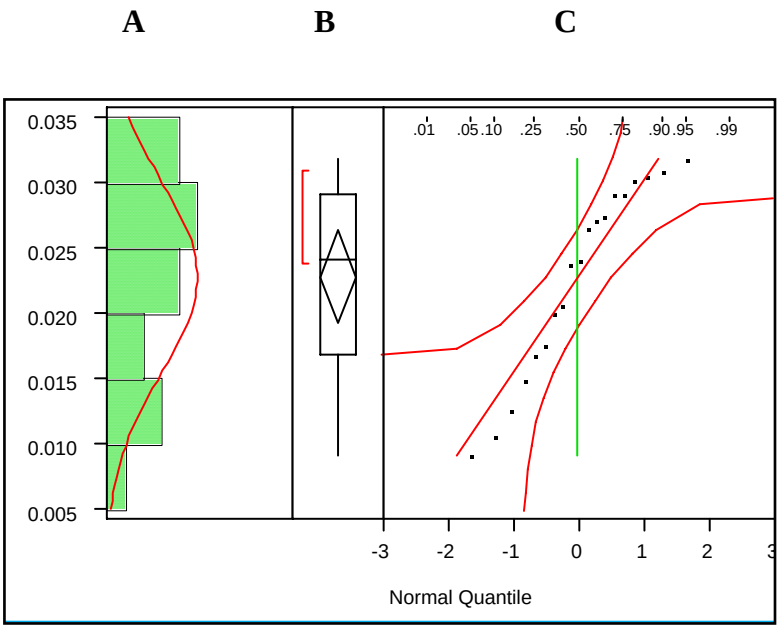


**Figure 20. Distribution of PV IL-1β Transformed (1/IL-1β) Data.** Histogram (A), Outlier Box Plot (B), and Normal Quantile Plot (C) of the distribution are shown.

Confirmation of the equality of variances of the transformed portal vein IL-1β data was done by using O'Brien and Brown-Forsythe Tests of homogeneity, which had F ratios that had p values of 0.22 and 0.12 (>0.05), respectively, and was assumed that there were no statistically significant differences among the experimental subjects (rats), and the variances of the subjects were equal.

**b) Oneway Analysis of Variance (Oneway Anova) of the Transformed Portal Vein Plasma IL-1β Levels, and Comparisons of the Means of Control, Sterile, and Septic Groups by using Tukey's Honest Significant Difference Test (Tukey-Kramer HSD):**

A total of 19 portal vein IL-1β observations were used for this analysis. The coefficient of determination (RSquare) of the whole model was 42%, which indicated that only 42% of the data could be explained by the oneway anova model. The whole model had an F ratio, which had a p value of 0.01, indicated that, at least one of the experimental groups was statistically different from the others in terms of portal vein IL-1β concentrations. The power of the whole model was 80%, which suggested that the experiment as done had enough power to detect the differences in the portal vein plasma IL-1β levels among the control, sterile and the septic groups.

The comparison of the means of portal vein IL-1β transformed levels of three experimental groups by using Tukey's Honest Significant Difference test (Tukey-Kramer HSD), suggested that only the mean of the sterile group was statistically different from the mean of the control group, and there was no statistically significant difference between the means of control and septic, and the means of sterile and septic groups.

**c) Means and 95% Confidence Intervals of Portal Vein Plasma IL-1β Levels in Original Values:**

The 95% confidence interval of the transformed data for each group was calculated as outlined previously. Figure 21 and Table 10 show the means and 95% confidence intervals of the portal vein plasma IL-1β levels in original values.

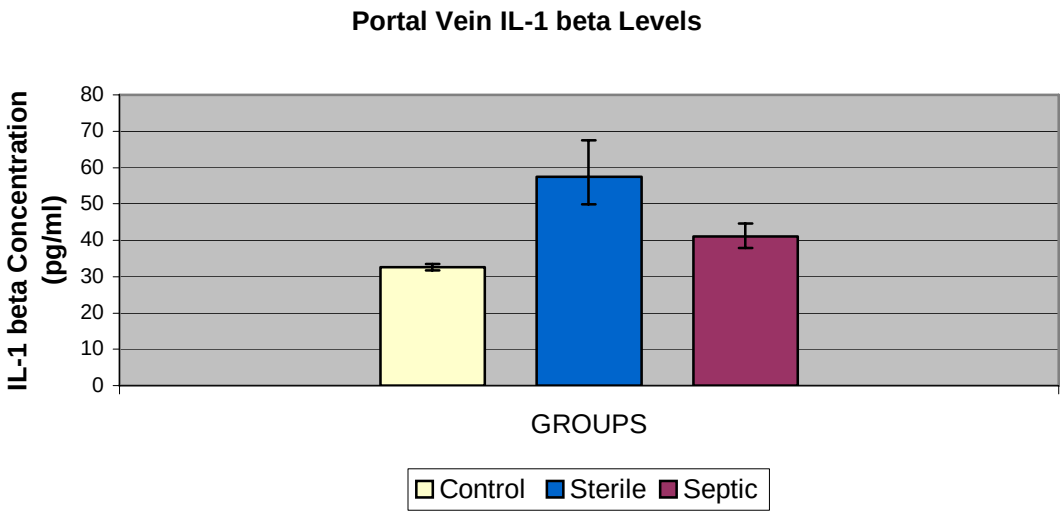


**Figure 21. The portal vein plasma IL-1β levels in control, sterile, and septic groups.** Means and standard error of the means are shown in original (non-transformed) values.

**Table 10. Means and 95% confidence intervals of the portal vein IL-1β concentrations are shown in original values.**

| Groups | Means (pg/ml) | 95% Confidence Intervals |
|---|---|---|
| Control | 32.59 | 31.77, 33.45 |
| Sterile | 57.39* | 49.89, 67.55 |
| Septic | 40.98 | 37.96, 44.52 |

*Significantly different from Control ($p<0.02$)

**d) Distributions of the Inferior Vena Cava Plasma IL-1β Raw and Transformed (1/IL-1β) Data:**

As we can see in Figure 22, the inferior vena cava IL-1β data was not normally distributed (The Shapiro-Wilk W test had a p value less than 0.0004).

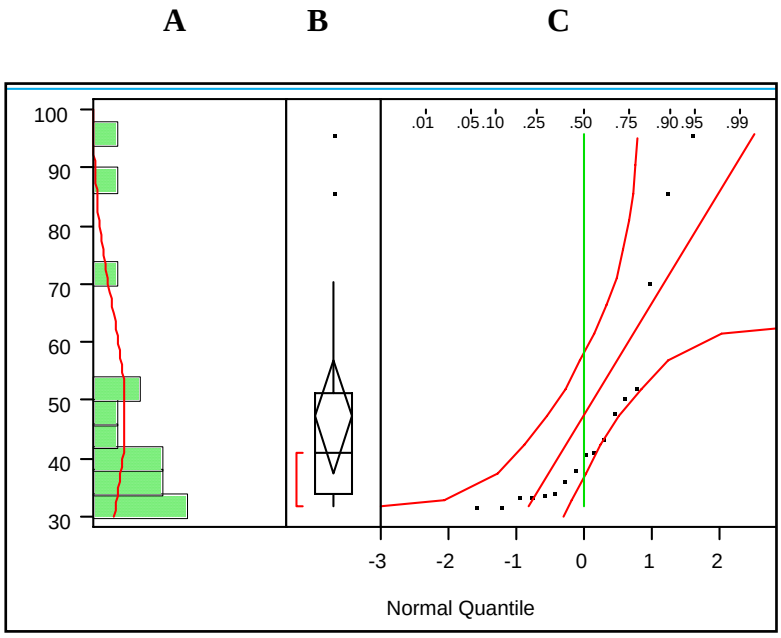


**Figure 22. Distribution of IVC IL-1β Raw Data.** Histogram (A), Outlier Box Plot (B), and Normal Quantile Plot (C) of the distribution are shown.

All data was transformed for statistical analyses. Figure 23 shows the distribution of transformed inferior vena cava IL-1β data, in which the reciprocal of inferior vena cava IL-1β raw data (1/IL-1β) was used to support the normal distribution. The Shapiro-Wilk W Test of the transformed data had a p value of 0.23, which was greater than the 0.05 alpha value.

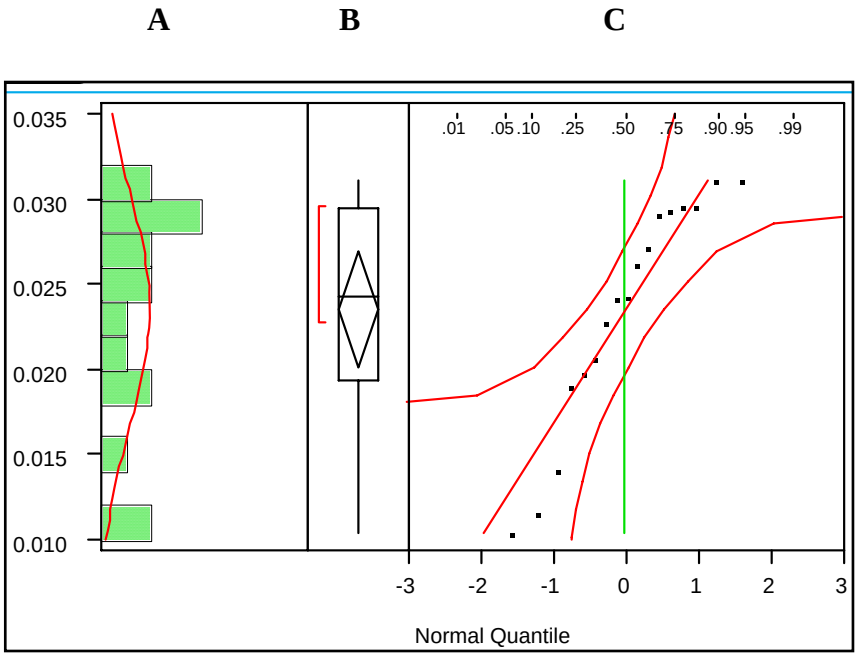


**Figure 23. Distribution of IVC IL-1β Transformed (1/IL-1β) Data.** Histogram (A), Outlier Box Plot (B), and Normal Quantile Plot (C) of the distribution are shown.

Confirmation of the equality of variances of the transformed IVC IL-1β data has been done by using O'Brien and Brown-Forsythe Tests of homogeneity, which had F ratios that had p values of 0.19 and 0.14 (>0.05), respectively, and was assumed that there were no statistically significant differences among the experimental subjects (rats), and the variances of the subjects were equal.

**e) Oneway Analysis of Variance (Oneway Anova) of the Transformed Inferior Vena Cava Plasma IL-1β Levels, and Comparisons of the Means of Control, Sterile, and Septic Groups by using Tukey's Honest Significant Difference Test (Tukey-Kramer HSD):**

A total of 17 inferior vena cava IL-1β observations were used for the statistical analysis. The coefficient of determination (RSquare) of the whole model was 33%, which indicated that only 33% of the data could be explained by the oneway anova model. The whole model had an F ratio, which had a p value of 0.06, indicated that, there was no statistically significant difference among the inferior vena cava IL-1β levels of the control, sterile and the septic groups at a chosen 0.05 alpha level.

**f) Means and 95% Confidence Intervals of Inferior Vena Cava Plasma IL-1β Levels in Original Values:**

The 95% confidence interval of the transformed data for each group was calculated as outlined previously. Figure 24 and Table 11 show the means and 95% confidence intervals of the inferior vena cava plasma IL-1β levels in original values.

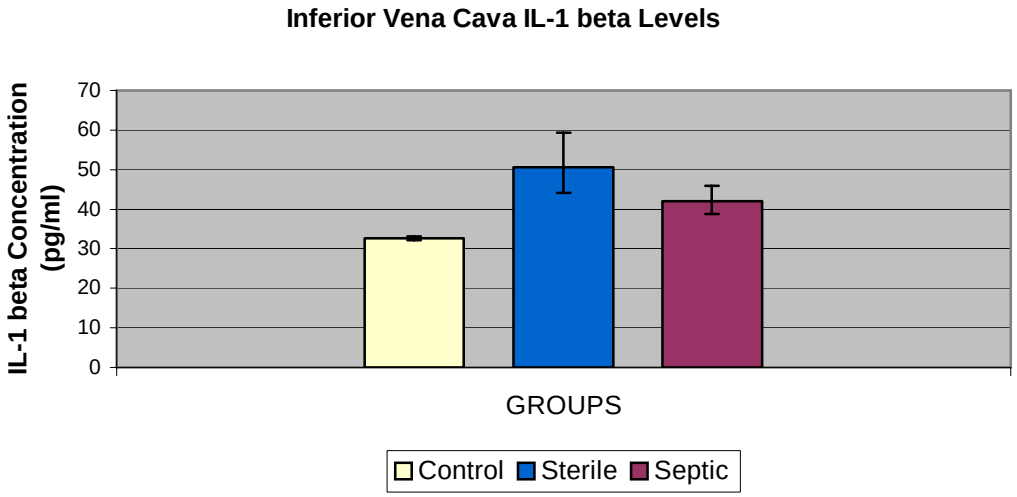


**Figure 24. The inferior vena cava plasma IL-1β levels in control, sterile, and septic groups.** Means and standard errors of the means are shown in original (non-transformed) values.

**Table 11. Means and 95% confidence intervals of the inferior vena cava IL-1β concentrations are shown in original values.**

| Groups | Means (pg/ml) | 95% Confidence Intervals |
|---|---|---|
| Control | 32.64 | 32.10, 33.19 |
| Sterile | 50.63 | 44.17, 59.31 |
| Septic | 42.07 | 38.76, 45.99 |

**g) Analysis of the Differences Between the Portal Vein and the Inferior Vena Cava Circulating IL-1β Concentrations in Sterile Abscess Group:**

The distribution of the differences between the portal vein and the inferior vena cava IL-1β levels in the sterile group was normally distributed, therefore we used the paired t-test to test for the significance in IL-1β levels between the two sources. The paired t-test gave us a mean difference of 6.17 between the two sources, and a t ratio, which had a p value of 0.03, indicating that there was a statistically significant difference between the plasma IL-1β levels of the portal vein and the inferior vena cava in the sterile abscess group. As seen in Figure 25, the two red lines around the line of fit (also red), the 95% confidence interval, do not include the black 45-degree reference line, which further confirmed that there was a statistically significant difference at the 0.05 alpha level. But we also have to keep in mind that the p value is so close to the alpha level, indicating that the significance is not statistically strong enough.

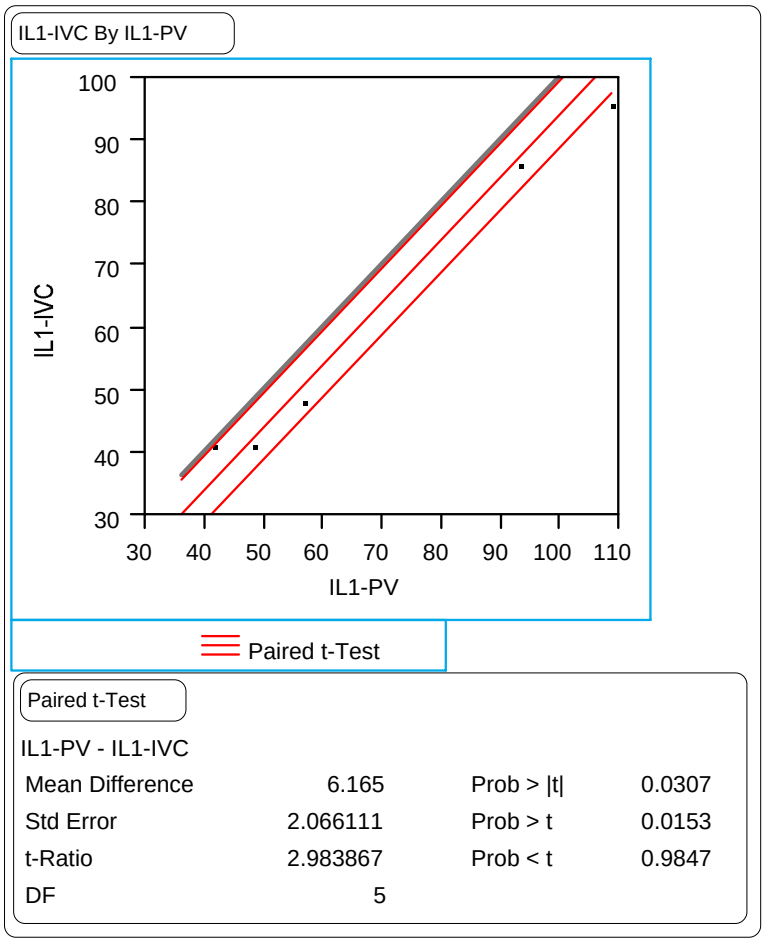


**Figure 25. Paired t-test of IL-1β levels of the inferior vena cava by portal vein in sterile group.** The black 45-degree reference line through the origin, red 45-degree line of fit and 2 red lines around the line of fit, which indicate 95% confidence interval are shown.

**h) Analysis of the Differences Between the Portal Vein and the Inferior Vena Cava Circulating IL-1β Concentrations in Septic Abscess Group:**

The distribution of the differences between the portal vein and the inferior vena cava IL-1β levels in the septic group was normally distributed, therefore we used the paired t-test to test for the significance in IL-1β levels between the two sources. The paired t-test gave us a mean difference of 0.16 between the two sources, and a t ratio, which had a p value of 0.95, indicating that there was no statistically significant difference between the plasma IL-1β levels of the portal vein and the inferior vena cava in the septic abscess group. Figure 26 depicts that, the two red lines around the line of fit (also red), the 95% confidence interval, include the black 45-degree reference line, which further confirmed that there was no statistically significant difference at the 0.05 alpha level.

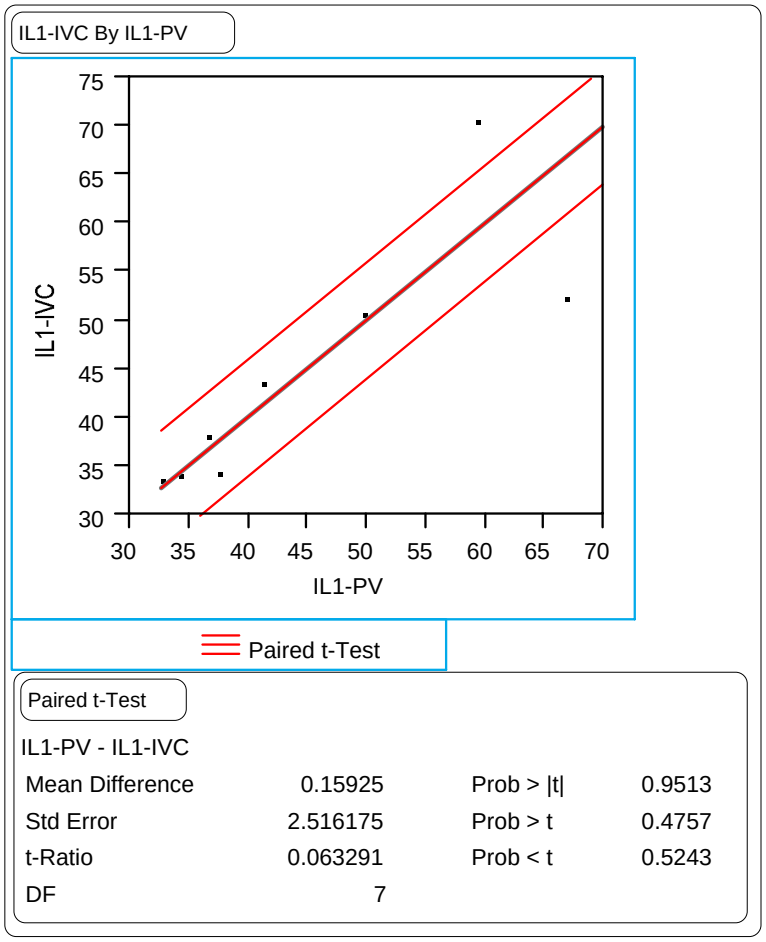


**Figure 26. Paired t-test of IL-1β levels of the inferior vena cava by portal vein in septic group.** The black 45-degree reference line through the origin, red 45-degree line of fit and 2 red lines around the line of fit, which indicate 95% confidence interval are shown.

**i) Linear Regression Analysis of the Transformed Portal Vein and Inferior Vena Cava IL-1β Values:**

Figure 27 shows a linear regression analysis of the portal vein and the inferior vena cava circulating IL-1β levels in all control, sterile, and septic groups. All the legends of the figure represent the transformed IL-1β data. The F ratio of the model had a p value less than 0.0001, suggested a statistically significant correlation between the IL-1β levels of the portal vein and the inferior vena cava. A coefficient correlation (R) value of 0.96, strongly suggested a direct correlation between the two sources of IL-1β.

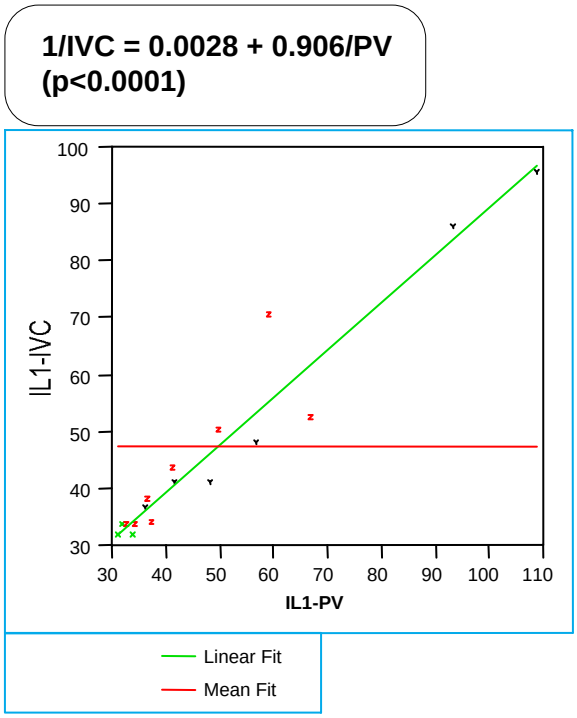


**Figure 27. The linear regression analysis of the portal vein and inferior vena cava IL-1β levels.** Linear fit and mean fit are shown.

**3) The Portal Vein and The Post-Hepatic Inferior Vena Cava Plasma Interleukin-6 (IL-6) Levels:**

**a) Distributions of the Portal Vein Plasma IL-6 Raw and Transformed (1/IL-6) Data:**

An examination of Figure 28 showed that the distribution of portal vein IL-6 data was not normally distributed. IL-6 values did not lie along the normal distribution curve in the histogram (A), there were outside values in the quantile box plot (B), and the mean was greater than the median. The data did not lie along with the normal distribution line in the normal quantile plot (C), and the plots were not between the 95% confidence curves. Finally, the Shapiro-Wilk W test had a p value of less than 0.0001, which all suggested that the data was not normally distributed.

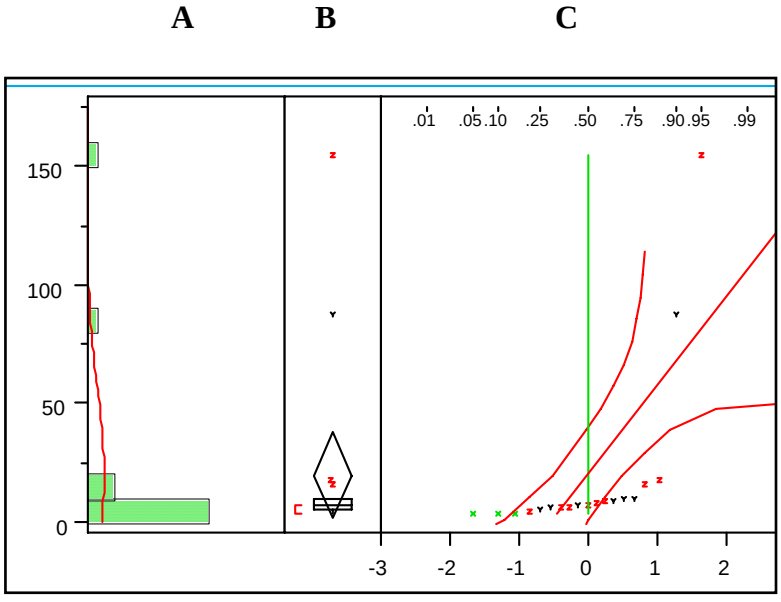


**Figure 28. Distribution of Portal Vein IL-6 Raw Data.** A: Histogram, B: Outlier Box Plot, and C: Normal Quantile Plot of the distribution are shown.

In order to statistically analyze the data, the data was transformed, so as to obtain a normal distribution. Figure 29 shows the distribution of the transformed portal vein IL-6 data, in which the reciprocal of the portal vein IL-6 raw data was used for the transformation.

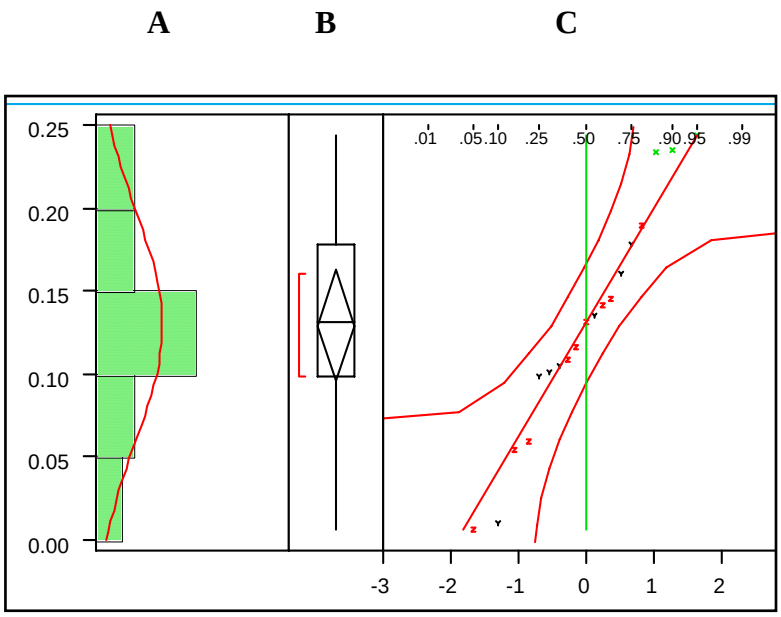


**Figure 29. Distribution of Portal Vein IL-6 Transformed (Reciprocal of original data) Data.** A: Histogram, B: Outlier Box Plot, and C: Normal Quantile Plot of the distribution are shown.

The normality of the distribution of the transformed (reciprocal) portal vein IL-6 data was confirmed by the histogram (A), the outlier box plot (B), the normal quantile plot (C), and the Shapiro-Wilk W test (Figure 29). The data was distributed along the normal distribution curve in the histogram, no outside values in the outlier box plot, the mean and the median values were almost equal, and the observations

lied more or less along the normal quantile plot line. Shapiro-Wilk W Test had a p value of 0.59, which was much greater than the 0.05 alpha value.

After confirming the normality of the distribution, we checked the equality of variances in order to be confident that our transformed data could be used for statistical analyses. O'Brien and Brown-Forsythe Tests of homogeneity of the transformed portal vein IL-6 data had F ratios that had probability (p) values of 0.52 and 0.24, respectively, which were much greater than 0.05 alpha values and we could assume that there were no statistically significant differences between the experimental subjects (rats), and the variances of the subjects were equal. Since there were no unequal variances among the experimental groups, we got a pooled estimate of error variance for each group. We then provided the two requirements for the analysis of the portal vein IL-6 data.

**b) Oneway Analysis of Variance (Oneway Anova) of the Transformed Portal Vein Plasma IL-6 Levels, and Comparisons of the Means of Control, Sterile, and Septic Groups by using Tukey's Honest Significant Difference Test (Tukey-Kramer HSD):**

The experimental groups (control, sterile and septic) were the predictor variables (X) and the reciprocal of the portal vein IL-6 concentrations were the response variables (Y) in our experimental design. We fitted Y by X, and had a whole model and oneway anova analysis of this model for transformed portal vein IL-6 levels.

There were a total of 19 portal vein IL-6 observations, and the coefficient of determination (RSquare) of the whole model was 49%, which indicated that 49% of the data could be explained by the oneway anova model. The whole model had an F ratio with a p value of 0.0043, indicated that, at least one of the experimental groups, in terms of portal vein IL-6 concentrations, statistically differed from the other or others. The power of the whole model was 90%, which showed that the experiment as done had enough power to detect the differences of the portal vein plasma IL-6 levels among the control, sterile and the septic groups.

Comparison of the means of portal vein IL-6 transformed levels of the three experimental groups using the Tukey's Honest Significant Difference test (Tukey-Kramer HSD) showed that the means of the sterile and septic groups were statistically different from that of the control group, while the means of sterile and septic groups were not statistically significantly different.

**c) Means and 95% Confidence Intervals of Portal Vein IL-6 Levels in Original Values:**

After analyzing the statistical differences among the experimental groups, we calculated the 95% confidence interval of the transformed data for each group. This was achieved by addition and subtraction of each group's standard error of the mean to the mean of the same group, respectively. We then converted these 95% confidence interval values of the transformed data back to the original form by simply retaking the reciprocal of these values. Figure 30 and Table 12 show the means and 95% confidence intervals of the portal vein plasma IL-6 levels in original values.

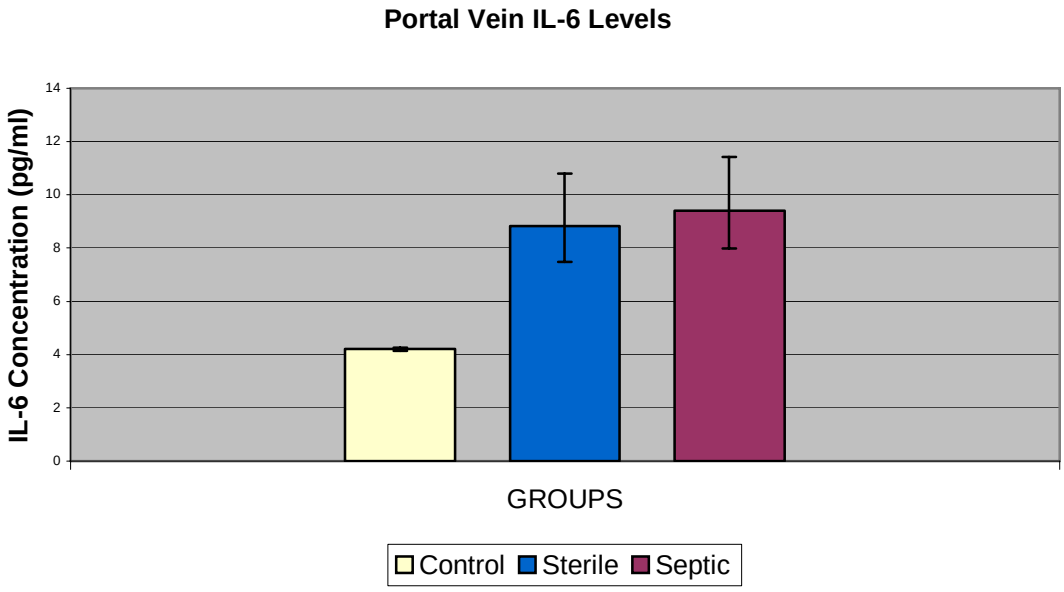


**Figure 30. Portal vein plasma IL-6 concentrations in control, sterile, and septic groups.** Means and standard error of the means are shown in original (non-transformed) values.

**Table 12. Means and 95% confidence intervals of the portal vein IL-6 concentrations are shown in original values.**

| Groups | Means (pg/ml) | 95% Confidence Intervals |
|---|---|---|
| Control | 4.20 | 4.14, 4.25 |
| Sterile | 8.83* | 7.47, 10.79 |
| Septic | 9.41* | 7.99, 11.43 |

*Significantly different from Control ($p<0.01$)

**d) Distributions of the Inferior Vena Cava Plasma IL-6 Raw and Transformed (1/IL-6) Data:**

As can be seen in Figure 31, the distribution of the inferior vena cava (IVC) IL-6 data is not normally distributed. IL-6 values were found not to lie along the normal distribution curve in the histogram (A), there were outside values in the quantile box plot (B), and the mean was greater than the median. The data did not lie along the normal distribution line in the normal quantile plot (C), and the plots were not between the 95% confidence curves. Finally, the Shapiro-Wilk W test had a p value of less than 0.0001, which all suggested that the data was not normally distributed.

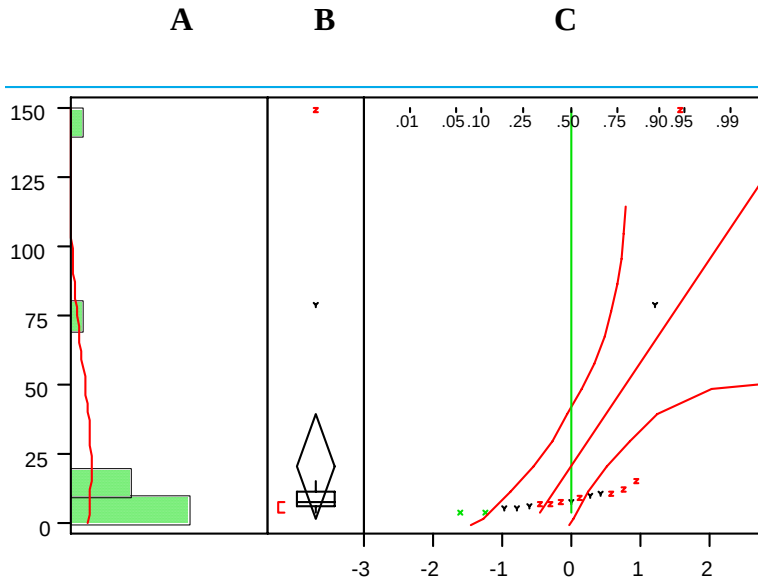


**Figure 31. Distribution of IVC IL-6 Raw Data.** Histogram (A), Outlier Box Plot (B), and Normal Quantile Plot (C) of the distribution are shown.

In order to statistically analyze our data, we transformed it. Figure 32 shows the distribution of the transformed inferior vena cava IL-6 data, in which the reciprocal of inferior vena cava IL-6 raw data was used for the transformation.

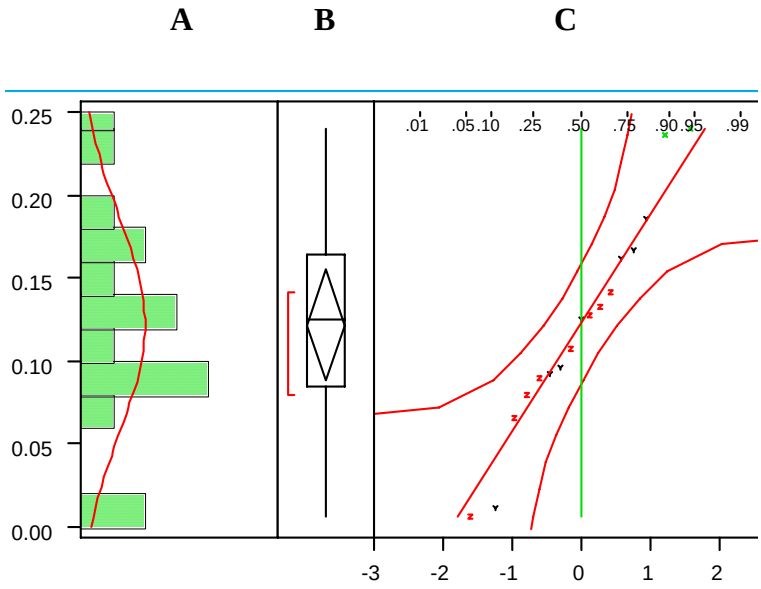


**Figure 32. Distribution of IVC Transformed IL-6 (Reciprocal of original data) Data.** Histogram (A), Outlier Box Plot (B), and Normal Quantile Plot (C) of the distribution are shown.

The normality of the distribution of the transformed (reciprocal) inferior vena cava IL-6 data was confirmed by the histogram (A), the outlier box plot (B), the normal quantile plot (C), and the Shapiro-Wilk W test, which had a p value of 0.72 (much greater than the 0.05 alpha value) (Figure 32).

Confirmation of the equality of variances of the transformed IVC IL-6 data was done by using O'Brien and Brown-Forsythe Tests of homogeneity, which had F ratios that had p values of 0.48 and 0.13 (>0.05), respectively, and was assumed that

there were no statistically significant differences among the experimental subjects (rats), and the variances of the subjects were equal.

**e) Oneway Analysis of Variance (Oneway Anova) of the Transformed Inferior Vena Cava Plasma IL-6 Levels, and Comparisons of the Means of Control, Sterile, and Septic Groups by using Tukey's Honest Significant Difference Test (Tukey-Kramer HSD):**

The predictor and response variables were as defined in section b for the portal IL-6 data, except that inferior vena cava was evaluated.

A total of 17 inferior vena cava IL-6 observations were used. The coefficient of determination (RSquare) of the whole model was 49%, which indicated that 49% of the data could be explained by the oneway anova model. The whole model had an F ratio, which had a p value of 0.0091, indicated that, at least one of the experimental groups was statistically different from the others in terms of inferior vena cava IL-6 concentrations. The power of the whole model was 84%, which showed that the experiment as done had enough power to detect the differences of the inferior vena cava IL-6 levels among the control, sterile and the septic groups, since the acceptable levels of power began at 70%.

When we compared the means of the inferior vena cava IL-6 transformed levels of the three experimental groups by using Tukey's Honest Significant Difference test (Tukey-Kramer HSD), we found that the means of the sterile and septic groups were statistically different from the mean of the control group, while

there was no statistically significant difference between the means of the sterile and septic groups.

**f) Means and 95% Confidence Intervals of Inferior Vena Cava Plasma IL-6 Levels in Original Values:**

After analyzing the statistical differences among the experimental groups, then we calculated the 95% confidence interval of the transformed data for each group by the addition and subtraction of each group's standard error of the mean to the mean of the same group, respectively. We converted these 95% confidence interval values of the transformed data back to the original form by retaking the reciprocal of these values. Figure 33 and Table 13 show the means and 95% confidence intervals of the inferior vena cava plasma IL-6 levels in original values.

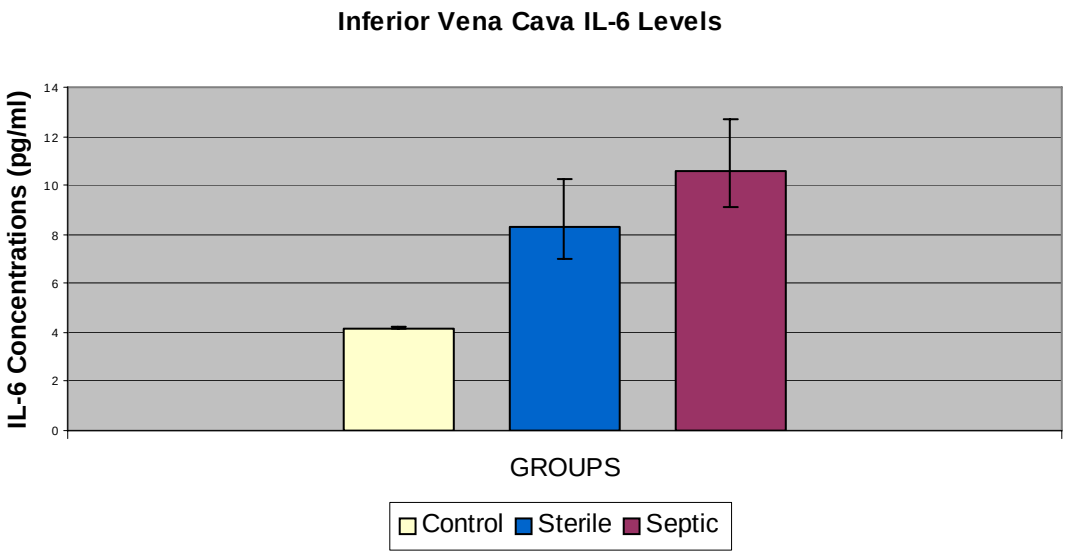


**Figure 33. Inferior vena cava plasma IL-6 levels in control, sterile, and septic groups.** Means and standard error of the means are shown in original (non-transformed) values.

**Table 13. Means and 95% confidence intervals of the inferior vena cava IL-6 concentrations are shown in original values.**

| Groups | Means (pg/ml) | 95% Confidence Intervals |
|---|---|---|
| Control | 4.18 | 4.15, 4.22 |
| Sterile | 8.31* | 7, 10.22 |
| Septic | 10.60* | 9.09, 12.72 |

*Significantly different from Control ($p<0.01$)

**g) Analysis of the Differences Between the Portal Vein and the Inferior Vena Cava Circulating IL-6 Concentrations in the Sterile Abscess Group:**

Again the difference between the portal vein and the inferior vena cava IL-6 levels in the sterile group was not normally distributed, therefore we used the Wilcoxon Signed-Rank non-parametric test in order to test the significance of the difference in IL-6 levels between these two sources. Wilcoxon Signed-Rank non-parametric test gave a mean difference of 1.47 between the two sources, and a t ratio, which had a p value of 0.27, which indicated that there was no statistically significant difference between the plasma IL-6 levels of the portal vein and the inferior vena in the sterile abscess group at a chosen hypothesized value of 0.

**h) Analysis of the Differences Between the Portal Vein and the Inferior Vena Cava Circulating IL-6 Concentrations in the Septic Abscess Group:**

The distribution of the differences between the portal vein and the inferior vena cava IL-6 levels in the septic group was normally distributed, therefore we used the paired t-test to test for the significance in IL-6 levels between the two sources.

The paired t-test gave us a mean difference of 1.16 between the two sources, and a t ratio, which had a p value of 0.26, indicating that there was no statistically significant difference between the plasma IL-6 levels of the portal vein and the inferior vena cava in the septic abscess group. As seen in Figure 34, the two red lines around the line of fit (also red), the 95% confidence interval, include the black 45-degree reference line, which further confirmed that there was no statistically significant difference at the 0.05 alpha level.

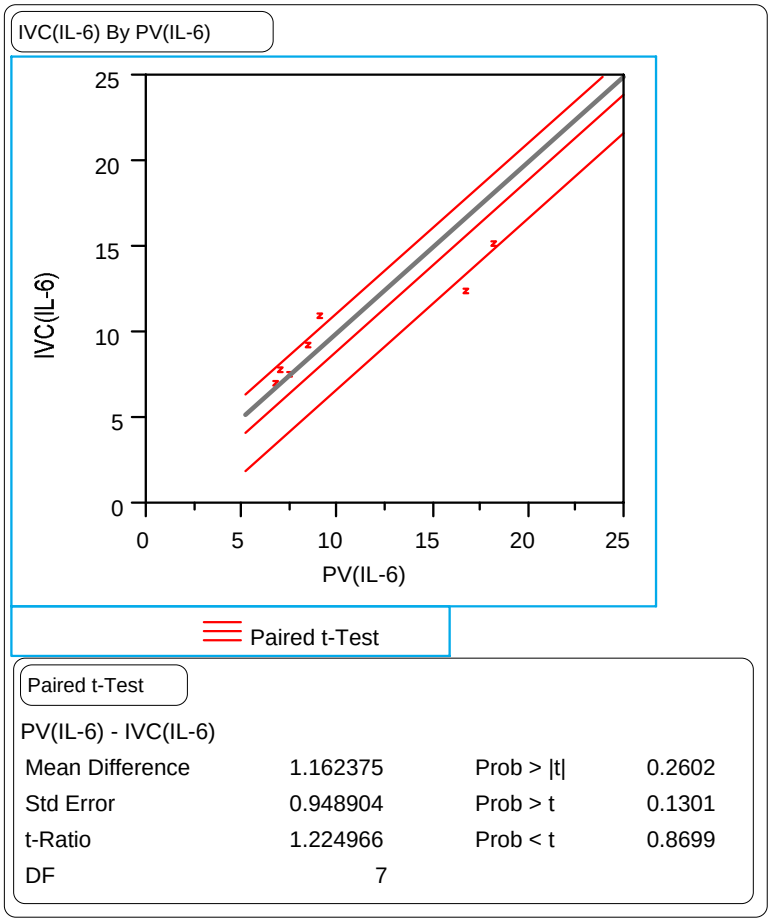


**Figure 34. Paired t-test of IL-6 levels of the inferior vena cava by portal vein in septic group.** The black 45-degree reference line through the origin, red 45-degree line of fit and 2 red lines around the line of fit, which indicate 95% confidence interval are shown.

### i) Linear Regression Analysis of the Transformed Portal Vein and Inferior Vena Cava IL-6 Values:

Linear regression analysis of the portal vein and the inferior vena cava IL-6 levels in all control, sterile, and septic groups is shown in Figure 35. All the values represent the reciprocal of the original data. The linear regression model had an F

ratio, which had a p value of less than 0.0001, which suggested the statistically significant correlation between the IL-6 levels of the portal vein and the inferior vena cava, and a coefficient correlation (R) value of 0.98, which indicated that there was a direct correlation between these two sources of IL-6.

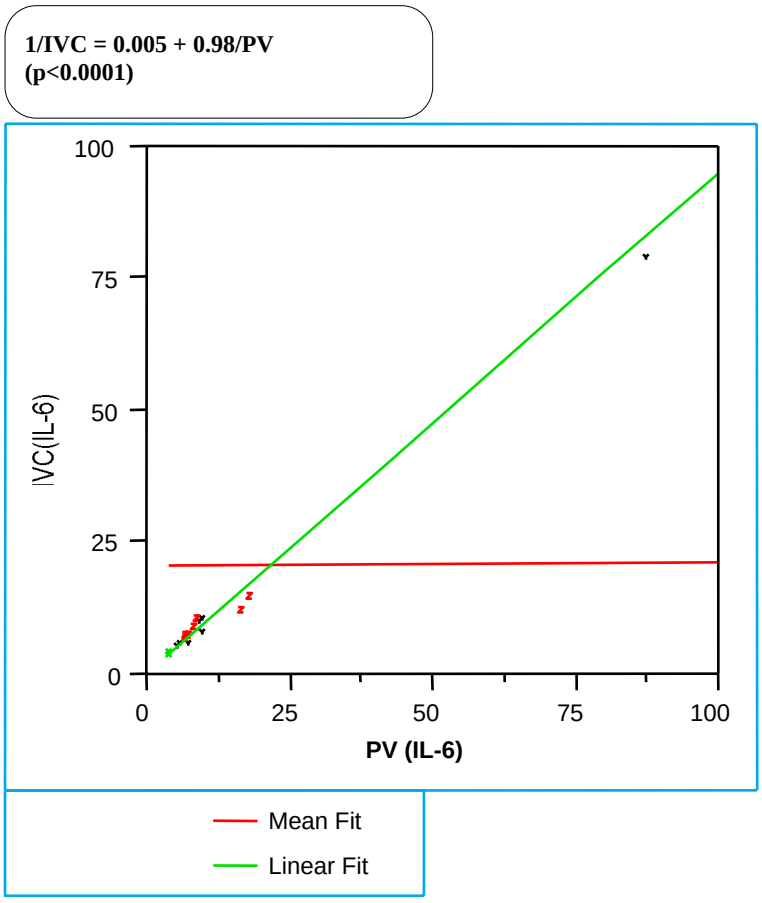


**Figure 35. The linear regression analysis of the portal vein and inferior vena cava IL-6 levels.** Linear fit and mean fit are shown.

## D) THE EFFECTS OF THE INTRA-ABDOMINAL SEPTIC AND STERILE ABSCESSES ON THE LIVER:

### 1) Hematoxylin & Eosin Stain of the Liver:

Figure 36 is a composite of control (A-C), sterile (D-F) and septic (G-I) livers stained with H&E, showing the basic morphology of the cells and the tissues.

Figure 36-A shows the control liver tissue at 10X magnification. Central veins and sinusoids are marked, and they show normal morphology with hepatocytes lying parallel to sinusoids.

Figure 36-D indicates the liver tissue of the sterile abscess group at 10X magnification, and has markedly dilated sinusoids when compared to control group.

Figure 36-G is the picture of the septic liver, and has also dilated sinusoids. The vasodilatation of the sinusoids in the septic liver is more intense and broadly distributed than in the sterile group.

In Figure 36-B-C, E-F, and H-I, the portal triads of the liver sections are shown in 20X and 40X magnifications. Figures 36-B-C are of control liver, which show the normal morphology of the portal triad at 20X and 40X magnifications, respectively. The relatively larger vessel is the portal vein, lying along side of the hepatic artery (thicker wall) and the bile duct. The bright red cells in the sinusoids and the portal triad indicate red blood cells. The dark blue and the relatively smaller cells in the sinusoids and around the walls of the portal vein and hepatic artery are white blood cells, and mostly neutrophils. The hepatocytes, which line the sinusoids, have

light bluish purple color with intra-cellular granules visible, and are larger than the white blood cells.

Figures 36-E-F show the liver of the sterile abscess group, with the portal triad shown at 20X and 40X magnifications, respectively. There is a markedly increased amount of white blood cell (inflammatory cell) infiltration in the sinusoids, especially around the portal triad.

Figure 36-H-I show the liver of the septic abscess group with portal triad shown at 20X and 40X magnifications, respectively. There is also an increased amount of white blood cell infiltration in the sinusoids around the portal triad of the septic liver, when compared to control liver. It appears that there is no difference between sterile and septic livers in terms of the location and the degree of the infiltration, but in the higher magnifications, it can also be seen that, the vasodilatation of the sinusoids of the septic liver is more intense than in the sterile one, with the least in the normal liver.

**2) Myeloperoxidase Stain of the Liver:**

Figure 37 shows the myeloperoxidase stain of control (A-C), sterile (D-F) and septic (G-I) livers at 10X, 20X and 40X magnifications, indicating the the inflammatory cell infiltration of the liver and differentiating the various inflammatory cells in the liver tissue samples. Portal triads are marked and shown in all sections along with the sinusoids surrounding them. The cells stained in blue color show the inflammatory cells in all samples. The darker blue-black stained cells indicate the

polymorphonuclear leukocytes, whereas the light blue stained cells show the monocytes in the circulation.

Figure 37 A-C show the control liver samples, which have baseline inflammatory cells in the circulation.

Figure 37 D-F and G-I show the liver samples of the sterile and septic abscess groups, respectively, and have markedly increased inflammatory cell infiltration in the sinusoids, which is more prominent around the portal triad.

The dark blue cells, which represent the polymorphonuclear leukocytes, are marked in 40X magnification of each group, and show a prominent increase in sterile and septic abscess groups when compared to control.

Regardless of the type of the inflammatory cells, the sterile and septic abscess livers have more infiltration than the control liver, and the infiltration is the most intense in the septic liver.

**3) Detection of Interleukin-6 (IL-6) Gene Expression in the Liver:**

Figure 38 shows the gene expression of IL-6, which is detected by *in situ* hybridization technique, in the liver samples of control (A-C), sterile (D-F) and septic (G-I) livers at 10X, 20X and 40X magnifications. Portal triads, central veins are marked, and IL-6 positive cells (purple-blue) are indicated by arrows.

Figure 38 A-C are the liver samples of the control group, and almost have no IL-6 positive cells, indicating no IL-6 gene expression in the non-stimulated control liver cells. A couple of mildly positive cells in this control group indicate the basal transcription of IL-6 gene.

Figure 38 D-F are the liver sections of sterile abscess group, and show significantly increased amount of IL-6 positive cells, indicating the increased IL-6 gene expression in the liver in response to the sterile intra-abdominal inflammation. The IL-6 positive cells of the liver in the sterile group are uniquely located and concentrated around the central vein and the portal triad regions. There are only a few IL-6 positive cells located in the liver parenchyma other than these two regions.

Figure 38 G-I are the septic liver samples. The IL-6 producing cells are also concentrated around the central vein and portal triad area in the septic livers. The only difference of the septic liver from the sterile liver in terms of IL-6 gene expression is the magnitude of the expression, which is more prominent in septic liver cells.

**4) Detection of Fibrinogen Gene Expression in the Liver:**

Figure 39 shows the gene expression of fibrinogen, which is detected by *in situ* hybridization technique, in the liver samples of control (A-C), sterile (D-F) and septic (G-I) groups at 10X, 20X and 40X magnifications. Portal triads, central veins are marked, and fibrinogen positive cells (purple-blue) are indicated by arrows.

Figure 39 A-C are the control liver samples, showing almost no fibrinogen positive cells throughout the liver, which indicates that there is almost no fibrinogen gene expression in this group. A couple of barely positive cells may indicate the basal fibrinogen gene expression.

Figure 39 D-F are the liver samples of the sterile intra-abdominal abscess group, which depict an increased amount of fibrinogen positive cells (purple-blue),

indicating the stimulation of fibrinogen gene expression in the sterile liver. The fibrinogen positive cells are located around the central vein area as is the location of IL-6 positive cells.

Figure 39 G-I are septic livers, and indicate the fibrinogen positive liver cells, which are bluish in color. The location of the fibrinogen positive cells in the septic liver is peri-central vein and portal triad. The only difference of the septic liver from the sterile liver in terms of fibrinogen expression is that, the gene expression is much more prominent and qualitatively appear to be of greater in the septic group.

**5) Gomori's One-Step Trichrome Stain of the Liver:**

Figure 40 shows the trichrome stain of control (A-C), sterile (D-F) and septic (G-I) livers at 10X, 20X and 40X magnifications, indicating the deposition of the collagenous connective tissue fibers in the liver. The central veins are marked in all tissue samples, and the greenish color stain represents the collagen fibers deposited in the liver samples, which are marked by arrows.

Figure 40 A-C show the liver samples of the control group, and the collagen deposition is less when compared to sterile and septic abscess groups (33 D-F and 33 G-I, respectively).

Figure 40 D-F represent the liver samples of the sterile abscess group, which show intense collagen deposition around the central vein and the sinusoids.

The collagen fiber deposition is markedly increased in the septic abscess group (Figure 40 G-I) when compared to sterile and control ones. The deposition is again prominent in and around the central vein area, extending through the sinusoids.

**6) Oil Red O Lipid Stain of the Liver:**

Figure 41 shows the lipid stain of control (A-C), sterile (D-F) and septic (G-I) livers at 10X, 20X and 40X magnifications, indicating the deposition of the lipid in the liver. The central veins are marked in tissue samples, and the red color lipid droplets are indicated by arrows.

Figure 41 A-C are control livers, and show very few lipid droplets, whereas Figures 41 D-F and G-I are sterile and septic abscess livers, respectively, and both show significantly increased amount and size of lipid droplets when compared to control liver, which is consistent with increased lipid deposition in the liver of the sterile and the septic abscess groups. The size of the lipid droplets is larger in the septic liver than in the sterile liver.

Lipid deposition in the liver samples is diffusely distributed throughout the liver parenchyma, where the concentration is much higher around the sinusoids in both sterile and septic groups.

# DISCUSSION

## A) MORTALITY AND MORBIDITY RATES OF SEPSIS/SIRS IN CHRONIC SEPTIC RAT FECAL-AGAR PELLET MODEL:

Sepsis is a systemic inflammatory response of the host against infection, regardless of the type of the microorganism (65). It is a clinical syndrome characterized by cardiovascular, respiratory, and metabolic responses (25). Sepsis is considered the most crucial causative factor in the evolution of multiple organ failure (MOF) in post-trauma and post-surgical patients (25), and is responsible for 50% to 80% of all deaths in surgical intensive care units by leading to MOF (9).

Many clinical and basic science studies have been initiated to investigate the underlying mechanisms of sepsis. The ultimate goal of these studies is to decrease the mortality from sepsis by developing new therapeutical modalities, however no specific therapy has yet been shown to decrease the morbidity and mortality from sepsis other than non-specific supportive management. Part of the unsuccessful therapeutical approaches tried was the lack of the animal models, which were consistent with the clinical progress of sepsis.

Many animal models have been used to investigate the underlying pathophysiological mechanisms of sepsis, and some treatment modalities have been found useful to decrease the mortality, but these modalities were not able to improve the clinical progress in septic patients in intensive care units, and even some attenuate the survival. The reason was that, these animal models used were only able to

investigate the very acute phase of sepsis, and were unable to answer the questions about the chronic and metabolic phases. In patients, sepsis usually follows a gradual pathway, starting with an acute hyperdynamic cardiovascular response, progressing to hypodynamic and hypercatabolic phase characterized with profound changes in carbohydrate, amino acid, and lipid metabolism (25, 66, 67), and ending with multiple organ failure and death. Most of the current animal models are only able to study the hyperdynamic acute-phase and do not give any information about the later phases, and so the therapeutical modalities applied to these models can not be applied to patients, and the reason why many clinical trials were unsuccessful was the lack of the information about the pathophysiology of the chronic phase of sepsis.

For this reason we used a well established and highly reproducible chronic septic rat fecal-agar pellet model, which reproduces some of the cardiovascular and metabolic alterations seen in septic patients, and was consistent with clinical progress of sepsis (67-73). We were able to study the effects of not only sepsis but also systemic inflammatory response syndrome with this particular animal model, and able to investigate the differences between the two systemic inflammatory responses and the role of the infectious organisms on this inflammatory process.

We produced an intra-abdominal septic abscess by implanting a previously sterilized then contaminated with $10^2$ CFU of E. coli and $10^9$ CFU of B. fragilis fecal-agar pellet into the intra-peritoneal cavity of the rats, as well as a sterile one by only inoculating pre-sterilized fecal-agar pellet, but bacteria, in order to study the systemic responses against sepsis/SIRS, since the clinical sepsis often develops after abdominal trauma or major abdominal surgery, and frequently is associated with an

intra-abdominal abscess, caused by mixed polymicrobial infections composed of aerobic organisms such as Escherichia coli as well as anaerobic organisms such as Bacteriodes fragilis (74-76).

We followed up the experimental subjects (rats) for a 72-hour period after pellet implantation, and focused on the relation between the abscess wall, portal circulation and the liver in terms of pro-inflammatory cytokines and their effects on acute-phase protein production.

Septic animals had a mortality rate of 0-100% in different batches depending on the amount of the bacteria inoculated into the pellet prior to implantation into the peritoneal cavity, whereas in the sterile abscess group no mortality occurred throughout the study. All the mortality seen in the septic group was during the first 48-hour post implantation period. All animals, which were inoculated with a sterile or septic pellet and which survived the initial peritonitis stage, formed an intra-abdominal abscess and survived until sampling at day 3. The reason for the high mortality rate, which occurred in the septic abscess group during the initial 24-48 hour period, was because of the acute disseminated peritonitis due to bacterial invasion. Once the abscess was totally walled off in both sterile and septic groups by the 48-hour post implantation period as described by Nakatani et al., and walled off abscess was responsible for the localizing the invading bacteria to a walled-off place in the abdominal cavity (60). An abscess is a localized inflammation by definition, and it plays a unique role in our model by limiting the invasion of the bacteria to the peritoneum, and preventing the high mortality rate seen in the septic group, but we

hypothesized that walled off abscess was also contributing to the development of the chronic inflammatory response seen in both sterile and septic abscess groups.

The septic pellets were inoculated with $10^2$ CFU of E. coli and $10^9$ CFU of B. fragilis. In seven different batches of rats, we observed different mortality rates ranging from 0% to 100%, as a result of the E. coli concentration in the septic pellets. The initial E. coli inoculum varied (0-221 CFU/pellet) in each batch of rats, while the amount of B. fragilis inoculated was constant in all seven batches ($10^9$ CFU/pellet). The linear regression analysis of the mortality rate by the amount of E. coli inoculated in each pellet showed a statistically significant close to perfect direct correlation, and the equation for linear regression analysis showed that; the septic mortality was 10.5 + 0.43 E. coli count, demonstrating that the septic mortality was close to 0 when there was no E. coli inoculated, and approached to 100% when the amount of E. coli was over 200 CFU/pellet. These results were consistent with the previously described data (74).

Even if B. fragilis did not seem to contribute to high septic mortality, it has been previously shown that it contributes to abscess formation, modulates skeletal muscle metabolism, and influences the systemic lactate concentrations in response to sepsis by lowering the proportion of active pyruvate dehydrogenase complex (74). Hyperlactetemia is a characteristic feature of the metabolic response to sepsis, and is a more consistent prognostic factor than TNF-$\alpha$ and IL-6 levels, and at very high levels (>20 mM/l) may also contribute to the high incidence of mortality (56, 74).

The morbidity of the animals due to the septic and the sterile intra-abdominal abscesses was evaluated by using parameters, such as weight changes, amount of

chow and water intake, and the general appearance. Following pellet implantation, both sterile and septic animals looked sick during the first 48-hour period due to the surgery, the inflammatory effect of the pellet and also due to the acute bacterial peritonitis in the septic animals. They had diarrhea, crusted eyes, and a lack of mobility, ate lower amounts of chow and drank less water, when compared to the control group. There were also weight changes due to metabolic responses of the septic process, which occurred after 24 hours (25, 67, 68, 71, 74). There was no statistically significant difference in the weights of the control, sterile and septic groups in pre-operative days 2 and 1 (p values were 0.57 and 0.56, respectively), but 24 hours after the implantation, both sterile and septic animals lost statistically significant amounts of weight, when compared to pre-operative levels (p: 0.0002 and p: 0.0001, respectively). Septic animals continued to loose weight until post-operative day 2, which was statistically significant (p: 0.006), when compared to 24-hour post-operative period, whereas sterile animals gained some weight by the post-operative day 2, when compared to 24-hour post-operative period, but this was not at statistically significant levels (p: 0.10).

The weight loss during the first 24-hour post operative period was because of stress due to surgery, since both sterile and septic groups lost statistically significant amounts of weight during this period, and there was no significant difference between the two groups. The weight loss after the post-operative 24-hour period was attributed to hypercatabolic phase seen in sepsis (25, 67, 68, 71, 74), since sterile animals started to gain weight in this period, while septic ones continued to loose statistically

significant amounts, since the hypercatabolic response was more intense in the septic group.

**B) THE ROLE OF THE INTRA-ABDOMINAL ABSCESS WALL IN THE COURSE OF SEPSIS/SIRS:**

Both sterile and septic pellets were totally walled off on post-operative day 3 (the day of sacrifice), but there was a difference in gross appearance between the two groups. Both abscess walls included whitish fibrous tissue, but the wall was much thicker and whiter in color in the septic abscess wall. This appears to reflect its increased intensity of the fibrotic reaction caused by the septic pellet.

The intensity of the inflammatory infiltration was investigated by looking at the histology of the sterile and the septic abscess walls using H&E stain, which did not show any significant difference between the two abscess walls, suggests that the body responses to both sterile and septic insults in a similar way, regardless of the presence of bacteria.

Both sterile and septic abscess walls showed an increased amount of IL-6 and fibrinogen gene expression as detected by polymerase chain reaction and *in situ* hybridization. Even though there was no quantitative difference of the expression of the IL-6 and the fibrinogen genes between the sterile and septic abscess walls, there was a marked difference of the morphology and the location of the IL-6 and fibrinogen producing cells between the sterile and septic abscess walls. Both IL-6 and fibrinogen expressing cells were fusiform and located in the intermediate layer (extracellular matrix) of the sterile abscess wall, whereas the IL-6 and fibrinogen

producing cells were round and located in the inner layer of the septic abscess wall near the necrotic center of the abscess, where most of the bacteria were seen, and which appears to have a stimulating effect in the gene expression of IL-6 and fibrinogen.

There was also a significant increase in the collagen deposition in the sterile and septic abscess walls by the post-operative day 3 as shown by trichrome stain. The septic wall had a concentrated and prominent accumulation of collagen fibers mostly located in the intermediate layer, whereas the sterile abscess wall had a scattered pattern and markedly less intense deposition, which was consistent with the gross anatomy of the abscess walls.

It has been previously shown by Vary et al. (67-73), as well as in this study, that intra-abdominal abscess formation has a distinct effect on the morbidity and mortality of the chronic septic rat fecal-agar pellet model. The acute disseminated peritonitis caused by gram negative (E. coli) and anaerobic (B. fragilis) bacteria is responsible for the early mortality seen in our septic rat model. Although a walled off intra-abdominal abscess formation decreases the mortality rate by encapsulation of the bacterial source, it cannot prevent the clinical course of sepsis/SIRS, which appears to be the direct effect of the pro-inflammatory cells in the abscess wall as the source of pro-inflammatory mediators, such as cytokines and acute-phase proteins, and the production of these inflammatory mediators appears to cause the chronic systemic effects of sepsis/SIRS.

**C) THE PLASMA LEVELS OF PRO-INFLAMMATORY CYTOKINES (TNF-α, IL-1β, IL-6) IN CHRONIC PHASE OF SEPSIS/SIRS:**

We looked at the circulating levels of three major pro-inflammatory cytokines, TNF-α, IL-1β, and IL-6, in all-experimental groups in post-operative day 3 and compared the results among each other. It was previously shown by Quinn et al. that, TNF-α and IL-1β are the acute pro-inflammatory cytokines and their circulating levels are mostly elevated in response to injury in the acute phase of chronic septic rat fecal-agar pellet model, whereas IL-6 is known as chronic or late phase pro-inflammatory cytokine (77).

In our experimental design, plasma samples were taken from both portal vein and inferior vena cava, in order to study not only the role of the intra-abdominal abscess wall in the portal vein cytokine levels, but also the contribution of the liver to the systemic circulation cytokine concentrations in response to sepsis/SIRS. The circulating levels of TNF-α and IL-1β did not show any significant differences among control, sterile and septic groups in either portal vein or inferior vena cava by post-operative day 3. On the other hand, circulating IL-6 levels in both portal vein and inferior vena cava on post-operative day 3 were statistically higher in both the sterile and septic groups, compared to the control group, but there was no statistically significant difference between the sterile and the septic groups.

These results suggest that, IL-6 is a chronic phase pro-inflammatory cytokine, which becomes significantly elevated in the portal blood in response to intra-abdominal abscess formation, and appears to be responsible for the systemic effects of sepsis. Whereas TNF-α and IL-1β are acute-phase pro-inflammatory cytokines,

which respond early to the infection/inflammation, and subside during the chronic phase, and appear to be responsible for the acute changes in response to sepsis/SIRS. The fact that there is no significant difference between the sterile and septic groups in terms of IL-6 plasma levels further confirms the importance of the inflammatory response mediated by the sterile inflammation in the circulating cytokine levels.

In our experimental design, we were able to study and compare the circulating cytokine levels of both portal vein and inferior vena cava in order to grossly localize their origin and determine what role the abscess wall plays in terms of initiating the systemic cytokine response to injury. In the chronic phase of sepsis (post-operative day 3 in our animal model), no statistically significant difference between the portal vein and the inferior vena cava circulating pro-inflammatory cytokine (TNF-$\alpha$, IL-1$\beta$, IL-6) levels in all experimental groups was observed.

Our *in situ* hybridization data as well as the above information suggested that, elevated circulating cytokine levels in the chronic phase of sepsis/SIRS, originated from the intra-abdominal abscess wall and carried out to the systemic circulation via the portal vein.

**D) THE ROLE OF THE LIVER IN THE CHRONIC PHASE OF SEPSIS/SIRS:**

Using the chronic septic rat pellet model, Vary et al. described previously that, both sterile and septic abscess groups showed statistically significant leukocytosis (elevated white blood cells in the systemic circulation) when compared to the control group, and leukocytosis in the septic group was statistically higher than in the sterile

group (74). In the light of this previously published data (74), we focused on the inflammatory cell infiltration of the liver. We showed the effects of intra-abdominal sterile and septic abscesses on the liver in terms of pro-inflammatory white blood cell infiltration by using routine Hematoxylin & Eosin and myeloperoxidase stains. The increased leukocyte infiltration (mainly polymorphonuclear leukocytes) observed in the liver was concentrated around the sinusoids and the portal triad in both sterile and septic abscess groups, when compared to control group. The infiltration of myeloperoxidase stained cells was more intense in the septic group than in the sterile group. These results suggest that, the intra-abdominal insult regardless of being sterile or septic causes a systemic reaction in the organism that further effects the liver as a remote organ by causing inflammatory cell infiltration and sequestration.

We further evaluated the metabolic changes that might occur in the liver during the intra-abdominal insult by examining the liver samples histologically using Oil Red O Lipid stains. The sterile and septic livers showed a significantly increased amount and size of lipid droplets throughout the parenchyma when compared to control livers. The changes in the hepatic lipid metabolism, in which ketone synthesis was inhibited and malonyl CoA synthesis was increased with a shift to increased hepatic free fatty acid metabolism and triglyceride formation has been discussed previously (25, 59, 68) in the chronic septic rat model. Our observations confirm these data by showing that the liver responds to an intra-abdominal abscess by increased lipid deposition in the hepatocytes, and these changes in the hepatic lipid metabolism shown histologically were more prominent in the septic group than in the sterile group.

The liver is known to possess Kupffer cells (specialized macrophages located in liver, especially within the sinusoids close to the entry of the portal triad), and these cells show elevated cytokine and acute-phase protein gene expression in response to injury. The location of the hepatic cellular element producing cytokines and its effect on acute-phase protein response of fibrinogen synthesis in intra-abdominal sepsis are not well documented in the literature. This study has investigated all these relations in detail. The ELISA data led us to choose IL-6 as the model pro-inflammatory cytokine, since IL-6 showed significantly elevated levels in the portal circulation of sterile and septic abscess animals in the chronic phase of the systemic response, and has been shown to induce fibrinogen synthesis, which appears to serve as a structural basis for the subsequent deposition of fibroblast synthesized collagen in the liver parenchyma.

IL-6 and fibrinogen gene expression was studied in the liver by using *in situ* hybridization and oligo DNA probes. Both IL-6 and fibrinogen genes were found to be expressed quantitatively at higher levels in the liver of sterile and septic abscess groups (the septic group had the most intense among the all three groups), when compared to the control group. The interesting data was that the cells, which expressed the IL-6 and the fibrinogen genes, were located solely around the central vein and portal triad. This is the first report showing the unique location of IL-6 and fibrinogen gene expression in the liver in response to intra-abdominal sterile and septic abscesses.

The fibrotic changes in the sterile and septic livers were depicted by using trichrome stain. Both sterile and septic livers had increased collagen deposition when

compared to the control livers, and the fibrotic changes were more prominent around the central vein area extending through the sinusoids, where the most intense IL-6 and fibrinogen gene expression was.

We concluded in the light of the data that, the liver has an important role as a remote organ in terms of IL-6 and fibrinogen gene expression in response to sepsis and SIRS, even though it doesn't contribute the systemic circulating levels of these pro-inflammatory proteins.

The unique and close location of the cells expressing IL-6 and fibrinogen genes in the liver confirms the heterogeneity of the liver parenchyma and suggests a direct paracrine effect of the hepatic central vein cells producing the IL-6 on those producing the fibrinogen. The consequent laying down of collagen with a proximity to the fibrinogen producing cells, appears to produce some degree of functional obstruction of the hepatic sinusoidal outflow, which induces hepatic sinusoidal congestion and appears to reduce the hepatic blood flow, and subsequently facilitates the production of superoxide radicals by the regulation of myeloperoxidase containing white blood cells, inducing the hepatic cellular response and chronic inflammatory changes in the intra-abdominal septic process.

Even though the septic liver shows a more intense inflammatory response and fibrotic changes, the data further supports the basic role of the sterile inflammation in contribution to remote organ injury independent of the septic contamination.

# SUMMARY AND CONCLUSIONS

The chronic septic rat fecal-agar pellet model is a reliable, highly reproducible, and well-established animal model, which reproduces some of the cardiovascular and metabolic alterations seen in septic patients, and is consistent with clinical progress of sepsis (67-73). It allows not only to study the effects of sepsis and systemic inflammatory response syndrome, but also to investigate the differences between the two systemic inflammatory responses and the role of the infectious organisms on this inflammatory process.

All the mortality is seen during the first 48-hour post implantation period due to acute disseminated bacterial peritonitis. All animals, which are inoculated with a sterile or septic pellet and which survive the initial peritonitis stage, form an intra-abdominal abscess and survive until sampling at day 3. An abscess is a localized inflammation by definition, and it plays a unique role in our model by limiting the invasion of the bacteria to the peritoneum, and preventing the high mortality rate seen in the septic group. The initial E. coli inoculum to the pellet has a statistically significant close to perfect direct correlation with the septic mortality rate, whereas B. fragilis has been previously shown to contribute to the abscess formation, modulate the skeletal muscle metabolism, and influence the systemic lactate concentrations in response to sepsis by lowering the proportion of active pyruvate dehydrogenase complex (74).

The morbidity of the sterile and the septic groups seen during the first 48-hour period is due to the surgery, the inflammatory effect of the pellet and also due to the acute bacterial peritonitis in the septic animals. They have diarrhea, crusted eyes, and a lack of mobility, eat lower amounts of chow and drink less water, and loose statistically significant amounts of weight secondary to the metabolic responses of the inflammatory process, when compared to the control group (25, 67, 68, 71, 74).

It has been previously shown by Vary et al. (67-73), as well as in this study, that both sterile and septic pellets are totally walled off by post-operative day 3 and an intra-abdominal abscess formation has a distinct effect on the morbidity and mortality of the chronic septic rat fecal-agar pellet model. Although a walled off intra-abdominal abscess formation decreases the mortality rate by encapsulation of the bacterial source, it cannot prevent the clinical course of sepsis/SIRS, which appears to be the direct effect of the pro-inflammatory cells in the abscess wall as the source of pro-inflammatory mediators, such as cytokines and acute-phase proteins, and the production of these inflammatory mediators appears to cause the chronic systemic effects of sepsis and SIRS.

It was previously shown by Quinn et al., as well as in this study that, TNF-$\alpha$ and IL-1$\beta$ are the acute pro-inflammatory cytokines and their circulating levels are mostly elevated in response to injury in the acute phase of chronic septic rat fecal-agar pellet model, whereas IL-6 is known as chronic or late phase pro-inflammatory cytokine, in which the levels are significantly higher in the portal circulation of the sterile and the septic abscess groups, when compared to the control group in response to an intra-abdominal abscess formation (77).

The intra-abdominal abscess, regardless of being sterile or septic, causes a systemic reaction in the organism that further effects the liver as a remote organ by causing inflammatory cell infiltration and sequestration. The liver responds to an intra-abdominal abscess by increased lipid deposition in the hepatocytes, secondary to the changes in the hepatic lipid metabolism as previously described in this model (25, 59, 68). The liver also has an important role as a remote organ in terms of IL-6 and fibrinogen gene expression in response to an intra-abdominal abscess, even though it doesn't contribute the systemic circulating levels of these pro-inflammatory proteins. The unique and close location of the cells expressing IL-6 and fibrinogen genes in the liver confirms the heterogeneity of the liver parenchyma and suggests a direct paracrine effect of the hepatic central vein cells producing the IL-6 on those producing the fibrinogen. The consequent laying down of collagen with a proximity to the fibrinogen producing cells, appears to produce some degree of functional obstruction of the hepatic sinusoidal outflow, which induces hepatic sinusoidal congestion and appears to reduce the hepatic blood flow, and subsequently facilitates the production of superoxide radicals by the regulation of myeloperoxidase containing white blood cells, inducing the hepatic cellular response and chronic inflammatory changes in the intra-abdominal septic process. Even though the septic liver shows a more intense inflammatory response and fibrotic changes, the data further supports the basic role of the sterile inflammation in contribution to remote organ injury independent of the septic contamination.

# BIBLIOGRAPHY


1. Faist E: Immunological trends in the treatment of the shock patient (presented at 4th International Shock Congress, Philadelphia, PA, June 1999)

2. Deutschman CS: Acute-phase responses and sirs/mods: the good, the bad, and the nebulous. Critical Care Medicine 26(10): 1630-32, 1998

3. Shephard RJ, Shek PN: Immune responses to inflammation and trauma: a physical training model. Canadian Journal of Physiology & Pharmacology 76: 469-472, 1998

4. Abraham E, Matthay MA, Dinarello CA, Glauser M, Parsons P, Fisher CJ, Repine JE: Consensus conference definitions for sepsis, septic shock, acute lung injury, and acute respiratory distress syndrome: Time for a reevaluation. Crit Care Med 28: 232-5, 2000

5. Schein M, Wise L: Epilogue: *In* Schein M, Wise L (eds): Cytokines and the Abdominal Surgeon. Austin: Landes Bioscience, 1998, pp 295-301

6. Deitch EA, Goodman ER: Prevention of multiple organ failure. Surgical Clinics of North America 79: 1471-1488, 1999

7. Baue AE: MOF/MODS, SIRS: An update. Shock 6 (suppl): 1-5, 1996

8. Tilney NL, Bailey GL, Morgan AP: Sequential system failure after rupture of abdominal aortic aneurysms: An unsolved problem in postoperative care. Ann Surg 178: 117-122, 1973

9. Deitch EA: Multiple organ failure: pathophysiology and potential future therapy. Ann Surg 216: 117-134, 1992

10. Rotstein OD, Meakins JL: Diagnostic and therapeutic challenges of intraabdominal infections. World J surg 14: 159-166, 1990

11. Gabay C, Smith MF, Eidlen D, Arend WP: Interleukin 1 receptor antagonist (IL-1Ra) is an acute-phase protein. Journal of Clinical Investigation 99: 2930-2940, 1997

12. Hardaway RM: A review of septic shock. The American Surgeon 66: 22-29, 2000

13. Border JR: Hypothesis: Sepsis, multiple organ failure and the macrophage. Arch Surg 123: 385-386, 1988

14. Bone RC: Sir Isaac Newton, sepsis, SIRS, and CARS. Crit Care Med 24: 1125-1128, 1996

15. Ertel WK: Pro- and anti-inflammatory cytokines following injury and sepsis (presented at 4th International Shock Congress, Philadelphia, PA, June 1999)

16. Giroir BP: BPI: Clinical success? (presented at 4th International Shock Congress, Philadelphia, PA, June 1999)

17. Lin E, Calvano SE, Lowry SF: Inflammatory cytokines and cell response in surgery. Surgery 127: 117-126, 2000

18. Spink J, Cohen J: Synergy and specificity in induction of gene activity by proinflammatory cytokines: potential therapeutic targets. Shock 7: 405-412, 1997

19. Lyoumi S, Tamion F, Petit J, et al.: Induction and modulation of acute-phase response by protein malnutrition in rats: comparative effect of systemic and localized inflammation on interleukin-6 and acute-phase protein synthesis. Journal of Nutrition 128: 166-174, 1998

20. Lin E, Calvano SE, Lowry SF: Disordered apoptosis as a mechanism for adverse outcome in critical illness. *In* Vincent JL (ed): Yearbook of Intensive Care and Emergency Medicine. Berlin, Springer-Verlag, 1997, pp91-99

21. Lin E, Calvano SE, Lowry SF: The biologic control of systemic inflammatory response. Curr Opin Crit Care 3: 299-307, 1997

22. Van der Poll, Lowry SF: Tumor necrosis factor in sepsis: Mediator of multiple organ failure or essential part of host defense? Shock 3: 1-12, 1995

23. Dinarello CA: Interleukin-1 and interleukin-1 antagonism. Blood 77: 1627-52, 1991

24. Schafer M, Carter L, Stein C: Interleukin-1 beta and corticotropin-releasing factor inhibit pain by releasing opioids from immune cells in immune tissue. Proc Natl Acad Sci USA 91: 4219-23, 1994

25. Siegel JH, Vary TC: Sepsis, abnormal metabolic control and the multiple organ failure syndrome. *In* Siegel JH (ed): Trauma: Emergency Surgery and Critical Care. New York, Churchill-Livingstone, 1987, pp 411-501

26. Abraham E, Regan RF: The effects of hemorrhage and trauma on interleukin-2 production. Arch Surg 120: 1341-46, 1983

27. Gabay C, Kushner I: Acute-phase proteins and other systemic responses to inflammation. The New England Journal of Medicine 340(6): 448-453, 1999

28. Biffl WL, Moore EE, Moore FA, et al.: Interleukin-6 delays neutrophil apoptosis. Arch Surg 131: 24-30, 1996

29. Rokita H, Branicki W, Wronska D, Borysiewicz LK, Koj A: Vaccinia virus-induced changes in cytokine-regulated acute-phase plasma protein synthesis by hepatoma cells. Biochemistry and Molecular Biology International 44(6): 1093-1104, 1999

30. Xing Z, Gauldie J, Cox G, Baumann H, Jordana M, Lei XF, et al.: IL-6 is an antiinflammatory cytokine required for controlling local or systemic acute inflammatory responses. J Clin Invest 101: 311-20, 1998

31. Tilg H, Trehu H, Atkins MB: Interleukin-6 (IL-6) as an antiinflammatory cytokine: induction of circulating IL-1 receptor antagonist and soluble tumor necrosis factor receptor p55. Blood 83: 113-8, 1994

32. Van Zee K J, Fischer E, Hawes AS, et al.: Effects of intravenous IL-8 administration in nonhuman primates. J Immunol 148: 1746-52, 1992

33. Steibhauser ML, Hogaboam CM, Lucaks NW, Strieter RM, Kunkel SL. Multiple roles for IL-12 in a model of acute septic peritonitis. J Immunol 162: 5437-43, 1999

34. Alleva DG, Kaser SB, Monroy MA, Fenton MJ, Belier DI: IL-15 functions as a potent autocrine regulator of macrophage proinflammatory cytokine production: evidence for differential receptor subunit utilization associated with stimulation or inhibition. J immunol 159: 2941-51, 1997

35. Bulfone-Paus S, Ungureanu D, Pohl T, Lindner G, Paus R, Ruckert R, et al.: Interleukin-15 protects from lethal apoptosis in vivo. Nat Med 3: 1124-8, 1997

36. McDonald PP, Russo MP, Ferrini S, Cassatella MA. Interleukin-15 (IL-15) induces NF-kappaB activation and IL-8 production in human neutrophils. Blood 92: 4828-35, 1998

37. Musso T, Calosso L, Zucca M, Millesimo M, Puliti M, Bulfone-Paus S, et al.: Interleukin-15 activates proinflammatory and antimicrobial functions in polymorphonuclear cells. Infect Immun 66: 2640-7, 1998

38. Oberholzer A, Steckholzer U, Okamura H, Kurimoto M, Trentz O, Ertel W: Increased circulating levels of interleukin-18 during severe sepsis in humans. Surg Forum 49: 88-90, 1998

39. Heinzel FP, Rerko DM, Ling P, et al.: Interleukin-12 is produced in vivo during endotoxemia and stimulates synthesis of gamma interferon. Infect Immunol 62: 4244-9, 1994

40. Dinarello CA: IL-18: A TH1-inducing, proinflammatory cytokine and new member of the IL-1 family. J Allergy Clin Immunol 103: 11-24, 1999

41. Keegan AD, Ryan JJ, Paul WE: IL-4 regulates growth and differentiation by distinct mechanisms. The immunologist 4: 194-8, 1996

42. Van der Poll T, Marchant A, Buurman WA, et al.: Endogenous IL-10 protects mice from death during septic peritonitis. J Immunol 155: 5397-401, 1995

43. Moldawer LL: IL-10: A counter-regulatory cytokine in septic shock (presented at 4th International Shock Congress, Philadelphia, PA, June 1999)

44. Etter, H, Althaus R, Eugster HP, Santamaria-Babi LF, Weber L, Moser R: IL-4 and IL-13 downregulate rolling adhesion of leukocytes to IL-1 or TNF-alpha-activated endothelial cells by limiting the interval of E-selectin expression. Cytokine 10: 395-403, 1998

45. Ramadori G, Christ B: Cytokines and the hepatic acute-phase response. Seminars in Liver Disease 19: 141-155, 1999

46. Bopst M, Haas C, Car B, Eugster HP: The combined inactivation of tumor necrosis factor and interleukin-6 prevents induction of the major acute-phase proteins by endotoxin. European Journal of Immunology 28: 4130-37, 1998

47. Weinhold B, Ruther U: Interleukin-6-dependent and –independent regulation of the human c- reactive protein gene. Biochemistry Journal 327: 425-429, 1997

48. Szalai AJ, Ginkel FW, Dalrymple SA, Murray R, McGhee JR, Volanakis JE: Testosterone and IL-6 requirements for human c- reactive protein gene expression in transgenic mice. The Journal of Immunology 165: 5294-5299, 1998

49. Alpana R, Schatten H, Ray BK: Activation of sp1 and its functional co-operation with serum amyloid a-activating sequence binding factor in synoviocyte cells trigger synergistic action of interleukin-1 and interleukin-6 in serum amyloid a gene expression. The Journal of Biological Chemistry 274(7): 4300-08, 1999

50. Ramadori G, Sipe JD, Dinarello CA, et al.: Pretranslational modulation of acute phase hepatic protein synthesis by murine recombinant interleukin (IL-1) and purified human IL-1. J Exp Med 162: 930-942, 1985

51. Andus T, Geiger T, Hirano T, et al.: Action of recombinant human interleukin 6, interleukin 1 beta and tumor necrosis factor alpha on the mRNA induction of acute-phase proteins. Eur J Immunol 18: 739-746, 1988

52. Castell JV, Gomez-Lechon MJ, David M, et al.: Interleukin-6 is the major regulator of acute phase protein synthesis in adult human hepatocytes. FEBS Lett 242: 237-239, 1989

53. Chaudry IH: Gender dimorphism and the effects of sex steroids in the divergent response to shock (presented at 4th International Shock Congress, Philadelphia, PA, June 1999)

54. Spitzer JA: Differences in chemokine and cytokine generation and function (presented at 4th International Shock Congress, Philadelphia, PA, June 1999)

55. Wissink S, van Heerde EC, van der Burg B, van der Saag PT: A dual mechanism mediates repression of NF-κB activity by glucocorticoids. Mol Endocrinol 12: 355-63, 1998

56. Vincent JL: The evaluation and future trends in the shock patient from the home to the hospital (presented at 4th International Shock Congress, Philadelphia, PA, June 1999)

57. Doherty JF, Golden MH, Remick DG, Griffin GE: Production of interleukin-6 and tumor necrosis factor-alpha in vitro is reduced in whole blood of severely malnourished children. Clin Sci (colch) 86: 347-351, 1994

58. Kushner I: The phenomenon of the acute-phase response. Ann NY Acad Sci 289: 39-48, 1982

59. Nakatani T, Sato T, Marzella L, Hirai F, Trump BF, Siegel JH: Hepatic and systemic responses to aerobic and anaerobic intra-abdominal abscesses in a highly reproducible chronic rat model. Circ Shock 13: 271-294, 1984

60. Nakatani T, Sato T, Trump BF, Siegel JH, Kobayashi K: Manipulation of the size and clone of an intra-abdominal abscess in rats. Res Exp Med 196: 117-126, 1996

61. Hanker JS, Laszlo J, Moore JO: The light microscopic demonstration of hydroperoxidase-positive phi bodies and rods in leukocytes in acute myeloid leukemia. Histochemistry 58: 241, 1978

62. Hanker JS, Ambrose WW, James CJ, et al.: Facilitated light microscopic cytochemical diagnosis of acute myelogenous leukemia. Cancer Res 39: 1635, 1979

63. Hanker JS, Chandross RJ, Weatherly NF et al.: Medusa cells: The morphology and cytochemistry of common amoeboid variants of eosinophils. Histochem J 12: 701, 1980

64. Gill GW, Frost JK, Miller KA: A new formula for a half-oxidized hematoxylin solution that neither overstains nor requires differentiation. Acta Cytol 18: 300, 1974

65. Wiles JB, Cerra FB, Siegel JH, et al.: The systemic septic response: Does the organism matter? Crit Care Med 8: 55-60, 1980

66. Siegel JH, Cerra FB, Coleman B, et al.: Physiologic and metabolic correlations in human sepsis. Surgery 86: 163-193, 1979

67. Vary TC, Siegel JH, Nakatani T, et al.: Biochemical basis for depressed ketogenesis in sepsis. J Trauma 26: 419-425, 1986

68. Vary TC, Siegel JH, Nakatani T, et al.: Effects of sepsis on activity of pyruvate dehydrogenase complex in skeletal muscle and liver. Am J Physiol 250 (Endocrinol Metab, 13): E634-E640, 1986

69. Vary TC, Siegel JH, Nakatani T, et al.: Regulation of glucose metabolism by altered pyruvate dehydrogenase activity: Potential site of insulin resistance in sepsis. J Parent Ent Nutr 10: 351-355, 1986

70. Vary TC, Siegel JH, Riukind AL: Clinical and therapeutic significance of metabolic patterns of lactic acidosis. *In* Cerra F (ed): Perspectives in Critical Care. St Louis, Quality Medical Publishing, Inc., 1988, pp 85-132

71. Vary TC, Siegel JH, Tall BD, et al.: Inhibition of skeletal muscle protein synthesis in septic intra-abdominal abscess. J trauma, 28: 981-988, 1988

72. Vary, TC, Siegel JH, Tall BD, et al.: Metabolic effects of partial reversal of pyruvate dehydrogenase activity by dichloroacetate in sepsis. Circ Shock 24: 3-18, 1988

73. Vary TC, Siegel JH, Zechnich A, et al.: Pharmacological reversal of abnormal glucose regulation, BCAA utilization and muscle catabolism in sepsis by dichloroacetate. J Trauma 28: 1301-1311, 1988

74. Vary TC, Siegel JH, Tall B, Morris JG: Role of anaerobic bacteria in intra-abdominal septic abscesses in mediating septic control of skeletal muscle glucose oxidation and lactic acidemia. The Journal of Trauma 29: 1003-1014, 1989

75. Altemeier WA: Intraabdominal abscesses. Am J Surg 125: 70-79, 1973

76. Swenson RM, Lorber B, Michealson TC, et al.: The bacteriology of intra-abdominal infections. Arch Surg 109: 398-399, 1974

77. Quinn LM: The host defense response to abscess formation: An investigation of plasma cytokine responses in an intra-abdominal septic rat model. *In*: A Thesis submitted to the Graduate School of Biomedical Sciences, UMDNJ. New Jersey, March, 1999